PACIFIC EARTHQUAKE ENGINEERING
RESEARCH CENTER

Interaction in Interconnected Electrical Substation Equipment Subjected to Earthquake Ground Motions

Armen Der Kiureghian
Jerome L. Sackman
Kee-Jeung Hong
University of California, Berkeley

A report to sponsor Pacific Gas & Electric Co.
San Francisco, California

PEER 1999/01
FEB. 1999

Interaction in Interconnected Electrical Substation Equipment Subjected to Earthquake Ground Motions

Armen Der Kiureghian
Jerome L. Sackman
Kee-Jeung Hong

Structural Engineering, Mechanics & Materials
Department of Civil & Environmental Engineering
University of California, Berkeley
Berkeley, California 94720

A report to sponsor
Pacific Gas & Electric Co.
San Francisco, California

Report No. PEER 1999/01
Pacific Earthquake Engineering Research Center
College of Engineering
University of California
Berkeley, California

February 1999

ABSTRACT

The survival of lifeline systems after a major earthquake in an urban area is essential for speedy delivery of first aid and for post-earthquake recovery. Of particular importance are electric power distribution systems. The research presented in this paper is part of a larger program aimed at assessing the seismic fragility of electrical substations that form critical nodes in power distribution systems.

A typical electrical substation consists of a complex set of interconnected equipment items, such as transformers, circuit breakers, surge arresters, capacitor banks, disconnect switches, etc., many of which support fragile elements such as ceramic bushings. These equipment items are usually connected to each other through rigid conductor buses or flexible cables. Due to dissimilar characteristics of these equipment items, significant dynamic interaction between them may occur during seismic disturbances if the connection is not sufficiently flexible. Post-earthquake field investigations have indicated that this kind of interaction may be responsible for some of the observed damage in electrical substations during recent earthquakes. Unfortunately no sound design guidelines or analysis methods are currently available that account for this effect.

This investigation aims at assessing the effect of interaction in interconnected equipment items and developing design guidelines for reducing the adverse nature of this effect. The study focuses on two equipment items with a single connecting element. Equipment items are modeled as linear, distributed-mass systems with one degree of freedom. Two distinct models of the connecting element are used: a linear spring-dashpot-mass element to represent a rigid bus with linear or linearized properties, and an extensible cable with negligible flexural rigidity to represent a flexible cable conductor. A set of dimensionless response ratios are defined that quantify the interaction effect on each equipment item relative to its response in a stand-alone configuration. A response ratio to quantify the force in the connecting element is also defined. Extensive analytical and numerical analyses are carried out to evaluate the influences of various system parameters on the interaction effect.

For the linear connecting element, a simple method of analysis utilizing a response spectrum specification of the ground motion is developed. Parametric investigations with this method reveal that the interaction tends to amplify the response of the higher frequency equipment item and de-amplify the response of the lower frequency equipment item relative to their respective stand-

alone responses. The amplification in the response of the higher frequency equipment item can be as large as a factor of 6 or greater. Parameters having major influences on this effect include the ratio of equipment frequencies, the ratio of equipment masses, the stiffness of the connecting element, the damping of the connecting element, and the location of attachment of the connecting element to each equipment item. Lesser influence is provided by the mass of the connecting element and the shape of the response spectrum. No interaction occurs between equipment items with identical frequencies and damping ratios, provided equal fractions of their masses act as external inertia forces. Specific guidelines for reducing the interaction effect on the higher frequency equipment item are described.

The response of the cable-connected equipment system is found to be highly nonlinear and asymmetric when the cable is taut. As a result, analysis by the response spectrum method is not possible. Instead, an algorithm for time history analysis is developed and numerical calculations are carried out for typical systems subjected to a selection of recorded ground motions. These investigations reveal that the interaction can significantly amplify the response of the higher frequency equipment item and moderately amplify the response of the lower frequency equipment item. Parameters having major influences on this effect include the equipment frequencies and the cable slackness. Due to the complex and unpredictable nature of the response, it is prudent to design the cable-connected system with sufficient cable slackness to avoid the adverse effect of interaction. A simple formula is developed that provides the minimum cable slackness in terms of the chord length of the cable and the maximum relative displacement between the stand-alone equipment items. Other specific guidelines for reducing the interaction effect on the cable-connected equipment items are also described.

Aside from the above results concerning the interaction effect, this report contains a number of new formulations and analytical results. These include closed form expressions for the modal properties of connected oscillators, formulas for the stiffness and geometric properties of the catenary cable, an algorithm for dynamic analysis of cable-connected equipment items, and a criterion for neglecting the flexural rigidity of a cable.

Last but not least, based on the experience gained in this study, a set of topics for further study are recommended that, in the view of the authors, would lead to a better understanding of the behavior of interacting equipment items and would result in more reliable and safer designs.

ACKNOWLEDGMENT

This study was supported by Contract No. Z-19-2-133-96 with the Pacific Gas & Electric Company through the Pacific Earthquake Engineering Research (PEER) Center. Valuable information provided by PG&E engineers, particularly Eric Fujisaki and Ed Matsuda, and by Dennis Ostrom are gratefully acknowledged. Thanks are also extended to our colleague, Gregory Fenves, for his role as the Project Manager within UC Berkeley.

TABLE OF CONTENTS

ABSTRACT..... i

ACKNOWLEDGMENT..... iii

TABLE OF CONTENTS..... iv

LIST OF FIGURES..... vi

NOMENCLATURE..... ix

CHAPTER 1 - INTRODUCTION..... 1

1.1 Introduction..... 1

1.2 Objectives and Scope..... 3

1.3 Organization of the Report..... 4

CHAPTER 2 – TWO EQUIPMENT ITEMS CONNECTED BY A LINEAR SPRING-DASHPOT ELEMENT..... 6

2.1 Introduction..... 6

2.2 Model of Equipment Item..... 6

2.3 Model of the Connected System..... 9

2.4 Modal Properties of the Connected System..... 11

2.5 Response of the Connected System..... 16

CHAPTER 3 – EFFECT OF INTERACTION IN LINEARLY CONNECTED EQUIPMENT ITEMS..... 22

3.1 Introduction..... 22

3.2 Response Ratios..... 22

3.3 Effect of Equipment Frequencies, Mass Ratio, and Stiffness of Connecting Element..... 24

3.4 Effect of Damping of the Connecting Element..... 26

3.5 Effect of Mass of the Connecting Element 31

3.6 Effect of Attachment Configuration..... 33

CHAPTER 4 – TWO EQUIPMENT ITEMS CONNECTED BY A CABLE 42

4.1 Introduction..... 42

4.2 Catenary Cable as Connecting Element..... 43

4.3 Analysis of the Cable-Connected System..... 48

4.4 Numerical Studies with Example Cable-Connected Systems..... 51

CHAPTER 5 – RECOMMENDATIONS AND GUIDELINES FOR DESIGN OF CONNECTED EQUIPMENT..... 76

5.1 Introduction..... 76

5.2 Major Findings..... 76

5.3 Guidelines for Design of Equipment Connected by Rigid Bus..... 80

5.4 Guidelines for Design of Equipment Connected by Flexible Cables 82

CHAPTER 6 - SUMMARY AND RECOMMENDATIONS FOR FURTHER STUDY 85

6.1 Summary..... 85

6.2 Recommendations for Further Study 86

APPENDIX A – CRITERION FOR NEGLECTING FLEXURAL STIFFNESS OF CABLE 88

REFERENCES..... 92

LIST OF FIGURES

CHAPTER 2

Figure 2.1 Single-degree-of-freedom models of equipment items 20

Figure 2.2 Two-degree-of-freedom linear models of connected equipment items 20

Figure 2.3 Normalized frequencies of the connected system 21

CHAPTER 3

Figure 3.1 Response ratios for connecting element for $l_1 / m_1 = l_2 / m_2$, $\omega_2 = 10\pi$ rad/s, $\zeta_1 = \zeta_2 = 0.02$ and $c_0 = 0$, based on the IEEE spectrum 36

Figure 3.2 Response ratios for connecting element for $l_1 / m_1 = l_2 / m_2$, $\omega_2 = 20\pi$ rad/s, $\zeta_1 = \zeta_2 = 0.02$ and $c_0 = 0$, based on the IEEE spectrum 37

Figure 3.3 Effect of damping of equipment items on response ratio R_2 for $l_1 / m_1 = l_2 / m_2$, $\omega_2 = 20\pi$ rad/s and $c_0 = 0$, based on the IEEE Spectrum 38

Figure 3.4 Effect of damping of connecting element on response ratios for $m_1 / m_2 = 2$, $l_1 / m_1 = l_2 / m_2$, $\omega_2 = 20\pi$ rad/s, $\kappa = 0.5$ and $\zeta_1 = \zeta_2 = 0.02$, based on the Kanai-Tajimi spectrum 38

Figure 3.5 Three-degree-of-freedom model of connected system with mass of the connecting element 39

Figure 3.6 Effect of mass of connecting element on response ratios for $m_1 / m_2 = 2$, $l_1 / m_1 = l_2 / m_2$, $\omega_2 = 20\pi$ rad/s, $\zeta_1 = \zeta_2 = 0.02$, $\kappa = 0.5$ and $c_0 = 0$, based on the IEEE spectrum 39

Figure 3.7 Tuned-mass damper effect of the connecting element on response ratios R_1 and R_2 for $m_1 / m_2 = 2$, $l_1 / m_1 = l_2 / m_2$, $\omega_2 = 20\pi$ rad/s, $\zeta_1 = \zeta_2 = 0.02$, $\kappa = 0.02$ and $c_0 = 0$, based on the IEEE spectrum 40

Figure 3.8 Example connected system with variable attachment points 41

Figure 3.9 Effect of attachment configuration on response ratios R_1 and R_2 for $m_1 / m_2 = 2$, $\omega_2 = 20\pi$ rad/s, $\zeta_1 = \zeta_2 = 0.02$, $\kappa = 0.5$ and $c_0 = 0$, based on the IEEE spectrum 41

CHAPTER 4

Figure 4.1 Catenary cable 58

Figure 4.2 Normalized horizontal cable force versus normalized sag 58

Figure 4.3 Normalized cable stiffness versus normalized sag 59

Figure 4.4 Rate of change of cable sag with respect to span length versus normalized sag 59

Figure 4.5 Cable configuration with virtual sag 60

Figure 4.6 Normalized sag versus slackness 60

Figure 4.7 Normalized horizontal cable force versus slackness 61

Figure 4.8 Normalized cable stiffness versus slackness 61

Figure 4.9 Normalized effective stiffness of example cable versus normalized sag, accounting for cable extensibility 62

Figure 4.10 Cable-connected equipment items 62

Figure 4.11 N-S component of Newhall record, 1994 Northridge earthquake 63

Figure 4.12 Displacement time histories for stand-alone and connected equipment items 64

Figure 4.13 Time history of the cable span length 65

Figure 4.14 Time history of the normalized cable force 65

Figure 4.15 Time history of the normalized effective cable stiffness 66

Figure 4.16 Selected accelerograms 67

Figure 4.17 Response ratios for five earthquakes as functions of the initial sag for

$\omega_1 = 2\pi$ rad/s and $\omega_2 = 10\pi$ rad/s 68

Figure 4.18 Response ratios for five earthquakes as functions of the initial sag for $\omega_1 = 2\pi$ rad/s and $\omega_2 = 10\pi$ rad/s with equipment positions switched 69

Figure 4.19 Response ratios for five earthquakes as functions of the initial sag for $\omega_1 = 4\pi$ rad/s and $\omega_2 = 10\pi$ rad/s 70

Figure 4.20 Change in slackness due to relative displacement Δ 71

Figure 4.21 Response ratios for five earthquakes as functions of the interaction parameter for $\omega_1 = 2\pi$ rad/s and $\omega_2 = 10\pi$ rad/s ($H / L_0 = 0$) 72

Figure 4.22 Response ratios for five earthquakes as functions of the interaction parameter for $\omega_1 = 2\pi$ rad/s and $\omega_2 = 10\pi$ rad/s with equipment positions switched ($H / L_0 = 0$) 73

Figure 4.23 Response ratios for five earthquakes as functions of the interaction parameter for $\omega_1 = 4\pi$ rad/s and $\omega_2 = 10\pi$ rad/s ($H / L_0 = 0$) 74

Figure 4.24 Response ratios for five earthquakes as functions of the interaction parameter for $\omega_1 = 2\pi$ rad/s and $\omega_2 = 10\pi$ rad/s ($H / L_0 = 0.5$) 75

APPENDIX A

Figure A1. Cable with no flexural stiffness 91

Figure A2. Horizontal support displacement of curved beam 91

NOMENCLATURE

A	cross-sectional area;
a_i	i th modal effective participation factor of the connected system;
c	damping coefficient of oscillator; also used to denote cable chord length;
c_0	damping coefficient of connecting element;
c_1	damping coefficient of lower-frequency equipment;
c_2	damping coefficient of higher-frequency equipment;
$\mathbf{C}$	damping matrix of connected system;
$D(\omega,\zeta)$	displacement response spectrum ordinate for frequency ω and damping ratio ζ;
dL	differential support displacement;
dM	differential bending moment;
$d\psi$	differential curvature;
E	elastic modulus;
h, h_0	cable sag;
H	vertical separation between cable supports;
$H_u(\omega)$	frequency response function of response quantity $u(t)$;
$\mathbf{H}(\omega)$	frequency response matrix of the connected system;
I	moment of inertia;
k	stiffness of oscillator;
k_0	stiffness of connecting element;
k_1	stiffness of lower-frequency equipment;
k_2	stiffness of higher-frequency equipment;
k_{eff}	effective cable stiffness including effect of axial deformation;
k_{cable}	stiffness due to cable action;
k_{flexure}	stiffness due to bending;
$\mathbf{K}$	effective stiffness matrix of connected system;
l	effective mass producing external inertia force;

l_1 effective mass producing external inertia force for lower-frequency equipment;

l_2 effective mass producing external inertia force for higher-frequency equipment;

L, L_0 cable span;

L_1, L_2 distances from lowest point of cable to left and right supports, respectively;

$\mathbf{L}$ external inertia force coefficient vector of connected system;

m mass of oscillator;

m_0 mass of connecting element;

m_1 mass of lower frequency equipment;

m_2 mass of higher frequency equipment;

M_i i th modal mass;

$\mathbf{M}$ effective mass matrix of connected system;

$\mathbf{P}_n$ effective external force vector at n th time step;

rms root mean square;

R_0 response ratio for connecting element;

R_1 response ratio for lower-frequency equipment;

R_2 response ratio for higher-frequency equipment;

$\mathbf{R}$ restoring force vector for the cable-connected system;

s, s_0 cable length;

s_1, s_2 cable lengths from lowest point to left and right supports, respectively;

t, t_i time;

T horizontal component of cable force;

$u(t)$ relative displacement response;

$u_1(t)$ relative displacement of lower-frequency connected equipment;

$u_{10}(t)$ relative displacement of lower-frequency stand-alone equipment;

$u_2(t)$ relative displacement of higher-frequency connected equipment;

$u_{20}(t)$ relative displacement of higher-frequency stand-alone equipment;

$\mathbf{u}$ relative displacement vector of connected system;

$\mathbf{u}_n$ relative displacement vector of connected system at n th time step;

w weight per unit length of cable;

x coordinate along a beam;

$\ddot{x}_g(t)$ ground acceleration;

y coordinate along equipment;

y_i coordinate at equipment attachment point;

$z(t)$ generalized coordinate;

α angle of inclination of cable chord with the horizontal;

α_i non-dimensional attachment coordinate;

β interaction parameter; also parameter in numerical integration scheme;

χ damping ratio parameter;

δ variation symbol;

Δ maximum relative displacement between stand-alone equipment items;

$\Delta\mathbf{P}_n^i$ effective residual force at i th iteration and n th time step;

$\Delta\mathbf{u}_n^i$ displacement vector increment at i th iteration and n th time step;

Δt time increment;

$\varepsilon_1, \varepsilon_2$ tolerances;

φ_i component of modal vector;

Φ_i i th modal vector;

$\Phi_{\ddot{x}_g\ddot{x}_g}(\omega)$ power spectral density of ground acceleration process;

γ parameter in numerical integration scheme;

γ_i i th modal participation factor;

κ stiffness ratio parameter;

λ, λ_i eigenvalues;

μ mass ratio parameter;

$\rho(y)$ distributed mass density;

ρ_{ij} cross-modal correlation coefficient;

ω circular frequency;

ω_1 natural circular frequency of lower-frequency equipment;

ω_2 natural circular frequency of higher-frequency equipment;

ω_g parameter of power spectral density function;

$\widetilde{\omega}_i$ modal frequencies;

Ω_i i th modal frequency of the connected system;

$\psi(y)$ displacement shape function,

ψ_i displacement shape function value at i th equipment attachment point;

ζ_1 modal damping ratio of lower-frequency equipment;

ζ_2 modal damping ratio of higher-frequency equipment;

ζ_g parameter of power spectral density function;

$\widetilde{\zeta}_i$ modal damping ratios;

Z_i modal damping ratios of the connected system.

CHAPTER 1
INTRODUCTION

1.1 Introduction

Recent earthquakes in Loma Prieta (1989), Northridge (1995) and Kobe (1996) have once again demonstrated their devastating effects on the built environment in urban centers. The resulting social and economic losses due to these earthquakes have been particularly severe because of the extensive damage experienced by critical lifeline systems, such as transportation networks, gas and water distributions systems, and power transmission and communication networks. This experience has further highlighted the need to strengthen the critical components of these systems so as to assure their functionality during future earthquakes.

An important element within the power transmission network is the electrical substation. This consists of a complex set of interconnected equipment items, such as transformers, circuit breakers, surge arresters, capacitor banks, disconnect switches, etc., many of which support fragile elements such as ceramic bushings or insulators. These equipment items are usually connected to each other through conductor buses or cables. In the event of an earthquake, these connections may induce dynamic interaction between the equipment items. Field investigations during recent earthquakes (Benuska 1990, Hall 1995) have indicated that the dynamic interaction between connected equipment items with dissimilar dynamic characteristics may have contributed significantly to the observed damage. Unfortunately no design guidelines or analysis methods are currently available that account for this effect.

This report aims at developing a thorough understanding of the effect of dynamic interaction on the response of interconnected electrical substation equipment subjected to earthquake ground motions that will lead to practical and effective design rules and guidelines. Towards that end, we develop simple models of interconnected dynamical systems that adequately represent equipment items and their connections in a typical substation. Equipment items are modeled as lumped- or distributed-mass systems with a

single degree of freedom. The connection is modeled either as a linear spring-dashpot or mass-spring-dashpot element, or as a cable. The ground motion is either described as a stochastic process defined in terms of its mean response spectrum or power spectral density, or is a recorded ground motion.

A set of dimensionless measures of seismic interaction are defined by relating the response of each equipment item in the connected system to its stand-alone response. A similar measure is defined for the connecting element. These measures of interaction allow the designer to determine if additional strength should be provided for each equipment item and the connecting element in order to assure its safety in the presence of the interaction effect. They also provide a basis for determining the proper intensity of base motion for qualification tests so as to indirectly account for the interaction effect.

For the linear connecting element, extensive parametric studies are carried out to understand the nature of the interaction effect and to identify the parameters that strongly influence it. The possibilities of adding a damping element or mass to the connecting element in order to reduce the adverse effects of interaction are explored. Also investigated is the influence of the attachment configuration.

The connecting cable is modeled as an ideal cable with no flexural stiffness, but account is made of its extensibility in an approximate manner. The response of the cable-connected system turns out to be strongly nonlinear when the cable is taut. Time history analyses with recorded ground motions are carried out in order to understand the behavior of the system and the influences of various parameters on the interaction effect. The main focus is on determining the required cable slackness to avoid adverse interaction effects. This is achieved by introducing a simple parameter involving the cable geometry and slackness, which is shown to be an acute predictor of the significance of the interaction effect.

A set of guidelines and recommendations for seismic design of interconnected electrical substation equipment items are developed based on the results derived from this study. Recommendations are made for reducing the effect of interaction in systems connected by a linear element or a cable.

1.2 Objectives and Scope

The objective of this study is to gain a deep understanding of the effect of interaction between connected electrical substation equipment items that are subjected to seismic disturbances with the final goal of developing simple and practical guidelines for design of such systems.

Attention in this study is focused on developing sufficiently simple models of equipment items and connecting elements for practical use that incorporate the essential features for accurately quantifying the interaction effect. These models, however, contain limitations that need to be recognized so that the results of this study are used appropriately. Specifically, the models used in this study are limited in the following ways:

a) Equipment items are modeled as linear, single-degree-of-freedom systems. While allowance is made for the mass of the equipment to be distributed, no account is made of contributions to the response arising from higher modes, nor of possible nonlinearities in the behavior of the stand-alone equipment. All energy dissipation mechanisms are idealized as viscous damping.

b) Connecting elements are idealized either as linear spring-dashpot or mass-spring-dashpot elements, or as idealized cables with no flexural stiffness and no inertia effects. In reality, rigid conductor buses with thermal expansion loops may experience hysteretic behavior as a result of plastic deformation in the loop, and flexible cable conductors may possess significant flexural rigidity and possibly inertia effects. These additional effects are not considered in this study. However, a criterion for the condition under which the effect of cable flexural stiffness can be neglected is described in the Appendix.

c) Consideration in this report is restricted to two equipment items with a single connecting element. The behavior of two equipment items with multiple connections, or that of more than two connected equipment items can be considerably different.

d) Consideration is given to only one component of the ground motion. Furthermore, no account is made of site response effects, other than that implicit in the assumed ground response spectrum, or the effect of soil-equipment interaction.

It would appear that this investigation is the first in-depth study of interconnected equipment items subjected to seismic motions. In spite of the limitations enumerated above, we believe the results reported here are applicable to many interconnected equipment items found in electrical substations, and the guidelines and recommendations should be useful in the safer design and analysis of such systems in the future.

1.3 Organization of the Report

In Chapter 2, the equipment items are modeled as lumped- or distributed-mass systems with one degree of freedom. The connecting element is modeled as a linear spring-dashpot element. The equations governing the motion of the 2-degree-of-freedom connected equipment system are derived by use of the method of virtual work. Closed form expressions are derived for the modal properties of this system. Rules for computing the responses of the stand-alone and connected equipment items based on the response spectrum method are described.

Chapter 3 begins with the introduction of three dimensionless response ratios that characterize the effect of interaction in the two equipment items and the connecting element. These ratios relate the response of each equipment and the connecting element to the corresponding responses in the stand-alone equipment configuration. The influences of various system parameters on these ratios are then investigated in a discriminating in-depth manner. The parameters include the stiffness, damping and mass of the connecting element, and the attachment configuration. Attention is also devoted to the influences of various equipment parameters. For the analysis of the damping effect, an approach based on random vibration theory that accounts for the non-classical damping of the system is employed, and for the analysis of the connecting mass effect, a 3-degree-of-freedom connected system is considered. The results in this chapter reveal the major influences on the seismic interaction between two equipment items connected by a linear element.

Chapter 4 deals with equipment items connected by a flexible cable. The chapter begins with an analysis of an ideal inextensible cable with no flexural stiffness. Closed form expressions are derived for various geometric and mechanical properties of the cable. These results are extended to account for the extensibility of the cable in an approximate manner. The equations of motion for cable-connected equipment items are derived and a step-by-step iterative solution algorithm is developed to determine response time-histories for prescribed ground accelerograms. Detailed numerical studies are presented for example systems subjected to five recorded earthquake ground motions with varied characteristics. The main focus is on determining the influence of the cable slackness on the interaction effect. The chapter ends with the introduction and evaluation of a parameter that determines when the interaction effect is significant..

Chapter 5 describes a set of guidelines and recommendation for seismic design and analysis of interconnected equipment items. These are based on the results derived in Chapters 3 and 4. A set of recommendations are presented for reducing the adverse effect of interaction in connected equipment items. For cable-connected equipment items, a simple expression for the minimum required cable slackness to avoid the interaction effect is presented.

A summary of the report and suggestions for further study are presented in Chapter 6.

CHAPTER 2

TWO EQUIPMENT ITEMS CONNECTED BY A LINEAR SPRING-DASHPOT ELEMENT

2.1 Introduction

In this chapter we describe models for characterization of electrical substation equipment. A simple linear, distributed mass, single-degree-of-freedom model is used that is characterized by its effective mass, stiffness and damping values, and its attachment configuration. Subsequently, a model is developed for two equipment items that are connected by a linear element consisting of a spring and a viscous damper. Closed form expressions are derived for the undamped modal properties of the two-degree-of-freedom connected system. These modal properties are used in conjunction with a modal combination rule to formulate expressions for the peak responses of the equipment items in both the stand-alone as well as connected configurations. These results form the basis for the investigation of interaction in the linear connected system that is the topic of Chapter 3.

2.2 Model of Equipment Item

A typical electrical substation contains a large variety of equipment items, e.g., transformers, circuit breakers, capacitor banks, surge arresters, disconnect switches, etc., many of which support fragile elements such as ceramic bushings. Often several different models or designs of the same equipment are stationed at the same location. Furthermore, the interconnections between the different equipment items are varied both in configuration and type. Given this plethora of configurations of equipment types and connections, from the viewpoint of risk assessment or seismic design, it is impractical to develop a detailed model of each equipment item. Furthermore, the information available on each equipment is rather limited and at best may consist of the overall mass and stiffness characteristics, or the fundamental frequency, and a measure of the energy dissipation capacity. Under these conditions, it is expedient to use a simple and general model

that is based on the limited information that is available and which captures the essential dynamic features of the equipment and the effect of its interconnection with other equipment items.

For the purpose of this study, an equipment item is modeled as a single-degree-of-freedom system. When the mass of the equipment is effectively lumped at a single point, then a simple mass-spring-dashpot system, as shown in Figure 2.1a, is an appropriate model. The equation of motion of the equipment item, when it is subjected to a base motion, is then given by

$$m\ddot{u} + c\dot{u} + ku = -m\ddot{x}_g \tag{2.1}$$

where m denotes the mass, c denotes the viscous damping coefficient, k denotes the spring stiffness, $\ddot{x}_g(t)$ denotes the base acceleration, and $u(t)$ denotes the displacement of the mass relative to the base. For a given equipment, the spring stiffness k can be determined by estimating the required force to move the mass in the horizontal direction by a unit amount. Alternatively, if an estimate of the fundamental circular frequency, ω, of the equipment is available, then the stiffness can be computed as $k = m\omega^2$. The viscous damping coefficient c may be determined in terms of the critical damping ratio, ζ, from $c = 2m\omega\zeta$. The value of ζ depends on the energy dissipation capacity of the equipment, including its support system. For typical substation equipment items, the damping ratio is expected to be very small, i.e., of the order of 0.01 to 0.05. As we will see later, this value does not significantly affect the nature of interaction between equipment items.

We will be concerned with attachments to the equipment item. For the model in Figure 2.1a, we assume the attachment is made to the lumped mass so that $u(t)$ represents the horizontal displacement of the attachment point relative to the base.

When the mass of an equipment is distributed over a domain, then a more detailed model is necessary. Such a system can be approximated with a single degree of freedom by employing an appropriate displacement "shape" function. As an example, consider an equipment item modeled as a cantilever beam, as shown in Figure 2.1b, with distributed mass density $\rho(y)$ and flexural stiffness $EI(y)$ along the vertical axis y. Let the dis-

placement of the system in time and space be described approximately by the separable function $u(y,t) = \psi(y)z(t)$, where $\psi(y)$ is the displacement shape function and $z(t)$ is the generalized coordinate that describes the variation of the displacement amplitude in time. Also let y_0 denote the point of an external attachment to the equipment. Using the method of virtual work (see the derivation for a more general system in the following section), one can show that the equation of motion for the displacement $u = u(y_0,t)$ of the equipment at the attachment point, assuming no force is acting at the attachment point, is

$$m\ddot{u} + c\dot{u} + ku = -l\ddot{x}_g \tag{2.2}$$

where

$$m = \int_0^L \rho(y)[\psi(y)]^2 dy \tag{2.3}$$

is the equivalent mass,

$$k = \int_0^L EI(y)[\psi''(y)]^2 dy \tag{2.4}$$

is the equivalent stiffness, and

$$l = \psi(y_0)\int_0^L \rho(y)\psi(y)dy \tag{2.5}$$

is the effective mass producing the external inertia force, where L denotes the length of the beam and $\psi''(x) = d^2\psi(x)/dx^2$. The shape function $\psi(x)$, which must satisfy geometric boundary conditions, may be chosen conveniently as the displacement shape under a suitable static load approximately representing the earthquake effect, e.g., an inverted triangularly distributed load.

It can be seen that (2.1) and (2.2) are identical except for the coefficient of the base acceleration on the right-hand side. The deviation of the quantity l from m is due to two factors: (a) the distributed nature of the mass, (b) the point of attachment. One can easily verify that (2.1) and (2.2) are identical when the mass is lumped at the attachment point

y_0. Note that when the mass is lumped at a point $\tilde{y}$, l will generally be different from m if $y_0 \neq \tilde{y}$.

2.3 Model of Connected System

Consider two equipment items modeled as described in the previous section and connected in the manner shown in Figures 2.2. For the more general model shown in Figure 2.2b, let $u_1(y,t) = \psi_1(y)z_1(t)$ and $u_2(y,t) = \psi_2(y)z_2(t)$ describe the displacements fields of the mass-distributed equipment items, where $\psi_1(y)$ and $\psi_2(y)$ are prescribed displacement shapes for each equipment and $z_1(t)$ and $z_2(t)$ are the corresponding generalized coordinates. Also, let y_1 and y_2 denote the coordinates of the respective attachment points. We assume the connecting element consists of a linear spring of stiffness k_0 and a linear viscous damper with coefficient c_0, which are placed in parallel in a horizontal position, as shown in Figure 2.2b. (If the connecting element is not in a horizontal position, then in what follows k_0 and c_0 must be replaced by $k_0\cos^2\alpha$ and $c_0\cos^2\alpha$, where α denotes the angle of inclination with the horizontal.) To develop the equations of motion by use of the method of virtual work, we consider virtual displacements of the system in the form $\delta u_1 = \psi_1(y)\delta z_1$ and $\delta u_2 = \psi_2(y)\delta z_2$. The equation of dynamic equilibrium when the connected system is subjected to a uni-directional base acceleration $\ddot{x}_g(t)$, neglecting the damping effects, is developed by setting the work done by the inertia and internal forces through the virtual displacements equal to zero. The equation takes the form

$$\begin{aligned}
&\int_0^{L_1}\rho_1(y)\left[\psi_1(y)\ddot{z}_1(t)+\ddot{x}_g(t)\right]\left[\psi_1(y)\delta z_1\right]dy+\int_0^{L_1}EI_1(y)\psi_1''(y)z_1(t)\left[\psi_1''(y)\delta z_1\right]dy\\
&+k_0\left[u_1(y_1,t)-u_2(y_2,t)\right]\left[\psi_1(y_1)\delta z_1-\psi_2(y_2)\delta z_2\right]\\
&+\int_0^{L_2}\rho_2(y)\left[\psi_2(y)\ddot{z}_2(t)+\ddot{x}_g(t)\right]\left[\psi_2(y)\delta z_2\right]dy+\int_0^{L_2}EI_2(y)\psi_2''(y)z_2(t)\left[\psi_2''(y)\delta z_2\right]dy=0
\end{aligned}\qquad (2.6)$$

The above equality must hold for all selections of δz_1 and δz_2. This requires that the coefficient terms for both δz_1 and δz_2 be zero. Employing the abbreviated notations

$u_i = u_i(y_i,t)$ and $\psi_i = \psi_i(y_i)$ and noting that $z_i = u_i / \psi_i$, $i = 1, 2$, the equations governing the displacements at the attachment point are obtained as

$$m_1\ddot{u}_1 + \left[c_1 + c_0\psi_1^2\right]\dot{u}_1 - c_0\psi_1^2\dot{u}_2 + \left[k_1 + k_0\psi_1^2\right]u_1 - k_0\psi_1^2 u_2 = -l_1\ddot{x}_g \tag{2.7a}$$

$$m_2\ddot{u}_2 + \left[c_2 + c_0\psi_2^2\right]\dot{u}_2 - c_0\psi_2^2\dot{u}_1 + \left[k_2 + k_0\psi_2^2\right]u_2 - k_0\psi_2^2 u_1 = -l_2\ddot{x}_g \tag{2.7b}$$

where m_i, k_i and l_i, $i = 1, 2$, are the effective properties defined as in (2.2)-(2.5). In order to account for energy dissipation of the system, damping terms similar to the stiffness terms have been added to the above equations. Note that c_1 and c_2 should be regarded as effective damping coefficients representing the distributed nature of damping in each equipment item.

The equations of motion (2.7) can be cast in the matrix form

$$\mathbf{M}\ddot{\mathbf{u}} + \mathbf{C}\dot{\mathbf{u}} + \mathbf{K}\mathbf{u} = -\mathbf{L}\ddot{x}_g \tag{2.8}$$

where $\mathbf{u} = [u_1 \;\; u_2]^{\mathrm{T}}$ is the vector of displacements of the two attachment points relative to the base, and $\mathbf{M}$, $\mathbf{C}$ and $\mathbf{K}$ are the effective mass, damping and stiffness matrices of the system given by

$$\mathbf{M} = \begin{bmatrix} m_1 & 0 \\ 0 & m_2 \end{bmatrix}, \quad \mathbf{C} = \begin{bmatrix} c_1 + c_0\psi_1^2 & -c_0\psi_1^2 \\ -c_0\psi_2^2 & c_2 + c_0\psi_2^2 \end{bmatrix}, \quad \mathbf{K} = \begin{bmatrix} k_1 + k_0\psi_1^2 & -k_0\psi_1^2 \\ -k_0\psi_2^2 & k_2 + k_0\psi_2^2 \end{bmatrix} \tag{2.9}$$

and $\mathbf{L} = [l_1 \;\; l_2]^{\mathrm{T}}$ is the external inertia force coefficient vector. It is noted that the stiffness and damping matrices are not symmetric. This is a consequence of expressing the equations of motion in terms of the displacements at the attachment points.

Up to this point we have not assigned scales to the displacement shape functions $\psi_1(y)$ and $\psi_2(y)$. From (2.9), it is evident that it is most convenient to scale these functions such that $\psi_1 = \psi_2 = 1$, i.e., scale $\psi_1(y)$ and $\psi_2(y)$ such that these functions attain unit values at the attachment points. With this scaling, the damping and stiffness matrices take the symmetric forms

$$\mathbf{C} = \begin{bmatrix} c_1 + c_0 & -c_0 \\ -c_0 & c_2 + c_0 \end{bmatrix}, \quad \mathbf{K} = \begin{bmatrix} k_1 + k_0 & -k_0 \\ -k_0 & k_2 + k_0 \end{bmatrix}. \tag{2.10}$$

For the conventional lumped-mass system shown in Figure 2.2a, the equations of motion take the same form as in (2.8) with $\mathbf{M}$ as in (2.9) and $\mathbf{C}$ and $\mathbf{K}$ as in (2.10), where m_i, c_i and k_i, $i = 1, 2$, now are the actual mass, damping and stiffness coefficients of the two oscillators. However, in this case $l_1 / m_1 = l_2 / m_2 = 1$. As mentioned earlier, for the more general system in Figure 2.2b, l_1 / m_1 and l_2 / m_2 typically are different from unity, as they depend on the distribution of mass and on the locations of the attachment points. Thus, the difference between the two systems in Figure 2.2a and 2.2b lies in the ratios l_i / m_i, $i = 1, 2$. It is noted that the eigen-properties of the two systems are identical.

For an arbitrary value of c_0, the connected system in general may not have classical modal damping, i.e., its undamped eigen-vectors may not be orthogonal with respect to the damping matrix. Initially, we neglect this effect and carry out analyses using undamped modal properties and approximate modal damping values. For this purpose, in the following section, closed-form expressions are derived for the undamped modal properties of the connected system. Subsequently, the effect of non-classical damping is investigated by random vibration analysis using a non-modal approach. As shown there, approximate modal analysis provides sufficiently accurate results for the system under consideration.

2.4 Modal Properties of the Connected System

In this section we derive closed-form expressions for the undamped modal properties of the 2-DOF connected system. The characteristic equation for the eigenvalues of the undamped connected system defined by the mass matrix in (2.9) and the stiffness matrix in (2.10) is

$$\begin{vmatrix} k_0 + k_1 - \lambda m_1 & -k_0 \\ -k_0 & k_0 + k_2 - \lambda m_2 \end{vmatrix} = 0 \tag{2.11}$$

where $\lambda = \Omega^2$ and Ω denotes the eigen-frequency of the system. Expanding the determinant, one obtains

$$\lambda^2 - \left[\frac{k_0 + k_1}{m_1} + \frac{k_0 + k_2}{m_2}\right]\lambda + \frac{k_0 k_1 + k_0 k_2 + k_1 k_2}{m_1 m_2} = 0 \tag{2.12}$$

It is convenient to define the connecting stiffness ratio

$$\kappa = \frac{k_0}{k_1 + k_2} \tag{2.13}$$

Using this notation and the expressions $\omega_1 = \sqrt{k_1 / m_1}$ and $\omega_2 = \sqrt{k_2 / m_2}$ for the natural frequencies of the stand-alone equipment items, (2.12) can be re-written in the form

$$\lambda^2 - a\lambda + b = 0 \tag{2.14}$$

where a and b are the positive quantities

$$a = (1+\kappa)(\omega_1^2 + \omega_2^2) + \kappa\left(\frac{m_1}{m_2}\omega_1^2 + \frac{m_2}{m_1}\omega_2^2\right) \tag{2.15a}$$

$$b = (1+2\kappa)\omega_1^2\omega_2^2 + \kappa\left(\frac{m_1}{m_2}\omega_1^4 + \frac{m_2}{m_1}\omega_2^4\right) \tag{2.15b}$$

The two roots of this equation are

$$\lambda_1 = \frac{a - \sqrt{a^2 - 4b}}{2} \tag{2.16a}$$

$$\lambda_2 = \frac{a + \sqrt{a^2 - 4b}}{2} \tag{2.16b}$$

The ordered modal frequencies of the connected system are obtained as $\Omega_1 = \sqrt{\lambda_1}$ and $\Omega_2 = \sqrt{\lambda_2}$ with $\Omega_1 \le \Omega_2$.

Let the modal vectors of the connected system, denoted Φ_i, $i = 1,2$, be scaled such that $\Phi_i = [1 \quad \varphi_i]^T$. Note that this vector defines the displacements of the two attachment points for each mode shape. The element φ_i is obtained by solving

$$\begin{bmatrix} k_0 + k_1 - \lambda_i m_1 & -k_0 \\ -k_0 & k_0 + k_2 - \lambda_i m_2 \end{bmatrix} \begin{Bmatrix} 1 \\ \varphi_i \end{Bmatrix} = 0 \tag{2.17}$$

After algebraic manipulations, the solution for φ_i is obtained in the form

$$\varphi_i = -\frac{1 + \dfrac{m_1}{m_2}\dfrac{\omega_1^2}{\omega_2^2}}{1 + \dfrac{m_2}{m_1}\dfrac{\omega_2^2}{\omega_1^2}} \times \frac{1 - (\Omega_i / \omega_1)^2}{1 - (\Omega_i / \omega_2)^2}, \quad i = 1,2 \tag{2.18}$$

It is seen that the modal frequencies and mode shapes of the connected system are fully described in terms of the stand-alone equipment frequencies ω_1 and ω_2, the mass ratio m_1 / m_2, and the connecting element stiffness ratio κ.

To evaluate the response of the system, we need to determine the modal participation factors. For the displacements at the attachment points, the participation factors are defined as (Chopra 1995)

$$\gamma_i = \frac{\Phi_i^{\mathrm{T}} \mathbf{L}}{M_i}, \quad i = 1, 2 \tag{2.19}$$

where

$$M_i = \Phi_i^{\mathrm{T}} \mathbf{M} \Phi_i = m_1 + m_2 \varphi_i^2, \quad i = 1, 2 \tag{2.20}$$

are the modal masses. Using (2.20) in (2.19), we have

$$\begin{aligned} \gamma_i = \frac{\Phi_i^{\mathrm{T}} \mathbf{L}}{M_i} &= \frac{l_1 + l_2 \varphi_i}{m_1 + m_2 \varphi_i^2} \\ &= \frac{\dfrac{l_1}{m_1}\dfrac{m_1}{m_2} + \dfrac{l_2}{m_2}\varphi_i}{\dfrac{m_1}{m_2} + \varphi_i^2}, \quad i = 1, 2 \end{aligned} \tag{2.21}$$

It is evident that the participation factors involve the ratios l_i / m_i, $i = 1, 2$. As mentioned earlier, these ratios depend on the distribution of mass of each equipment and the location of its attachment point.

It is also necessary to determine the modal damping ratios for the connected system. We denote them as Z_1 and Z_2. These ratios are determined from the formula

$$Z_i = \frac{\Phi_i^T \mathbf{C} \Phi_i}{2\Omega_i M_i}, \quad i = 1, 2 \tag{2.22}$$

This approach essentially ignores the contributions of the cross-modal terms $\Phi_i^T \mathbf{C} \Phi_j$, $i \neq j$, which are non-zero when the system is non-classically damped. The specific values for c_1 and c_2 are obtained by assuming damping ratios ζ_1 and ζ_2 for the stand-alone equipment items and using the relation $c_i = 2\omega_i \zeta_i m_i$. A rigorous treatment of the non-classical damping effect is presented in Section 3.4 of Chapter 3.

Before proceeding further, it is worthwhile to examine the special case when the two oscillators have identical frequencies, i.e., $\omega_1 = \omega_2 = \omega$. In that case, the two frequencies of the connected system are

$$\Omega_1 = \omega \tag{2.23a}$$

$$\Omega_2 = \omega \sqrt{1 + \kappa \left(2 + \frac{m_1}{m_2} + \frac{m_2}{m_1} \right)} \tag{2.23b}$$

Substituting these results in (2.18) yields an indefinite result for φ_1 and $\varphi_2 = -m_1 / m_2$. To obtain Φ_1, we invoke the orthogonality of the mode shapes with respect to the mass matrix, which results in $\Phi_1 = [1 \ 1]^T$ and $\Phi_2 = [1 \ -m_1 / m_2]^T$. It is clear that when the two oscillators have identical frequencies, the first mode of the connected system does not involve any interaction between the two oscillators since the corresponding mode shape does not produce any deformation of the connecting spring.

It is also worthwhile to investigate the limiting cases when κ approaches zero and infinity. When $\kappa \to 0$, i.e., a connecting element with negligible stiffness, the connected system becomes a two degree of freedom system with frequencies approaching $\Omega_1 = \omega_1$ and $\Omega_2 = \omega_2$. The corresponding mode shapes in this case approach $\Phi_1 = [1 \ 0]^T$ and $\Phi_2 = [0 \ 1]^T$, respectively. When $\kappa \to \infty$, i.e., an ideally rigid connecting element, the

lower frequency of the connected system approaches $\Omega_1 = \sqrt{(k_1 + k_2)/(m_1 + m_2)}$, whereas the second frequency approaches infinity. In this case, the connected system is equivalent to a system with only one degree of freedom.

Before closing this section, it is worthwhile to numerically examine the frequencies of the connected system. We consider the equipment mass ratios $m_1 / m_2 = 0.5$ and 5, the range of stand-alone equipment frequency ratios $0.1 \leq \omega_1 / \omega_2 \leq 1$, and the connecting element stiffness ratio values $\kappa = 0$, 0.2, 1 and ∞. Note that for the range of frequency ratios considered, equipment 1 has a frequency equal to or lower than the frequency of equipment 2. As mentioned above, the extreme values $\kappa = 0$ and $\kappa = \infty$ correspond to the unattached configuration of the two equipment items and to the case of an ideally rigid connecting element, respectively. The value $\kappa = 0.2$ is likely representative of a typical rigid bus connecting element with a thermal expansion loop, whereas the value $\kappa = 1$ is representative of a connecting element with a large but not unrealistic stiffness.

Figure 2.3 shows plots of the normalized modal frequencies Ω_i / ω_2, $i = 1,2$. Note that the curves for $\kappa = 0$ are equivalent to the frequency ratios ω_1 / ω_2 and ω_2 / ω_2. It can be seen that the fundamental frequency of the connected system, Ω_1, is greater than the stand-alone frequency, ω_1, of the lower frequency equipment item, except at $\omega_1 / \omega_2 = 1$ where it is equal to ω_1. The second modal frequency of the connected system, Ω_2, is always greater than the stand-alone frequency, ω_2, of the higher frequency equipment item. The differences between the frequencies of the connected system and the corresponding frequencies of the stand-alone equipment items grow with increasing stiffness ratio κ. This is expected, since the system becomes stiffer with addition of the connecting spring. The mass ratio m_1 / m_2 appears to have a greater influence on the fundamental frequency of the system than on its second modal frequency. It is evident that the stiffness of the connecting element has a strong influence on the behavior of the connected system.

2.5 Response of the Connected System

Our main interest in this study is to determine the effect of interaction on the restoring force in each equipment item and the force in the connecting element, when the connected system is subjected to a seismic ground motion. Given the shape functions $\psi_1(y)$ and $\psi_2(y)$, the internal forces in the two equipment items are directly proportional to the displacements $u_1(t)$ and $u_2(t)$ of the respective attachment points. Furthermore, the restoring force in the connecting element is proportional to the relative displacement, $u_2(t) - u_1(t)$. Hence, in the following analysis we focus our attention on these displacement responses rather than forces. In Chapter 4, we introduce dimensionless ratios describing the effects of interaction on the two equipment items and the connecting element. Because of the proportionality between the displacement and force responses, these ratios will be the same for the above mentioned forces responses as well.

Initially, we describe the ground motion in terms of the response spectrum. This manner of specification of the ground motion is convenient for seismic analysis of linear systems. In previous studies dealing with the impact of earthquakes on electrical substation equipment, the site-specific response spectrum has been found to correlate well with observed damage (Tsai 1993, Matsuda 1996). Furthermore, for electrical substation equipment, IEEE (1997) design guidelines recommend the use of a particular response spectrum. In a subsequent analysis, we employ a description of the ground motion in terms of a power spectral density in order to investigate the effect of non-classical damping.

By definition, the displacement response spectrum is a function $D(\omega,\zeta)$ representing the maximum absolute displacement of a single-degree-of-freedom oscillator of frequency ω and damping ratio ζ when its base is subjected to the specified ground acceleration $\ddot{x}_g(t)$. The "design" response spectrum specified in codes, such as that in the IEEE (1997) guidelines, is a smooth function representing the mean value of $D(\omega,\zeta)$ over an ensemble of ground motions with specified frequency content, intensity and duration.

The response spectrum can be used to compute the maximum responses in both the connected system as well as the stand-alone equipment items. Let $u_{10}(t)$ and $u_{20}(t)$ denote the displacements at the attachment points of the two equipment items in their stand-alone configurations. The maximum absolute values of these responses are given directly in terms of the response spectrum as

$$\max|u_{i0}(t)| = \frac{l_i}{m_i} D(\omega_i, \zeta_i), \; i = 1, 2 \tag{2.24}$$

where ω_i and ζ_i are the corresponding frequency and damping ratio, respectively. The maximum responses of the connected system, $\max|u_1(t)|$, $\max|u_2(t)|$ and $\max|u_2(t) - u_1(t)|$, as well as the maximum absolute relative displacement between the two stand-alone equipment items, $\max|u_{20}(t) - u_{10}(t)|$, can be determined by use of a modal combination rule. For this purpose, we make use of the CQC modal combination rule (Der Kiureghian 1981). According to this rule, the maximum absolute value of a generic response $u(t)$ of an n-degree-of-freedom linear system is given by

$$\max|u(t)| = \sqrt{\sum_{i=1}^{n}\sum_{j=1}^{n} a_i a_j \rho_{ij} D(\tilde{\omega}_i, \tilde{\zeta}_i) D(\tilde{\omega}_j, \tilde{\zeta}_j)} \tag{2.25}$$

where a_i are effective participation factors, $D(\tilde{\omega}_i, \tilde{\zeta}_i)$ is the displacement response spectrum ordinate associated with the frequency $\tilde{\omega}_i$ and damping ratio $\tilde{\zeta}_i$ of mode i of the system, and ρ_{ij} is the correlation coefficient between the responses of modes i and j. A reasonable approximation for the correlation coefficient is obtained by using a white-noise representation of the input excitation, for which ρ_{ij} is given by (Der Kiureghian 1980)

$$\rho_{ij} = \frac{8\sqrt{\tilde{\zeta}_i \tilde{\zeta}_j}(\tilde{\omega}_i \tilde{\zeta}_j + \tilde{\omega}_j \tilde{\zeta}_i)(\tilde{\omega}_i \tilde{\omega}_j)^{3/2}}{(\tilde{\omega}_i^2 - \tilde{\omega}_j^2)^2 + 4\tilde{\zeta}_j \tilde{\zeta}_i \tilde{\omega}_i \tilde{\omega}_j (\tilde{\omega}_i^2 + \tilde{\omega}_j^2) + 4(\tilde{\zeta}_i^2 + \tilde{\zeta}_j^2)\tilde{\omega}_i^2 \tilde{\omega}_j^2} \tag{2.26}$$

When modes with frequencies higher than the predominant frequency of the ground motion are involved, a more accurate approximation given by Der Kiureghian and Nakamura

(1993), which also involves the shape of the response spectrum, can be used. However, numerical investigations with a large number of example two-degree-of-freedom connected systems established that the simple approximation in (2.26) is sufficiently accurate for the present application. Hence, for the present study we make use of the approximation in (2.26), which, conveniently, involves only the modal frequencies and damping ratios of the system. With this approximation, to evaluate (2.25) for a given response spectrum, we only need to determine $\widetilde{\omega}_i$, $\widetilde{\zeta}_i$ and the effective participation factors a_i, $i = 1, 2$, for each response quantity of interest.

To determine the maximum relative displacement between the two stand-alone equipment items, $\max|u_{20}(t) - u_{10}(t)|$, we consider these items as parts of a single system with two degrees of freedom. Obviously, the modal frequencies are $\widetilde{\omega}_1 = \omega_1$ and $\widetilde{\omega}_2 = \omega_2$, and the modal damping ratios are $\widetilde{\zeta}_1 = \zeta_1$ and $\widetilde{\zeta}_2 = \zeta_2$. Furthermore, one can easily determine that the effective modal participation factors of the system for the response under consideration are $a_1 = -l_1 / m_1$ and $a_2 = l_2 / m_2$. Hence, using (2.24) and (2.25), we have

$$\max|u_{20}(t) - u_{10}(t)| = \sqrt{\max|u_{10}(t)|^2 - 2\rho_{12} \max|u_{10}(t)| \max|u_{20}(t)| + \max|u_{20}(t)|^2} \qquad (2.27)$$

The above simple expression is valuable for design of equipment items to be connected, as it provides an estimate of the maximum relative displacement that can occur in the stand-alone configuration. Obviously, this response measure will have a direct influence on the interaction between the two equipment items. Note that the measure is easily computed, as all quantities on the right-hand side are given in terms of the stand-alone equipment properties. It is worth noting that for the special case $\omega_1 = \omega_2$ and $\zeta_1 = \zeta_2$, i.e., equipment items with identical frequencies and damping ratios, we have $\rho_{12} = 1$ and $\max|u_{20}(t) - u_{10}(t)| = 0$. This shows that equipment items with identical frequencies and damping ratios do not interact if they are connected by a linear spring-dashpot element. For cable-connected equipment items to be investigated in Chapter 4, a more appropriate measure is the maximum relative displacement between the two equipment items defined by

$$\Delta = \max\left[u_{20}(t) - u_{10}(t)\right] \tag{2.28}$$

This quantity can also be computed by (2.27), provided the response spectrum ordinate $D(\omega_i, \zeta_i)$ used in (2.24) is defined as the maximum positive displacement of an oscillator rather than its maximum absolute value, as is commonly done. However, the difference between the two response spectra ordinates normally does not exceed a few percent. Hence, for all practical purposes, Δ can be taken equal to the value computed from (2.27) using the conventional response spectrum. We note that this is a conservative approximation since Δ in general is equal to or smaller than $\max|u_{20}(t) - u_{10}(t)|$.

For the connected system, the modal frequencies and damping ratios are as given in the preceding section, i.e., $\tilde{\omega}_i = \Omega_i$ and $\tilde{\zeta}_i = Z_i$, $i = 1, 2$. Thus, it is only necessary to determine the effective participation factors a_i for each of the response quantities. For each mode, a_i is the product of the modal participation factor γ_i and the response of interest when the system is deformed into its i-th mode shape. For the three response quantities mentioned earlier, these coefficients, for $i = 1, 2$, are

$$a_i = \gamma_i \quad \text{for } \max|u_1(t)| \tag{2.29a}$$

$$= \varphi_i \gamma_i \quad \text{for } \max|u_2(t)| \tag{2.29b}$$

$$= (\varphi_i - 1)\gamma_i \quad \text{for } \max|u_2(t) - u_1(t)| \tag{2.29c}$$

It is evident from (2.18) and (2.21) that a_i are functions only of the ratio ω_1 / ω_2 of the stand-alone equipment frequencies, the mass ratio m_1 / m_2, the ratios l_1 / m_1 and l_2 / m_2, and the connecting element stiffness ratio κ. Using the CQC rule in (2.25), the peak responses of the connected system are obtained in terms of these known system quantities, the modal damping ratios Z_1 and Z_2 obtained from (2.22), and the response spectrum shape $D(\omega, \zeta)$.

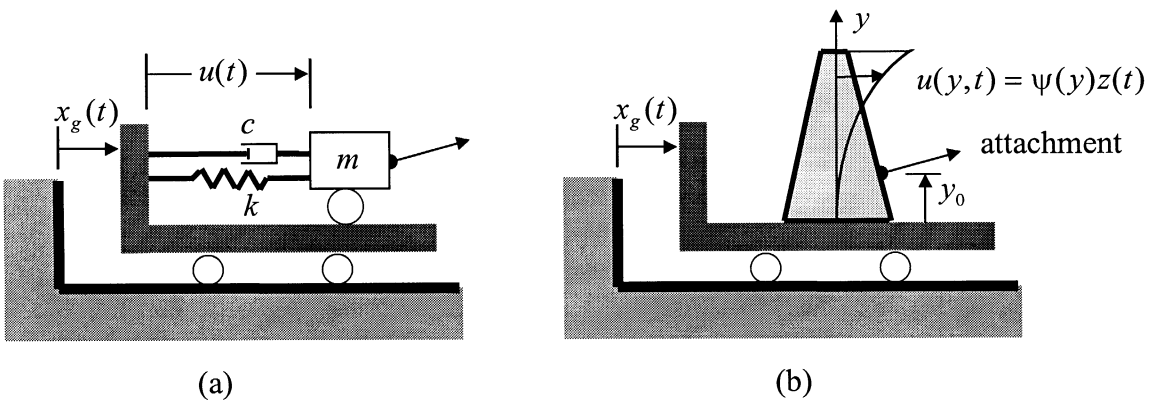

Figure 2.1 Single-degree-of-freedom models of equipment items

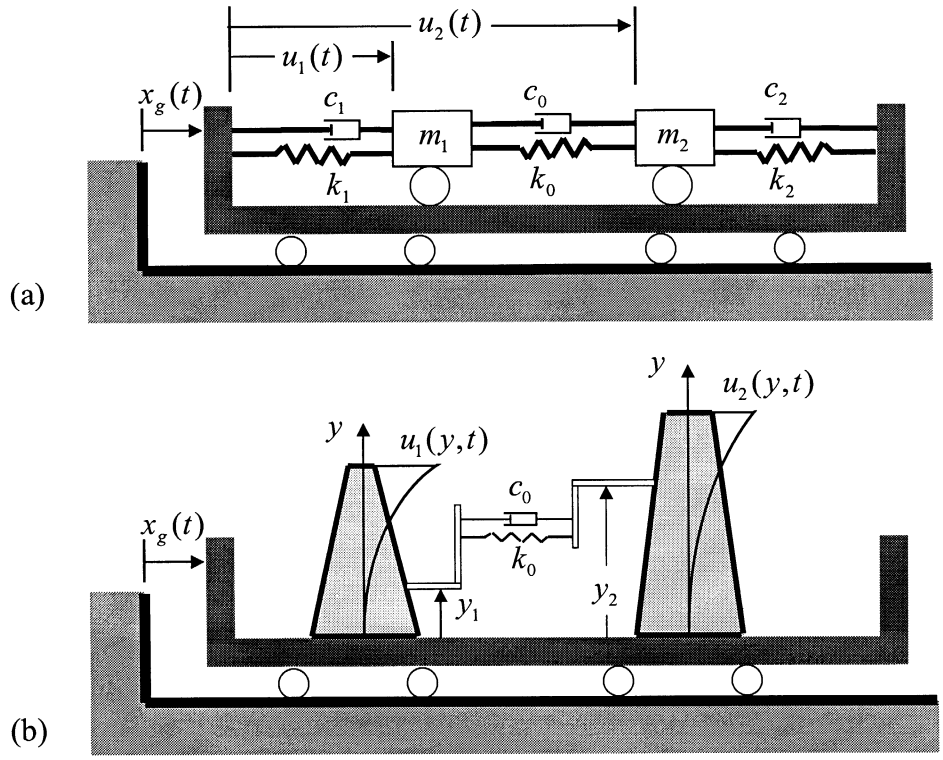

Figure 2.2 Two-degree-of-freedom linear models of connected equipment items

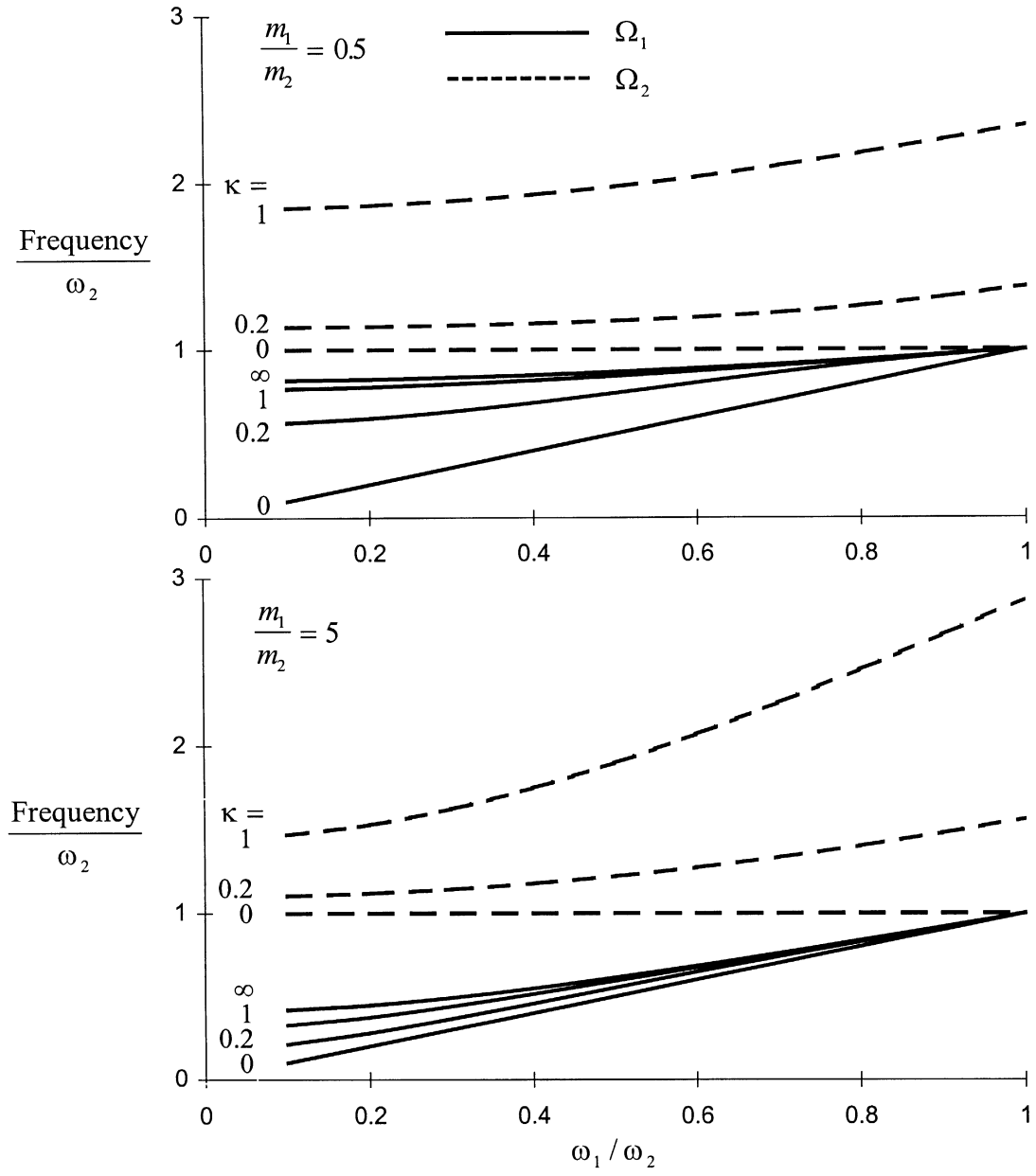

Figure 2.3 Normalized frequencies of the connected system

CHAPTER 3

EFFECT OF INTERACTION IN LINEARLY CONNECTED EQUIPMENT ITEMS

3.1 Introduction

This chapter examines the effect of interaction in two equipment items connected by a linear spring-dashpot or spring-dashpot-mass element. We first introduce three dimensionless response ratios that characterize the effect of interaction on the individual equipment items and on the connecting element. Subsequently, through a set of carefully planned parameter studies, we examine the influences of various key parameters on the interaction effect. Investigated are the influences of the equipment frequencies and mass ratio, the stiffness, damping and mass of the connecting element, and the attachment configuration of the connecting element.

3.2 Response Ratios

In order to evince the effect of interaction in connected equipment items, we relate the peak response of each equipment item in the connected system to the peak response in its stand-alone configuration. For this purpose, we introduce the response ratios

$$R_i = \frac{\max|u_i(t)|}{\max|u_{i0}(t)|}, \quad i = 1,2 \tag{3.1}$$

where $u_i(t)$ is the displacement of the i-th equipment item in the connected system relative to the ground, and $u_{i0}(t)$ is the same response in the stand-alone equipment. The above dimensionless ratios provide measures of the interaction effect in the connected system. A value greater than unity for one of the above response ratios indicates that, on account of the interaction effect, the response of the corresponding equipment item in the connected system is amplified relative to its response in the stand-alone configuration, and a value smaller than unity indicates that it is de-amplified. It is important

to recall that the internal forces in the two equipment items are directly proportional to their displacement responses. Hence, the above ratios are equally applicable to force responses in the two equipment items. Since the peak stand-alone responses are readily available from (2.24), the above ratios provide the kind of information that an engineer would need in order to determine whether the equipment items in the connected system are safe.

For the connecting element, we introduce the response ratio

$$R_0 = \frac{\max|u_2(t) - u_1(t)|}{\max|u_{20}(t) - u_{10}(t)|}. \tag{3.2}$$

The response quantity represented by the denominator of the above ratio is the maximum absolute relative displacement between the two stand-alone equipment items. This quantity is readily available from (2.27). In absence of interaction information, one may tend to use this response quantity to make an estimate of the force acting in the connecting element. The numerator of the ratio represents the actual absolute relative displacement between the two equipment items in the connected system. Recall again that the relative displacement between the two equipment items is proportional to the restoring force acting in the connecting element. Hence, the response ratio R_0 provides the necessary information to determine the peak restoring force in the connecting element from the estimate of that force based on the readily available stand-alone relative displacement response, $\max|u_{20}(t) - u_{10}(t)|$.

In the remainder of this chapter, we investigate the influences of various parameters on the response ratios R_0, R_1 and R_2 for two equipment items connected by a linear spring-dashpot or spring-dashpot-mass element. Unless specified otherwise, the response spectrum shape specified by the IEEE guidelines (1997) is used. Note that the amplitude of this spectrum need not be specified, since it does not affect the above response ratios.

3.3 Effect of Equipment Frequencies, Mass Ratio, and Stiffness of Connecting Element

To investigate the influence of the stiffness of the connecting element on the interaction between the two equipment items, we examine the response ratios R_0, R_1 and R_2 for the values $\kappa = 0.2$, 1 and ∞ of the connecting stiffness ratio. For the other system parameters, we consider the values $m_1 / m_2 = 0.5$ and 5, $\omega_2 = 10\pi$ rad/s and 20π rad/s (= 5 Hz and 10 Hz, respectively), $0.1 \le \omega_1 / \omega_2 \le 1$, $\zeta_1 = \zeta_2 = 0.02$ and 0.05, and $c_0 = 0$. We assume the attachment configuration is such that $l_1 / m_1 = l_2 / m_2$. As mentioned earlier, the extreme value $\kappa = \infty$ represents an ideally rigid connecting element; $\kappa = 0.2$ represents a typical case, and $\kappa = 1$ represents the case of a large but not unrealistic value of the connecting stiffness. Two values of ω_2 are selected to examine the effect of a change in the absolute values of the equipment frequencies. By shifting the modal frequencies relative to a fixed response spectrum shape, in essence, we obtain an understanding of the influence of the frequency content of the ground motion on the interaction between the two equipment items. Note that for the range of frequency ratios considered, equipment 1 always has a frequency lower than or equal to the frequency of equipment 2.

Figures 3.1 and 3.2 show plots of R_0, R_1 and R_2 for $\omega_2 = 10\pi$ rad/s and $\omega_2 = 20\pi$ rad/s, respectively, for both values of the mass ratio and for the damping ratios $\zeta_1 = \zeta_2 = 0.02$. Figure 3.3 shows the response ratio R_2 for $\omega_2 = 20\pi$ rad/s and $\zeta_1 = \zeta_2 =$ 0.02 and 0.05. The following noteworthy observations can be made from the results reported in these figures:

a) At $\omega_1 / \omega_2 = 1$, i.e., equipment items with identical frequencies, $R_1 = R_2 = 1$, regardless of the values of κ, m_1 / m_2 and ω_2. This is because, for identical frequencies, the two equipment items have identical displacements and, therefore, the connecting element is not activated. In this special case there is no interaction effect. It is noted that the response ratio R_0 has an indefinite value for this special case, as both the numerator and denominator in (3.2) are zero. The limits shown in Figures 3.1 and 3.2 were obtained numerically.

b) The response ratio R_0, which describes the ratio of the deformation in the connecting element to the maximum separation of the two stand-alone equipment items, remains smaller than unity, typically smaller than 0.6, for all cases. This ratio tends to decrease with increasing connecting stiffness ratio κ, and increase with increasing mass ratio m_1 / m_2. The trend with the frequency ratio ω_1 / ω_2, however, is not monotonic, as the ratio tends to assume its largest value for an intermediate frequency ratio between 0.1 and 1. It appears that the connecting element can be safely designed for less than 60% of the maximum separation between the stand-alone equipment items for a wide range of practical situations.

c) For all values of κ, m_1 / m_2 and $\omega_1 / \omega_2 < 1$, interaction de-amplifies the response of the lower frequency equipment, i.e., $R_1 < 1$, and amplifies the response of the higher frequency equipment, i.e., $R_2 > 1$. These effects grow with increasing κ and tend to "saturate" near the limiting case $\kappa = \infty$. Increasing the mass ratio m_1 / m_2 for fixed values of the other parameters tends to decrease the effect of interaction on the lower frequency equipment item but increases the same effect on the higher frequency equipment item. The effect of interaction also generally grows with increasing separation between the two frequencies. Exceptions are evident in R_1 over narrow bands of frequency. These are due to sharp changes in the shape of the IEEE response spectrum at these frequencies. It is noted that for the large but not unrealistic value $\kappa = 1$ of the connecting stiffness ratio, the amplification in the response of the higher frequency equipment can be as large as a factor of 8 for $m_1 / m_2 = 5$ and $\omega_1 / \omega_2 = 0.1$. This shows that interaction between connected equipment items can have a severe adverse effect on the equipment item with higher frequency.

d) The effect of the frequency content of the ground motion, as characterized by the shape of the IEEE response spectrum, on the response ratios R_0, R_1 and R_2 can be determined by comparing the curves in Figures 3.1 and 3.2, which are respectively for $\omega_2 = 10\pi$ rad/s and $\omega_2 = 20\pi$ rad/s, for the corresponding values of κ and m_1 / m_2. One can show that, for a fixed frequency ratio ω_1 / ω_2, these response ratios are en-

tirely independent of the absolute values of the individual equipment frequencies if the input excitation is a white noise process. Therefore, the deviations between the corresponding curves in Figures 3.1 and 3.2 can be interpreted as the influence of the non-white frequency content inherent in the IEEE spectrum. It is evident from this comparison that the response ratios R_0, R_1 and R_2 are at most moderately dependent on the shape of the spectrum, or, equivalently, on the positions of the equipment frequencies ω_1 and ω_2 relative to the spectrum. This is undoubtedly due to the definition of these quantities as response ratios rather than absolute responses, as well as the fact that the IEEE response spectrum represents a wide-band excitation. It follows that quantitative results derived for R_0, R_1 and R_2 for a given ω_1 / ω_2 are approximately applicable to a wide range of equipment items with the same ratio of stand-alone frequencies, as long as the excitation is not overly narrow band.

e) To investigate the effect of the damping ratio of the individual equipment items, Figure 3.3 compares the response ratio R_2 for the damping ratios $\zeta_1 = \zeta_2 = 0.02$ (solid or dashed lines) and $\zeta_1 = \zeta_2 = 0.05$ (square marks) for the case with $\omega_2 = 20\pi$ rad/s. In both cases, the connecting element is assumed to have no damping, i.e., $c_0 = 0$. It can be seen that the equipment damping values have virtually no influence on the response ratio R_2. Although not shown here, the same is true for response ratios R_0 and R_1. Of course the individual equipment damping values influence the absolute responses in both the stand-alone and connected systems. However, these influences are similar so that the response ratios for all practical purposes remain invariant.

3.4 Effect of Damping of the Connecting Element

As mentioned before, for an arbitrary value of the damping coefficient c_0, the connected system shown in Figure 2.2 and described by (2.8)-(2.10) in general is not classically damped. In a non-classically damped system, the eigen-vectors are complex valued. The conventional response spectrum method described in Section 2.5 is not applicable to such a system without making an approximation. Although a response spectrum method for non-classically damped systems is available (Igusa and Der Kiureghian 1985), it is more

convenient to investigate the influence of c_0 and the non-classical damping effect by random vibration analysis. For this purpose, we compute and compare the exact values of R_0, R_1 and R_2 for selected values of c_0 with results obtained by approximate modal analysis using damping ratios in (2.22). The input ground acceleration is considered to be a stationary, filtered white-noise process defined by the Kanai-Tajim power spectral density function (Clough and Penzien 1993).

For stationary random vibration analysis, we need to determine the frequency response function for each response quantity of interest. The frequency response functions for the connected system are obtained by finding the steady-state solution of (2.8) for $\ddot{x}_g(t) = \exp(\mathrm{i}\omega t)$. The result, using the damping and stiffness matrices in (2.10), is

$$\mathbf{u}_{\text{steady state}}(\omega) = -\mathbf{H}(\omega)\mathbf{L}\exp(\mathrm{i}\omega t) \tag{3.3}$$

where

$$\begin{aligned}\mathbf{H}(\omega) &= (-\omega^2\mathbf{M} + \mathrm{i}\omega\mathbf{C} + \mathbf{K})^{-1} \\ &= \begin{bmatrix} -\omega^2 m_1 + \mathrm{i}\omega(c_0 + c_1) + k_0 + k_1 & -\mathrm{i}\omega c_0 - k_0 \\ -\mathrm{i}\omega c_0 - k_0 & -\omega^2 m_2 + \mathrm{i}\omega(c_0 + c_2) + k_0 + k_2 \end{bmatrix}^{-1} \\ &= \frac{1}{\Delta}\begin{bmatrix} -\omega^2 m_2 + \mathrm{i}\omega(c_0 + c_2) + k_0 + k_2 & \mathrm{i}\omega c_0 + k_0 \\ \mathrm{i}\omega c_0 + k_0 & -\omega^2 m_1 + \mathrm{i}\omega(c_0 + c_1) + k_0 + k_1 \end{bmatrix}\end{aligned} \tag{3.4}$$

$$\Delta = \left[-\omega^2 m_1 + \mathrm{i}\omega(c_0 + c_1) + k_0 + k_1\right]\left[-\omega^2 m_2 + \mathrm{i}\omega(c_0 + c_2) + k_0 + k_2\right] - (\mathrm{i}\omega c_0 + k_0)^2 \tag{3.5}$$

and $\mathrm{i} = \sqrt{-1}$. The elements of the vector $-\mathbf{H}(\omega)\mathbf{L}$ are the frequency-response functions of the attachment point displacements $u_1(t)$ and $u_2(t)$ of the connected system. We denote these as $H_{u_1}(\omega)$ and $H_{u_2}(\omega)$, respectively. For the relative displacement response, $u_2(t) - u_1(t)$, the corresponding frequency response function is $H_{u_2-u_1}(\omega) = H_{u_2}(\omega) - H_{u_1}(\omega)$.

For the stand-alone equipment responses $u_{10}(t)$ and $u_{20}(t)$, the frequency response functions are obtained as steady-state solutions of (2.2) for $\ddot{x}_g(t) = \exp(\mathrm{i}\omega t)$. The result is

$$H_{u_{i0}}(\omega) = -\frac{l_i}{m_i}\frac{1}{\omega_i^2 - \omega^2 + 2i\zeta_i\omega_i\omega}, \quad i = 1,2 \tag{3.6}$$

For the response $u_{20}(t) - u_{10}(t)$, the frequency response function is given by $H_{u_{20}-u_{01}}(\omega) = H_{u_{20}}(\omega) - H_{u_{10}}(\omega)$.

For the ground acceleration, we consider a stationary, filtered white-noise process defined by the well known Kanai-Tajimi power spectral density (Clough and Penzien 1993)

$$\Phi_{\ddot{x}_g\ddot{x}_g}(\omega) = \frac{\omega_g^4 + 4\zeta_g^2\omega_g^2\omega^2}{(\omega_g^2 - \omega^2)^2 + 4\zeta_g^2\omega_g^2\omega^2}\Phi_0 \tag{3.7}$$

The parameters ω_g and ζ_g of this model control the predominant frequency and band-width of the process, respectively, and are related to the properties of the local site. For the present analysis, we use $\omega_g = 5\pi$ rad/s and $\zeta_g = 0.6$, which are appropriate for firm ground. The parameter Φ_0 is related to the intensity of the ground motion; however, it need not be specified for the subsequent analysis of the response ratios.

Since the mean of a peak stationary process is approximately proportional to its root-mean-square (rms) value (Der Kiureghian 1980), it is convenient in the present analysis to define the response ratios R_0, R_1 and R_2 in terms of the rms responses of the connected and stand-alone equipment systems instead of the peak values. Hence, for the analysis in this section, we define the response ratios as

$$R_i = \frac{\text{rms}[u_i(t)]}{\text{rms}[u_{i0}(t)]}, \quad i = 1,2 \tag{3.8}$$

$$R_0 = \frac{\text{rms}[u_2(t) - u_1(t)]}{\text{rms}[u_{20}(t) - u_{10}(t)]} \tag{3.9}$$

The rms responses are computed from the generic expression

$$\text{rms}[u(t)] = \sqrt{\int_{-\infty}^{+\infty} |H_u(\omega)|^2 \Phi_{\ddot{x}_g\ddot{x}_g}(\omega) d\omega} \tag{3.10}$$

where $u(t)$ represents any of the responses $u_1(t)$, $u_2(t)$ or $u_2(t)-u_1(t)$ of the connected system, or the responses $u_{10}(t)$, $u_{20}(t)$ or $u_{20}(t)-u_{10}(t)$ of the stand-alone system, and $H_u(\omega)$ denotes the corresponding frequency response function.

In order to investigate the effect of the damping of the connecting element, we introduce the dimensionless parameter

$$\chi = \frac{c_0}{c_1 + c_2} \tag{3.11}$$

This parameter relates the viscous damping coefficient of the connecting element to the sum of the viscous damping coefficients of the two stand-alone equipment items. The damping of the connecting element may arise from material damping, friction at the connections, or hysteretic behavior of the connecting element, e.g., of the thermal expansion loop in a rigid bus. Although these energy dissipation mechanisms are not viscous in nature, for the purpose of the present study a simple viscous damping model is sufficient. When the energy dissipation mechanism arises from material damping or friction at the connections, c_0 would tend to be small in relation to c_1 and c_2 and χ would have a small value. However, when the energy dissipation mechanism arises from hysteretic behavior of the connecting element or its parts, e.g., the thermal expansion loop in a rigid bus, then c_0 may have a larger value, possibly of the same order as c_1 and c_2. Furthermore, it is possible to envision a dashpot specifically placed between the two equipment items to dissipate energy. In the following, we investigate the beneficial effect of such a connecting damping element to reduce the adverse effect of interaction.

Figure 3.4 shows plots of R_1 and R_2 for $m_1/m_2 = 2$, $\omega_2 = 20\pi$ rad/s, $0.1 \le \omega_1/\omega_2 \le 1$, $\zeta_1 = \zeta_2 = 0.02$, $\kappa = 0.5$ and $\chi = 0$, 1 and 10. The attachment configuration is assumed to be such that $l_1/m_1 = l_2/m_2$. For each value of χ two sets of curves are shown. The solid curves are the exact results computed by use of the equations derived earlier in this section. The dashed curves are the approximate results obtained by modal random vibration analysis using the approximate damping ratios in (2.22). As mentioned earlier, the latter analysis neglects the fact that the undamped mode shapes of the connected system

are not orthogonal with respect to the damping matrix. The value $\chi = 0$ corresponds to a connecting element with no or negligible damping and is the case considered in all the analyses in the preceding and subsequent sections. For this case, the approximate modal damping ratios computed from (2.22) are in the range 0.007-0.020, depending on the values of m_1 / m_2, κ and ω_1 / ω_2. The case $\chi = 1$ corresponds to a connecting element that has a damping coefficient similar in magnitude to the damping coefficients of the individual equipment items. As mentioned earlier, this value might be appropriate for certain rigid-bus conductors that include thermal expansion loops that experience plastic deformation during the earthquake. For this value of χ, the approximate modal damping ratios computed from (2.22) are in the range 0.015-0.105, depending on the values of m_1 / m_2, κ and ω_1 / ω_2. The case $\chi = 10$ corresponds to a connecting element that has a damping coefficient one order of magnitude larger than the damping coefficients of the individual equipment items. Such a value might be appropriate if special damping devices are added to the connecting element. Our aim from considering this case is to investigate whether such a device would have a significant beneficial effect for the connected equipment items. For this case, the approximate modal damping ratios computed from (2.22) are in the range 0.02-0.95, depending on the values of m_1 / m_2, κ and ω_1 / ω_2. The following noteworthy observations can be derived from the results in Figure 3.4:

a) For small damping of the connecting element, the effect of non-classical damping in the connected system is insignificant. This is evident from the fact that the solid and dashed lines in Figure 3.4 virtually coincide for small values of χ. This verifies the accuracy of the response spectrum analyses performed in the preceding and subsequent sections that assume classical damping and employ the undamped mode shapes of the connected system.

b) Increasing the damping of the connecting element significantly reduces the amplification in the response of the higher frequency equipment item that is induced by the interaction effect. This damping also tends to further de-amplify the response of the lower frequency equipment item relative to its stand-alone response. Whether or not

damping values in the connecting element as high or higher than the damping in the individual equipment items can be implemented is an issue that is left to a future study.

3.5 Effect of Mass of the Connecting Element

The previous analyses assumed that the mass of the connecting element had a negligible influence on the response of the connected system. In this section, we investigate the validity of this assumption. Furthermore, we wish to investigate the possibility of adding a mass to the connecting element in order to diminish the adverse effect of interaction on the higher frequency equipment item.

To investigate the effect of the mass of the connecting element, we investigate the 3-degree-of-freedom system shown in Figure 3.5, which consists of the two equipment items modeled as single-degree-of-freedom systems with assigned displacement shape functions, and a connecting element modeled as a spring-dashpot-mass element. The mass m_0 may represent an equivalent lumped mass for a connecting element with distributed mass, e.g., a rigid or flexible bus, or it may represent an actual lumped mass placed on the connecting element. Note that the stiffness and damping elements on each side of this mass are selected in such a manner that when $m_0 \to 0$ the system in Figure 3.5 becomes equivalent to the system in Figure 2.2b. For the analysis in this section, we introduce the dimensionless mass parameter

$$\mu = \frac{m_0}{m_1 + m_2} \tag{3.12}$$

The analyses in the preceding sections were for systems with $\mu = 0$.

Let $u_0(t)$ denote the displacement of the mass m_0 relative to the ground. The equations of motion for the 3-degree-of-freedom system in Figure 3.5 are formally the same as (2.7) with $\mathbf{u} = [u_0 \;\; u_1 \;\; u_2]^T$, $\mathbf{L} = [m_0 \;\; l_1 \;\; l_2]^T$ and the mass, damping and stiffness matrices given by

$$\mathbf{M}=\begin{bmatrix} m_0 & 0 & 0 \\ 0 & m_1 & 0 \\ 0 & 0 & m_2 \end{bmatrix},\quad \mathbf{C}=\begin{bmatrix} 4c_0 & -2c_0 & -2c_0 \\ -2c_0 & 2c_0+c_1 & 0 \\ -2c_0 & 0 & 2c_0+c_2 \end{bmatrix},\quad \mathbf{K}=\begin{bmatrix} 4k_0 & -2k_0 & -2k_0 \\ -2k_0 & 2k_0+k_1 & 0 \\ -2k_0 & 0 & 2k_0+k_1 \end{bmatrix} \tag{3.12}$$

where it has been assumed that the equipment displacement shape functions are scaled to have unit values at the attachment points. Determination of the modal properties of this system requires the solution of a bi-cubic equation. While closed-form expressions can be derived, they are too complex to provide insight into the behavior of the system. Hence, we carry out numerical calculations for this system.

We first examine the effect of a small connecting element mass on the response ratios R_1 and R_2. Figure 3.6 shows plots of these response ratios for $m_1/m_2=2$, $\omega_2=20\pi$ rad/s, $0.1\le\omega_1/\omega_2\le 1$, $\zeta_1=\zeta_2=0.02$, $\kappa=0.5$, $c_0=0$, and $\mu=0$, 0.1 and 0.2. The attachment configuration is assumed to be such that $l_1/m_1=l_2/m_2=1$. The input excitation is defined by the IEEE response spectrum. It can be seen that increasing the mass of the connecting element amplifies the responses of both equipment items. However, the amplifications are relatively modest as long as μ remains small. For the higher frequency equipment item, the amplification due to the mass of the connecting element appears to be independent of the frequency of the lower frequency equipment item. For the lower frequency equipment item, the amplification in the response due to the mass of the connecting element is greatest when ω_1 approaches ω_2. For such values, the response ratio R_1 becomes greater than unity, indicating an amplification in the response of the lower frequency equipment item relative to its stand-alone response. However, this amplification is not significant for realistic values of the connecting element mass (e.g., it is only a factor of 1.32 for $\mu=0.2$) and should not be cause for serious concern.

Next, we explore the possibility of using the mass m_0 of the connecting element as a tuned-mass damper to reduce the effect of interaction between the two equipment items. Considering the frequency $\omega_0=\sqrt{4k_0/m_0}$ of the connecting element when the equipment masses m_1 and m_2 are fixed, we examine two cases: (a) connecting element tuned

to equipment 1, i.e., $\omega_0 = \omega_1$, and (b) connecting element tuned to equipment 2, i.e., $\omega_0 = \omega_2$. One can easily show that these cases correspond to the mass ratios

$$\mu_1 = 4\kappa \frac{\frac{m_1}{m_2} + \left(\frac{\omega_2}{\omega_1}\right)^2}{\frac{m_1}{m_2} + 1} \quad \text{and} \quad \mu_2 = 4\kappa \frac{\left(\frac{\omega_1}{\omega_2}\right)^2 \frac{m_1}{m_2} + 1}{\frac{m_1}{m_2} + 1} \tag{3.13}$$

respectively. Numerical investigations reveal, however, that a reduction in the response due to the effect of tuned-mass damping occurs only when κ is small. For example, Figure 3.7 shows the response ratios R_1 and R_2 as a function of μ for the parameter values $m_1 / m_2 = 2$, $l_1 / m_1 = l_2 / m_2 = 1$, $\omega_2 = 20\pi$ rad/s, $\omega_1 / \omega_2 = 0.5$ and 1, $\kappa = 0.02$, $\zeta_1 = \zeta_2 = 0.02$, and $c_0 = 0$. Unlike the steady increase in the response ratios R_1 and R_2 with μ observed in Figure 3.6, the curves here do not show monotonic behavior. For $\omega_1 / \omega_2 = 0.5$, a dip in the curve for R_2 appears around $\mu = 0.045$, which nearly coincides with the value $\mu_2 = 0.04$ computed from (3.13). This is the tuned-mass damper effect of the connecting mass on the higher frequency equipment item. The corresponding value for the lower frequency equipment item from (3.13) is $\mu_1 = 0.16$. Indeed, the curve for the response ratio R_1 for $\omega_1 / \omega_2 = 0.5$ shows a decreasing trend for μ around 0.16. For $\omega_1 / \omega_2 = 1$, (3.13) yields $\mu_1 = \mu_2 = 0.08$. The curve for R_1 in Figure 3.7 for this frequency ratio shows a shallow dip, whereas the curve for R_2 shows a slowdown in the rate of increase. We note, however, that all these reductions in the response due to the tuned-mass damper effect are relatively insignificant, and that they occur at small values of κ for which the interaction effect between the two equipment items is not of seriously detrimental nature. Hence, we find the idea of adding a mass to the connecting element to act as a tuned-mass damper not to be an effective design strategy.

3.6 Effect of Attachment Configuration

When the attachment point on either equipment item is different from the point of its effective lumped mass, the corresponding l_i / m_i ratio is different from unity. While the expressions for the eigen-properties of the system remain unchanged, the response ratios

R_0, R_1 and R_2 are affected on account of the dependence of the modal participation factors (2.21) on l_i / m_i, $i = 1, 2$. It turns out that, for the linear 2-degree-of-freedom model in Figure 2.2b, the response ratios remain invariant for any $l_1 / m_1 = l_2 / m_2$. This happens because the same scale factor applies to both the connected and stand-alone systems. It follows that the attachment configuration has an influence on the response ratios only when $l_1 / m_1 \neq l_2 / m_2$. This effect can be investigated by computing the response ratios R_0, R_1 and R_2 by varying l_1 / m_1 and l_2 / m_2. However, it is more revealing to carry out calculations with a specific system in mind, as described below.

Consider the system shown in Figure 3.8, which consists of two rigid bars with uniform mass distributions, restrained by two linear torsional springs at their bases, and connected by a linear spring-dashpot element at attachment points $y_1 = \alpha_1 L_1$ and $y_2 = \alpha_2 L_2$, where $0 < \alpha_1, \alpha_2 \leq 1$. For rigid bars, the displacement shapes are $\psi_1(y) = y / (\alpha_1 L_1)$ and $\psi_1(y) = y / (\alpha_1 L_1)$, which are scaled to have unit amplitudes at the attachment points. Using (2.3) and (2.5), one obtains $m_i = \rho_i L_i / (3\alpha_i^2)$ and $l_i = \rho_i L_i / (2\alpha_i)$, $i = 1, 2$, where ρ_i is the mass per unit length of bar i. It follows that $l_i / m_i = 3\alpha_i / 2$, $i = 1, 2$.

Figure 3.9 shows plots of the response ratios R_1 and R_2 for $m_1 / m_2 = 2$, $\omega_2 = 20\pi$ rad/s, $0.1 \leq \omega_1 / \omega_2 \leq 1$, $\zeta_1 = \zeta_2 = 0.02$, $\kappa = 0.5$, $c_0 = 0$ and the following attachment configurations: $\alpha_1 = \alpha_2 = 2/3$, i.e., attachment points at 2/3 the length of each equipment, which results in $l_1 / m_1 = l_2 / m_2 = 1$ (solid lines); $\alpha_1 = 1$ and $\alpha_2 = 1/3$, i.e., attachment points at top of equipment 1 and 1/3 the length of equipment 2, which results in $l_1 / m_1 = 3/2$ and $l_2 / m_2 = 1/2$ (dashed lines); and $\alpha_1 = 1/3$ and $\alpha_2 = 1$, i.e., attachment points at 1/3 the length of equipment 1 and at top of equipment 2, which results in $l_1 / m_1 = 1/2$ and $l_2 / m_2 = 3/2$ (dotted lines). It is noted that the solid curves here apply to any attachment configuration such that $\alpha_1 = \alpha_2$, including the case when the attachments are at the top of both bars.

It is evident from Figure 3.9 that the attachment configuration of the connecting element can have a dramatic influence on the response ratios R_1 and R_2, particularly on the ratio R_2 for the higher frequency equipment item. It is clear that the response ratio for an equipment item increases when its attachment point is moved towards its base, and it decreases when the attachment point is moved towards its top. Hence, attaching the connecting element near the base of the higher frequency equipment item would produce the most adverse interaction effect. It is also worth noting that, depending on the attachment configuration, the interaction effect can actually amplify the response of the lower frequency equipment item as well (see the dotted curve for R_1 near $\omega_1 / \omega_2 = 1$, where R_1 is greater than unity). However, this response amplification is no where as critical as the amplification of the higher frequency equipment response.

In real systems, the attachment points on equipment items are most often dictated by restrictions related to functionality of the system, such as clearance for electrical conductors. As a result, from the viewpoint of mitigating seismic effects, one may not have a real choice in the location of attachment points other than those dictated by the functionality requirements.

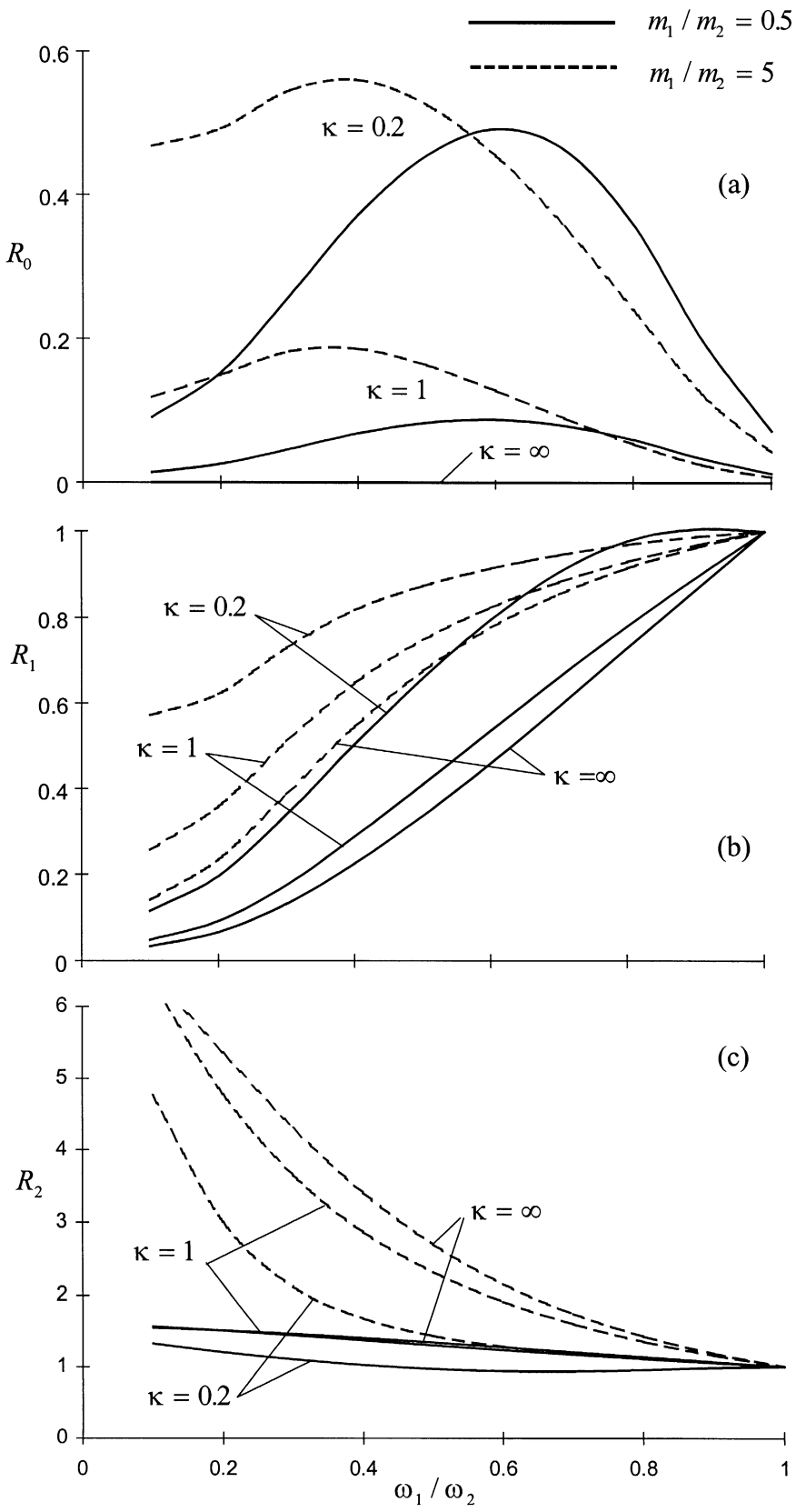

Figure 3.1 Response ratios for connecting element for $l_1 / m_1 = l_2 / m_2$, $\omega_2 = 10\pi$ rad/s, $\zeta_1 = \zeta_2 = 0.02$ and $c_0 = 0$, based on the IEEE spectrum

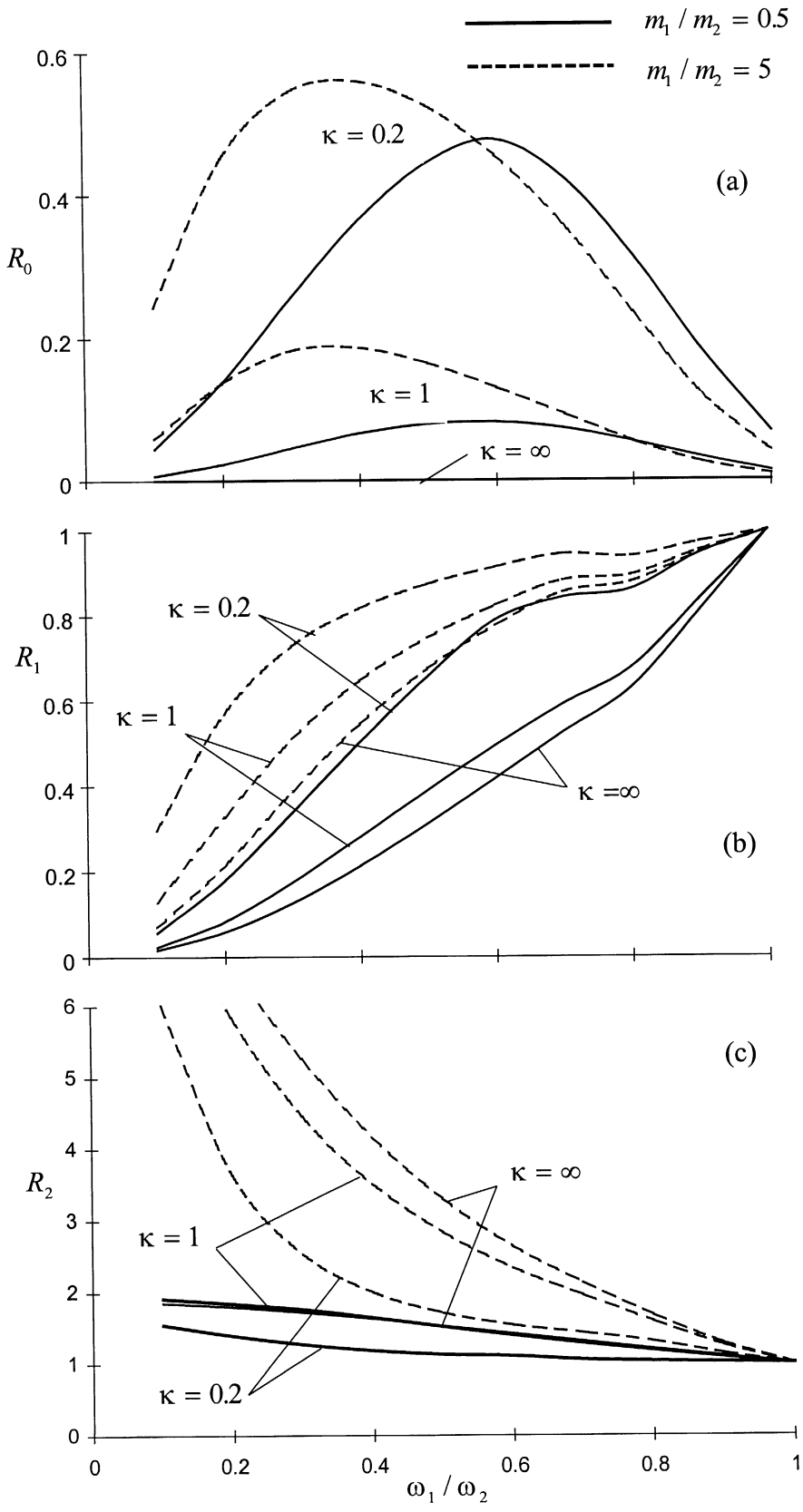

Figure 3.2 Response ratios for connecting element for $l_1 / m_1 = l_2 / m_2$, $\omega_2 = 20\pi$ rad/s, $\zeta_1 = \zeta_2 = 0.02$ and $c_0 = 0$, based on the IEEE spectrum

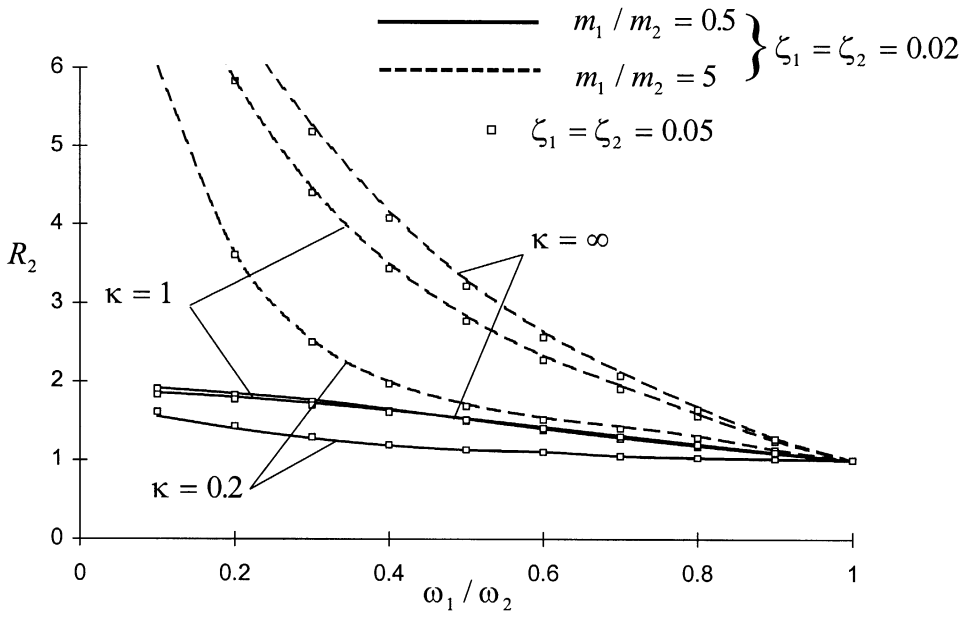

Figure 3.3 Effect of damping of equipment items on response ratio R_2 for $l_1 / m_1 = l_2 / m_2$, $\omega_2 = 20\pi$ rad/s and $c_0 = 0$, based on the IEEE Spectrum

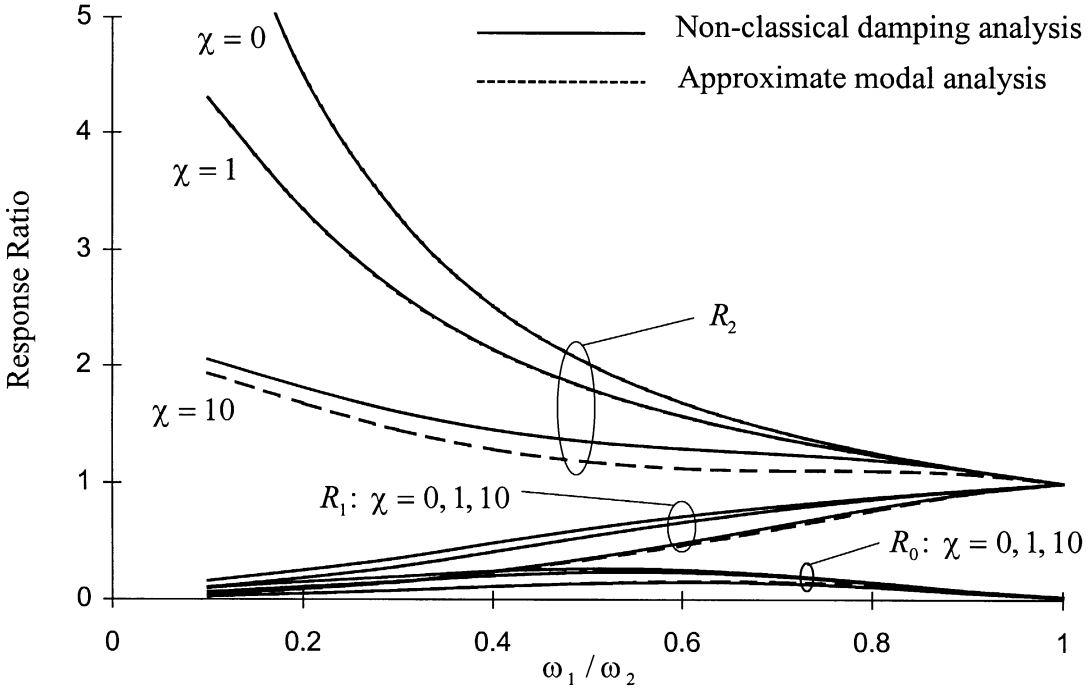

Figure 3.4 Effect of damping of connecting element on response ratios for $m_1 / m_2 = 2$, $l_1 / m_1 = l_2 / m_2$, $\omega_2 = 20\pi$ rad/s, $\kappa = 0.5$ and $\zeta_1 = \zeta_2 = 0.02$, based on the Kanai-Tajimi spectrum

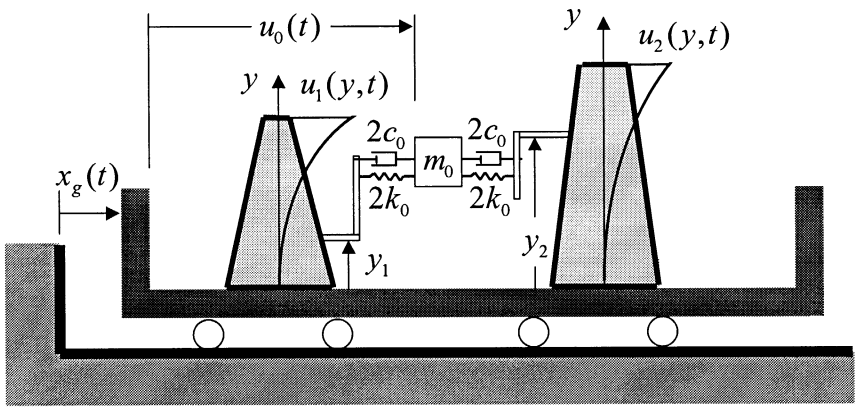

Figure 3.5 Three-degree-of-freedom model of connected system with mass of the connecting element

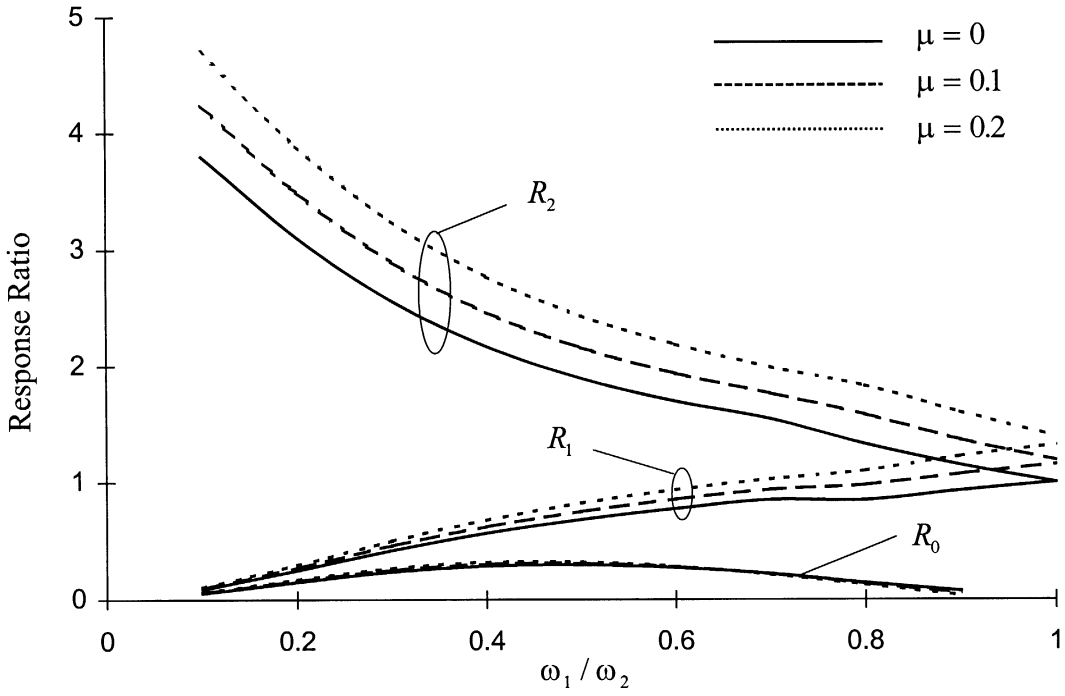

Figure 3.6 Effect of mass of connecting element on response ratios for $m_1 / m_2 = 2$, $l_1 / m_1 = l_2 / m_2$, $\omega_2 = 20\pi$ rad/s, $\zeta_1 = \zeta_2 = 0.02$, $\kappa = 0.5$ and $c_0 = 0$, based on the IEEE spectrum

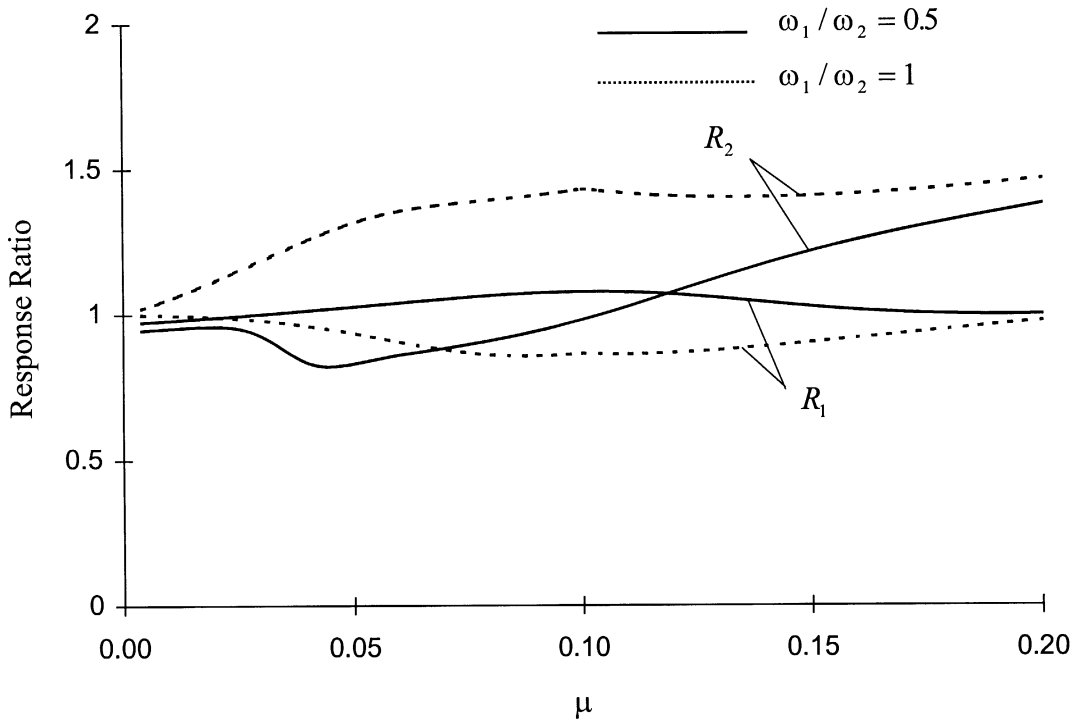

Figure 3.7 Tuned-mass damper effect of the connecting element on response ratios R_1 and R_2 for $m_1 / m_2 = 2$, $l_1 / m_1 = l_2 / m_2$, $\omega_2 = 20\pi$ rad/s, $\zeta_1 = \zeta_2 = 0.02$, $\kappa = 0.02$ and $c_0 = 0$, based on the IEEE spectrum

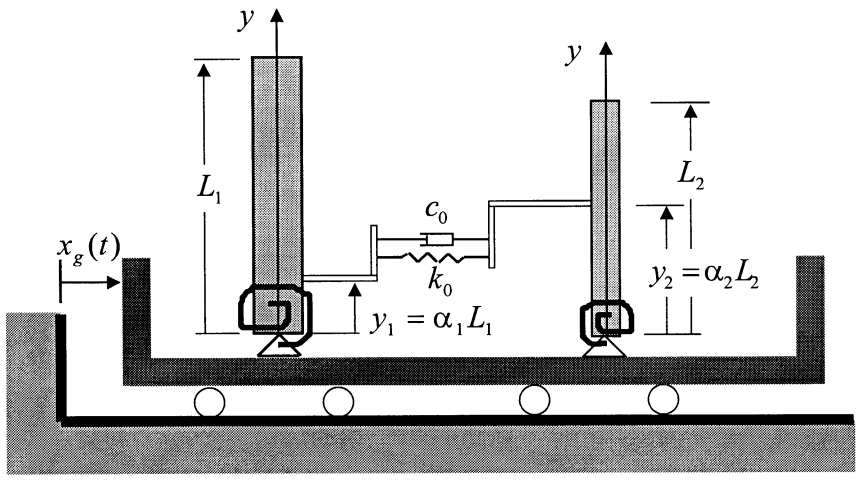

Figure 3.8 Example connected system with variable attachment points

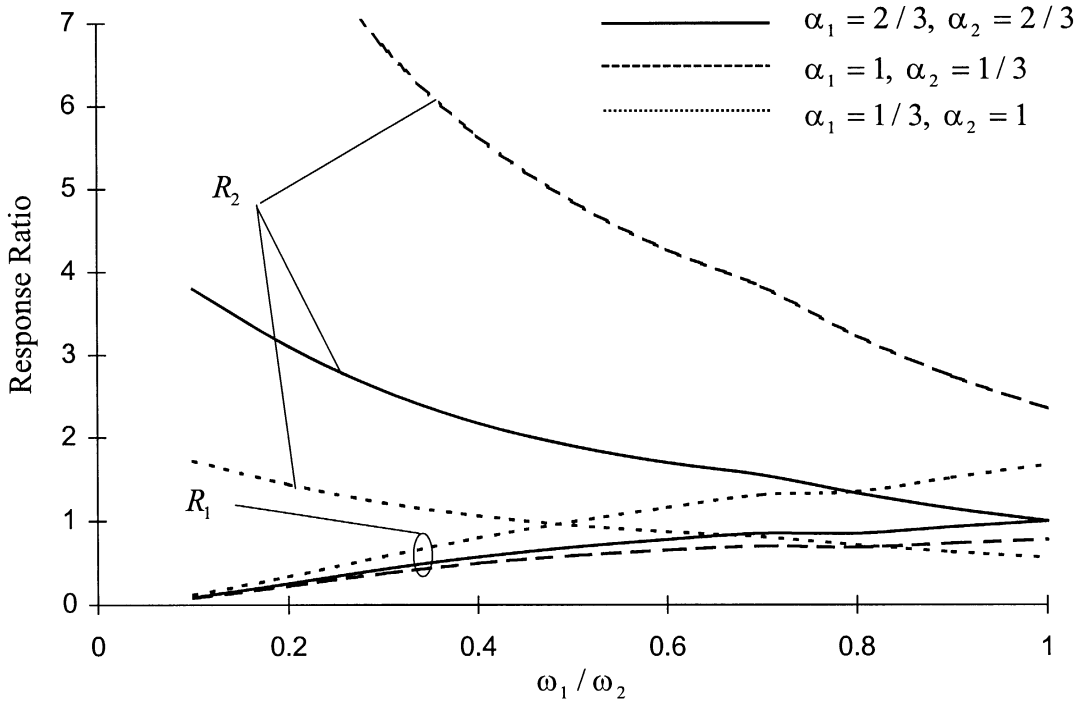

Figure 3.9 Effect of attachment configuration on response ratios R_1 and R_2 for $m_1 / m_2 = 2$, $\omega_2 = 20\pi$ rad/s, $\zeta_1 = \zeta_2 = 0.02$, $\kappa = 0.5$ and $c_0 = 0$, based on the IEEE spectrum

CHAPTER 4

TWO EQUIPMENT ITEMS CONNECTED BY A CABLE

4.1 Introduction

Many equipment items in electrical substations are connected to each other by flexible conductors, typically cables made of braided aluminum wires. In this chapter we investigate the effect of interaction between equipment items connected by idealized cables. It is assumed that the cable has no flexural stiffness and that no load other than self-weight is acting on the cable. Furthermore, inertia effects associated with the mass of the cable are considered to be negligible.*

In Section 4.2, the connecting cable is first modeled as having zero flexural and infinite extensional rigidity. A criterion under which the flexural stiffness of the cable can be neglected is described in Appendix A. Subsequently, the effect of extensibility is accounted for in an approximate manner. Closed form expressions are derived for various geometric and mechanical properties of the cable. Graphs displaying these expressions in dimensionless form are produced for convenient engineering analysis and design.

In Section 4.3, the equations of motion are derived for a 2-degree-of-freedom system consisting of two equipment items connected by a cable. Due to strong geometric nonlinearity and asymmetry inherent in the system, the response spectrum method cannot be used. Instead, an iterative numerical integration method is used to compute the response of the system to specific ground motions. Full account is made of the axial extensibility of the cable.

The effect of interaction in cable-connected equipment items is investigated in Section 4.4 by a comprehensive examination of the response ratios R_1 and R_2, which were defined in Chapter 3, for a range of parameter values. These results are used to identify a simple interaction parameter, defined in terms of the geometry of the cable, its slackness, and the maximum relative displacement of the stand-alone equipment items. It is shown

* See Epilogue on page 94.

that this parameter is an acute predictor of the expected severity of the interaction effect between the two equipment items.

4.2 Catenary Cable as Connecting Element

Consider an ideal inextensible cable with no flexural stiffness in equilibrium under its own weight, as shown in Figure 4.1. It is well known that such a cable takes on the catenary shape (Meriam and Kraige 1992). In the coordinate system of Figure 4.1, the shape of the cable is defined by the expression

$$y = \frac{T}{w}\left[\cosh\left(\frac{wx}{T}\right) - 1\right] \tag{4.1}$$

where w is the weight per unit length of the cable and T is the horizontal component of the cable force, which is constant throughout the cable. We first consider the case where the lowest point of the cable is below both supports. Let H be the vertical separation between the end supports, L the span length, L_1 and L_2 the horizontal distances from the lowest point of the cable to the left and right supports, respectively, and h the sag, which is defined as the vertical distance between the lowest point of the cable and the lower support, as shown in Figure 4.1. Given w, H, L and h, the unknown quantities are L_1, L_2 and T. Substituting the end point coordinates $(-L_1, h)$ and $(L_2, h+H)$ in the preceding equation, we have

$$h = \frac{T}{w}\left[\cosh\left(\frac{wL_1}{T}\right) - 1\right] \tag{4.2a}$$

$$h + H = \frac{T}{w}\left[\cosh\left(\frac{wL_2}{T}\right) - 1\right] \tag{4.2b}$$

These equations together with the identity

$$L_1 + L_2 = L \tag{4.2c}$$

are used to solve for the unknowns. It is useful to recast the above equations in the non-dimensional form

$$\frac{h}{L} = \frac{T}{wL}\left[\cosh\left(\frac{wL}{T}\frac{L_1}{L}\right) - 1\right] \tag{4.3a}$$

$$\frac{h+H}{L} = \frac{T}{wL}\left[\cosh\left(\frac{wL}{T}\frac{L_2}{L}\right) - 1\right] \tag{4.3b}$$

$$\frac{L_1}{L} + \frac{L_2}{L} = 1 \tag{4.3c}$$

Given H/L, the normalized cable force $T/(wL)$ can be determined as a function of the normalized sag h/L by numerically solving the above set of transcendental equations. Figure 4.2 shows the corresponding plots for $H/L = 0$, 0.1 and 0.5. It is noted that the tension force is highly sensitive to small values of the normalized sag h/L, and that it asymptotically approaches infinity as $h/L \to 0$. Naturally, the tension force in the actual cable is bounded by the plastic limit load of the cable, which depends on the effective diameter of the cable and the yield strength of its material. It follows that for small h/L, the axial deformation of the cable will have an important influence on the stiffness of the cable. This effect is accounted for later in this section.

The instantaneous or tangent stiffness of the cable for horizontal separation of its supports is the derivative dT/dL. To determine this quantity, we take derivatives of (4.2) with respect to L, which after elementary algebraic manipulations, and noting that H is a constant, result in

$$\frac{dh}{dL} = \frac{wL}{T}\left[\frac{h}{L} - \frac{L_1}{L}\sinh\left(\frac{wL}{T}\frac{L_1}{L}\right)\right]\frac{dT}{wdL} + \sinh\left(\frac{wL}{T}\frac{L_1}{L}\right)\frac{dL_1}{dL} \tag{4.4a}$$

$$\frac{dh}{dL} = \frac{wL}{T}\left[\frac{h+H}{L} - \frac{L_2}{L}\sinh\left(\frac{wL}{T}\frac{L_2}{L}\right)\right]\frac{dT}{wdL} + \sinh\left(\frac{wL}{T}\frac{L_2}{L}\right)\frac{dL_2}{dL} \tag{4.4b}$$

$$\frac{dL_1}{dL} + \frac{dL_2}{dL} = 1 \tag{4.4c}$$

The preceding represents a system of three linear algebraic equations for the unknown dimensionless derivatives dh/dL, $dT/(wdL)$, dL_1/dL and dL_2/dL. One more equa-

tion is needed to solve for these unknowns. It is obtained by observing that the length, s, of the inextensible cable remains constant with respect to variations in L. Let $s = s_1 + s_2$, where s_1 and s_2 are the lengths of the cable from its lowest point to the left and right supports, respectively. It is well known that for the catenary cable

$$s_1 = \frac{T}{w}\sinh\left(\frac{wL_1}{T}\right) \text{ and } s_2 = \frac{T}{w}\sinh\left(\frac{wL_2}{T}\right) \tag{4.5}$$

so that

$$s = \frac{T}{w}\left[\sinh\left(\frac{wL_1}{T}\right) + \sinh\left(\frac{wL_2}{T}\right)\right] \tag{4.6}$$

Differentiating (4.6) with respect to L, one obtains

$$0 = \frac{wL}{T}\left[\frac{s}{L} - \frac{L_1}{L}\cosh\left(\frac{wL}{T}\frac{L_1}{L}\right) - \frac{L_2}{L}\cosh\left(\frac{wL}{T}\frac{L_2}{L}\right)\right]\frac{dT}{wdL} + \cosh\left(\frac{wL}{T}\frac{L_1}{L}\right)\frac{dL_1}{dL} + \cosh\left(\frac{wL}{T}\frac{L_2}{L}\right)\frac{dL_2}{dL} \tag{4.7}$$

Solving the system of simultaneous linear equations (4.4) and (4.7), after lengthy algebraic manipulations, we obtain

$$\frac{dT}{wdL} = \frac{T}{wL}\frac{\left(\frac{s}{L}\frac{h}{L} + \frac{H}{L}\frac{s_1}{L}\right)\frac{wL}{T} + \frac{s}{L}}{\left(\frac{s}{L}\frac{h}{L} + \frac{H}{L}\frac{s_1}{L}\right)\frac{wL}{T} + \frac{s}{L} + \left(\frac{H}{L}\right)^2 - \left(\frac{s}{L}\right)^2} \tag{4.8}$$

$$\frac{dh}{dL} = \frac{wL}{T}\frac{dT}{wdL}\left[\frac{h}{L} + \left(\frac{H}{L} - \frac{wL}{T}\frac{s_2}{L}\right)\frac{s_1}{L}\frac{L}{s}\right] + \frac{wL}{T}\frac{s_1}{L}\frac{s_2}{L}\frac{L}{s} \tag{4.9}$$

These expressions are plotted in Figures 4.3 and 4.4, respectively, against the normalized sag h/L for $H/L = 0$, 0.1 and 0.5. It is noted that the stiffness of the ideal catenary cable rapidly grows as h/L decreases, approaching infinity as $h/L \to 0$ when $H/L = 0$. While in the subsequent analysis of the cable-connected system we do not make use of (4.9), this formula is nevertheless valuable as it relates changes in the sag to changes in the span length of the cable.

The above analysis is based on the assumption that a minimum point of the cable exists between the two end support points. For $H > 0$, it is possible that the cable have

no minimum point between the two end supports, as is shown in Figure 4.5. The equations developed earlier remain valid for such a case, as long as one uses negative values for L_1 and s_1 with the sag defined by extrapolating the catenary cable curve in the manner shown in Figure 4.5. This "virtual" sag, however, cannot be directly measured in the field. For such cases, a more convenient measure is the slackness of the cable, which we define as $s/c-1$, where s is the length of the cable and $c=\sqrt{L^2+H^2}$ is the chord length as defined in Figure 4.5. This dimensionless quantity measures the excess of the cable length over the chord length. The catenary shape provides a unique relation between the slackness $s/c-1$ and the normalized sag h/L, including for the case of virtual sag. This relation is plotted in Figure 4.6 for selected values of H/L, where values of the virtual sag are shown as negative. Note that as $s/c-1\to 0$, $h/L\to -\infty$ when $H/L>0$. The relation between the normalized sag and the slackness can be used to determine the normalized cable force and cable stiffness directly in terms of s/c. These plots are computed by use of (4.1)-(4.8) and are shown in Figures 4.7 and 4.8, respectively.

Two observations in Figures 4.7 and 4.8 are noteworthy. First we note that the curves for $T/(wL)$ and $dT/(wdL)$ are insensitive to H/L when plotted against the slackness $(s/c-1)$. In fact, the curves for $H/L=0$, 0.1 and 0.2 are practically indistinguishable. It follows that for a constant slackness the force and stiffness properties of the catenary cable are essentially invariant to the configuration of its support points. The second observation relates to the three diamond-shaped marks on the curves in these figures. From left to right, these marks correspond to the configurations of the cable for $H/L=0.1$, 0.2 and 0.5, for which the minimum point of the cable (with zero slope) occurs at the lower support. Segments of the curves to the right of these points correspond to configurations of the cable as in Figure 4.1, and segments of the curves to the left of these points correspond to the configurations of the cable as in Figure 4.5. For $H/L=0$, the minimum point of the cable always lies between the two supports. Thus, as opposed to Figures 4.2 and 4.3 that apply only to the cable configuration in Figure 4.1, Figures 4.7 and 4.8 are applicable to catenary cables of arbitrary configuration.

In the preceding analyses, we assumed an inextensible cable. Of course in a real cable there is axial deformation. The influence on the stiffness of the cable from this deformation becomes significant when the slackness $s/c-1$ approaches zero. In the limit as $s/c-1 \to 0$, the stiffness of the cable approaches its extensional stiffness in the horizontal direction, which, provided the cable remains within the elastic range, is equal to $(EA/s)\cos^2\alpha$, where E denotes the elastic modulus of the material, A denotes the cross sectional area of the cable, and α denotes the angle of inclination of the chord with the horizontal so that $\cos\alpha = L/c$. For $s/c-1$ not close to zero, the cable stiffness is governed by its geometry, as previously described. In between these two limiting regimes, there is a transition zone where both contributions are important. In order to obtain an approximation of the cable stiffness for this range, we assume that the total flexibility of the cable is the sum of its flexibilities arising from its shape and its axial deformation. In essence, we are assuming that the effective stiffness of the cable is equivalent to the stiffness of two springs in series, one representing the cable stiffness and the other the axial stiffness. Based on this approximation, the effective stiffness of the cable, denoted k_{eff}, that combines both contributions is given by the relation

$$\frac{1}{k_{\text{eff}}} = \frac{sc^2}{EAL^2} + \frac{dL}{dT} \tag{4.10}$$

It is useful to write this expression in the dimensionless form

$$\frac{k_{\text{eff}}}{w} = \frac{\dfrac{dT}{wdL}\dfrac{EAL^2}{wsc^2}}{\dfrac{dT}{wdL} + \dfrac{EAL^2}{wsc^2}} \tag{4.11}$$

One should note that, due to the extensibility of the cable, the length s now is not a constant, as it depends on the tension force in the cable. This effect would be important for an exceptionally taut cable. In using the preceding approximation, it is appropriate to use the current value of the cable length to compute the stiffness term dT/dL.

As an example, consider a cable of span $L = 5\,\text{m}$, vertical separation $H/L = 0$, and normalized axial stiffness $EA/ws \cong 537{,}000$. (The specified axial stiffness is that of an

aluminum cable of an equivalent solid cross section of 5cm diameter.) Figure 4.9 shows the dimensionless effective stiffness k_{eff} / w of the cable as a function of both h / L and $s/c-1$. It can be seen that as $h / L \to 0$ or $s/c-1 \to 0$, the effective stiffness of the cable makes a rapid transition from that of the ideal inextensible cable stiffness, dT / dL, to that of the axial stiffness, EAL^2 / sc^2.

4.3 Analysis of the Cable-Connected System

Consider two equipment items, possibly with distributed mass, modeled as linear, viscously damped, single-degree-of-freedom systems, connected by a cable of weight w per unit length, initial span length L_0 and initial sag h_0, both measured in the static equilibrium position of the system, and the vertical separation H, as shown in Figure 4.10. If the cable does not have a minimum point between the two supports, then h_0 will denote the virtual sag, as defined in Figure 4.5. For the two equipment items, the displacement shape functions $\psi_1(y)$ and $\psi_2(y)$ are scaled to have unit values at the attachment points y_1 and y_2 with the cable. Note that $H = |y_1 - y_2|$. Given this information, the initial length of the cable, s_0, and the initial horizontal cable tension force, T_0, are determined from (4.2) and (4.6).

In the following analysis we neglect the inertia effect of the cable mass. This is justified by the finding in Section 3.5 that indicated only a small influence of the mass of the connecting element on the interaction effect, provided that the mass of the cable is small in relation to the sum of the masses of the two equipment items. Based on (2.7), the equation of motion of the system, relative to its static equilibrium position under the weight of the cable, can be written as

$$\mathbf{M}\ddot{\mathbf{u}} + \mathbf{C}\dot{\mathbf{u}} + \mathbf{R}(\mathbf{u}) = -\mathbf{L}\ddot{x}_g \tag{4.12}$$

where $\mathbf{u} = [u_1 \;\; u_2]^{\mathrm{T}}$ is the vector of displacements at the attachment points relative to the base (including the static displacements due to the weight of the cable), $\mathbf{M}$ is the mass matrix in (2.9), $\mathbf{C}$ is the damping matrix in (2.10) and $\mathbf{L}$ is as defined following (2.9). $\mathbf{R}(\mathbf{u})$ denotes the vector of restoring forces, which in general depends on the displaced

shape of the system. The restoring force vector for the cable-connected system is given by

$$\mathbf{R}(\mathbf{u}) = \begin{Bmatrix} k_1 u_1 - T(L) \\ k_2 u_2 + T(L) \end{Bmatrix} \tag{4.13}$$

where

$$L = L_0 + [u_2(t) - u_2(0)] - [u_1(t) - u_1(0)] \tag{4.14}$$

is the current span length.

The preceding equations are nonlinear because of the nonlinear dependence of T on L. We employ a step-by-step numerical integration scheme to solve these equations. The time axis is discretized into a set of equally spaced points $t_0, t_1, \ldots, t_n, \ldots$, with $t_0 = 0$ and $\Delta t = t_{n+1} - t_n$. The Newmark integration algorithm together with a Newton iteration scheme at each step are utilized. The Newmark algorithm is based on the approximation of the velocity and displacement at step $n+1$ in terms of the same responses at step n and an assumed shape of the acceleration increment. The general form is

$$\dot{\mathbf{u}}_{n+1} = \dot{\mathbf{u}}_n + (1-\gamma)\Delta t \ddot{\mathbf{u}}_n + \gamma \Delta t \ddot{\mathbf{u}}_{n+1} \tag{4.15a}$$

$$\mathbf{u}_{n+1} = \mathbf{u}_n + \Delta t \dot{\mathbf{u}}_n + (0.5-\beta)\Delta t^2 \ddot{\mathbf{u}}_n + \beta \Delta t^2 \ddot{\mathbf{u}}_{n+1} \tag{4.15b}$$

where $\mathbf{u}_n = \mathbf{u}(t_n)$, β and γ are parameters dependent on the assumed shape of the acceleration increment. Here, we use $\beta = 0.25$ and $\gamma = 0.5$, which correspond to the approximation of the acceleration over the time step by a constant equal to its average over the increment. The preceding equations are solved for $\dot{\mathbf{u}}_{n+1}$ and $\ddot{\mathbf{u}}_{n+1}$ in terms of the solutions $\mathbf{u}_n$, $\dot{\mathbf{u}}_n$ and $\ddot{\mathbf{u}}_n$ at the previous step and the displacement $\mathbf{u}_{n+1}$ at the new step. Substituting these in (4.12), one obtains

$$\left[\frac{1}{\beta \Delta t^2}\mathbf{M} + \frac{\gamma}{\beta \Delta t}\mathbf{C}\right]\mathbf{u}_{n+1} + \mathbf{R}(\mathbf{u}_{n+1}) = \mathbf{P}_{n+1} \tag{4.16}$$

where

$$\mathbf{P}_{n+1} = -\mathbf{L}\ddot{x}_g(t_{n+1}) + \mathbf{M}\left[\frac{1}{\beta\Delta t^2}\mathbf{u}_n + \frac{1}{\beta\Delta t}\dot{\mathbf{u}}_n + \left(\frac{1}{2\beta}-1\right)\ddot{\mathbf{u}}_n\right]$$
$$+ \mathbf{C}\left[\frac{\gamma}{\beta\Delta t}\mathbf{u}_n + \left(\frac{\gamma}{\beta}-1\right)\dot{\mathbf{u}}_n + \left(\frac{\gamma}{2\beta}-1\right)\Delta t\ddot{\mathbf{u}}_n\right] \tag{4.17}$$

is the effective external force vector. The nonlinear equation (4.16) is solved by Newton iterations using the following set of equations:

$$\left[\frac{1}{\beta\Delta t^2}\mathbf{M} + \frac{\gamma}{\beta\Delta t}\mathbf{C} + \mathbf{K}(\mathbf{u}_{n+1}^{i-1})\right]\Delta\mathbf{u}_{n+1}^{i} = \Delta\mathbf{P}_{n+1}^{i-1} \tag{4.18a}$$

$$\mathbf{u}_{n+1}^{i} = \mathbf{u}_{n+1}^{i-1} + \Delta\mathbf{u}_{n+1}^{i} \tag{4.18b}$$

$$\Delta\mathbf{P}_{n+1}^{i} = \Delta\mathbf{P}_{n+1}^{i-1} - \left[\frac{1}{\beta\Delta t^2}\mathbf{M} + \frac{\gamma}{\beta\Delta t}\mathbf{C}\right]\Delta\mathbf{u}_{n+1}^{i} - \left[\mathbf{R}(\mathbf{u}_{n+1}^{i}) - \mathbf{R}(\mathbf{u}_{n+1}^{i-1})\right] \tag{4.18c}$$

where $\mathbf{u}_{n+1}^{i}$ denotes the i-th trial value of $\mathbf{u}_{n+1}$ and $\mathbf{K}(\mathbf{u}) = d\mathbf{R}(\mathbf{u})/d\mathbf{u}$ in (4.18a) is the derivative of the restoring force vector with respect to the displacement vector, which is commonly known as the tangent stiffness matrix. Using (4.13) and (4.14), this matrix is

$$\mathbf{K} = \begin{bmatrix} k_1 + \dfrac{dT}{dL} & -\dfrac{dT}{dL} \\ -\dfrac{dT}{dL} & k_2 + \dfrac{dT}{dL} \end{bmatrix} \tag{4.19}$$

where the cable stiffness term dT/dL must be computed from (4.8) using the current geometry of the cable. The Newton iteration proceeds as follows: The i -th displacement increment $\Delta\mathbf{u}_{n+1}^{i}$ is computed from (4.18a) using information from the previous iteration. This is used in (4.18b) to compute a new estimate $\mathbf{u}_{n+1}^{i}$ of the displacement vector, which is then used in (4.18c) to update the effective residual force $\Delta\mathbf{P}_{n+1}^{i}$. The iteration count is increased by 1 and the process is repeated until convergence is achieved. The convergence criterion used is $\left\|\Delta\mathbf{P}_{n+1}^{i}\right\| / \left\|\Delta\mathbf{P}_{n+1}^{0}\right\| < \varepsilon_1$ and $\left\|\Delta\mathbf{P}_{n+1}^{i}\right\| < \varepsilon_2$, where $\varepsilon_1 = 10^{-6}$ and $\varepsilon_2 = 10^{-2}$. The initial values $\mathbf{u}_{n+1}^{0} = \mathbf{u}_n$, $\mathbf{R}_{n+1}^{0} = \mathbf{R}(\mathbf{u}_n)$ and $\Delta\mathbf{P}_{n+1}^{0} = \mathbf{P}_{n+1} - \mathbf{P}_n$ are employed at the beginning of each time step.

The above analysis neglected the axial deformation of the cable. As we have noted before, this effect can be important for taut cables. Let $EAL^2/(sc^2)$ denote the axial stiffness of the cable, where s, L and c are the current length, span and chord length of the cable, accounting for its elongation and horizontal support displacements. To approximately account for the contribution of axial deformation, we simply replace dT/dL with k_{eff} as defined in (4.11) so that (4.19) becomes

$$\mathbf{K} = \begin{bmatrix} k_1 + k_{\text{eff}} & -k_{\text{eff}} \\ -k_{\text{eff}} & k_2 + k_{\text{eff}} \end{bmatrix}. \tag{4.20}$$

Note that in computing dT/dL from (4.8), the current length of the cable and its span should be used.

4.4 Numerical Studies with Example Cable-Connected Systems

For the analysis in this section, we first consider two equipment items connected by an aluminum cable having the cross-sectional area $A = 19.6\,\text{cm}^2$ (equivalent to a solid cable of 5cm diameter), weight per unit length $w = 52.2$ N/m, elastic modulus $E = 7 \times 10^6\,\text{N/cm}^2$, initial span length $L_0 = 5\,\text{m}$ (under static equilibrium conditions), vertical separation $H = 0$, and variable initial normalized sag h_0/L_0. The equipment items are considered to have the masses $m_1 = 1000\,\text{kg}$ and $m_2 = 500\,\text{kg}$, an attachment configuration such that $l_1/m_1 = l_2/m_2 = 1$, stand-alone frequencies $\omega_1 = 2\pi\,\text{rad/s}$ and $\omega_2 = 10\pi\,\text{rad/s}$, and damping ratios $\zeta_1 = \zeta_2 = 0.02$. The cable is assumed to have zero damping, i.e., $c_0 = 0$. The mass of the cable is approximately 27kg and its inertia effect is assumed to be negligible.

The initial cable stiffness normalized by its weight per unit length, $k_{\text{eff},0}/w$, is strongly dependent on the initial sag, as is evident in Figure 4.3. For example, with $H = 0$, for $h_0/L_0 = 0.05$, $k_{\text{eff},0}/w = 192$, whereas for $h_0/L_0 = 0.10$, $k_{\text{eff},0}/w = 25.9$. For the considered equipment items, these correspond to initial values of the connecting stiffness ratio $\kappa = k_{\text{eff},0}/(k_1 + k_2)$ equal to 0.0188 and 0.0025, respectively. These indi-

cate very small initial stiffness values of the connecting cable. However, during the seismic disturbance, the effective stiffness of the cable varies dramatically and κ assumes large values, as we will shortly see.

We first examine the response of the cable-connected system with the initial normalized sag $h_0 / L_0 = 0.05$ to the N-S component of the Newhall record of the 1994 Northridge earthquake, which is shown in Figure 4.11. The initial cable length for this normalized sag is $s_0 = 5.033\,\text{m}$. For this record, Figure 4.12 shows the displacement responses of the two equipment items in both the stand-alone, $u_{10}(t)$ and $u_{20}(t)$, and connected, $u_1(t)$ and $u_2(t)$, configurations. The maximum stand-alone displacements are $\max|u_{10}(t)|=0.3375\text{m}$ and $\max|u_{20}(t)|= 0.0162\,\text{m}$ and the maximum separation between the two stand-alone equipment items is $\Delta = \max[u_{20}(t) - u_{10}(t)] = 0.3163\,\text{m}$. The two stand-alone responses are significantly different because of the large separation between the equipment frequencies (1Hz and 5Hz, respectively). These time histories tend to have nearly symmetric peaks relative to the equilibrium position with nearly zero averages over time. The displacement time histories $u_1(t)$ and $u_2(t)$ of the connected system start from the static equilibrium positions $u_1(0)$ and $u_2(0)$, respectively, which are not zero. These responses exhibit strongly skewed peaks relative to the equilibrium position, with non-zero averages over time and larger displacements occurring towards the side that slackens the cable. This is a clear indication of nonlinearity in the response. Note also that the response of equipment 1 in the connected system has a higher frequency content than its stand-alone response. This is due to the contribution of the added stiffness provided by the cable and equipment 2. More significantly, we observe a large increase in the peak response of equipment 2 (the higher frequency equipment item) in the connected system relative to its stand-alone response, and a moderate increase in the peak response of equipment 1. The ratio of the peak responses of equipment 2 in the connected and stand-alone configurations is $R_2 = 7.62$. The ratio for equipment 1 is $R_1 = 1.48$.

Figure 4.13 shows the time history of the cable span $L(t)$ as defined in (4.14). The strong nonlinearity in the response is clearly evident from the marked skewness of this

time history. Whereas the span shortens to a minimum of 4.53m, its maximum value is only 5.046m, which is larger than the original length of the cable $s_0 = 5.033\,\text{m}$. It is evident that, for this system, the axial deformation of the cable is important.

Figure 4.14 shows the time history of the normalized cable force $T(t)/(wL_0)$, plotted on a semi-logarithmic scale. The response shows peak forces at various instances of time that are more than two orders of magnitude greater than the initial cable force. These occur at instances at which the cable is stretched almost straight. Obviously such large forces could be damaging to the attached equipment, including the cable-to-equipment connections.

Figure 4.15 shows the time history of normalized effective cable stiffness, $k_{\text{eff}}(t)/w$, plotted on a semi-logarithmic scale. Relative to its initial value, the effective stiffness increases by more than three orders of magnitude and decreases by almost two orders of magnitude at certain instants during the response. At many instants, the effective stiffness caps at a constant value, which is nearly equal to the axial stiffness of the cable. At these instants, the cable is stretched almost straight. The stiffness ratio κ, which had an initial value of 0.0188, reaches 51 at these points. This means that at these instances the effective stiffness of the cable is 51 times the sum of the stiffnesses of the two equipment items.

The example described above is a rather extreme case, as the normalized sag of the cable is only 5%. To gain insight into the influence of the sag on the interaction between the two equipment items, we compute the response ratios R_1 and R_2 for the system under consideration as functions of the normalized initial sag h_0/L_0 for the five earthquake records shown in Figure 4.16. Recall that R_1 and R_2 represent ratios of the peak equipment responses in the connected system to the corresponding responses in the stand-alone system. The results are shown in Figure 4.17. It is seen that the effect of interaction is particularly adverse on the higher frequency equipment item as the response ratio R_2 is much greater than unity for several of the ground motions. The response ratio R_1 also has values greater than unity for certain ranges of the normalized initial sag. This is be-

cause of the specific frequency content of the selected ground motions. For example, the spectrum for the Tabas LN record shows a deep trough at the frequency of 2π rad/s, which happens to coincide with the frequency ω_1 of equipment 1. As a result of this coincidence, any change in the natural frequency of the system, such as that induced by the connection of equipment 1 to equipment 2, amplifies the response of equipment 1. The most salient observation from this figure is that the interaction effect tends to diminish with increasing normalized initial sag of the cable. It appears that for the present system the interaction effect is insignificant for a normalized initial sag greater than about 0.15.

To demonstrate the sensitivity of the nonlinear interaction effect on the details of the ground motion, we repeat the above analysis while switching the positions of the two equipment items. (This is equivalent to changing the sign of the ground motion while maintaining the equipment positions.) The results for the response ratios R_1 and R_2 are shown in Figure 4.18. For a linear system, such a change would not have any influence on the maximum absolute responses. However, because of the particular nonlinearity of the system, which causes a strong asymmetry in the response, the switching of the positions of the two equipment items (or the direction of the motion) significantly affects the response ratios. This can be seen by comparing the curves in Figure 4.17 with the corresponding curves in Figure 4.18. In particular, the peak value of R_2, which is 7.62 in Figure 4.17, reduces to 6.05 for the case in Figure 4.18. This comparison serves to demonstrate the particular nature of the nonlinearity in the cable-connected system.

A quantity that strongly influences the degree of interaction between the cable-connected equipment items is the maximum amount that the two stand-alone equipment items move away from one another. We define this quantity as

$$\Delta = \max[u_{20}(t) - u_{10}(t)] \tag{4.21}$$

Two factors determine the magnitude of Δ. One is the displacement spectral ordinates of the ground motion at the equipment frequencies, particularly that of the lower frequency equipment. As shown in (2.24), the peak values of $u_{10}(t)$ and $u_{20}(t)$ are proportional to these spectral ordinates. Ordinarily, the lower the equipment frequencies, the larger will

be the spectral ordinates and, therefore, the peak stand-alone responses as well as the peak of their difference, Δ. Naturally, the lower-frequency equipment item will tend to have a larger displacement and, therefore, dominate Δ. The second factor is the separation between the two equipment frequencies. We note, in particular, that when the two equipment items have identical frequencies and damping ratios $\Delta = 0$ regardless of the frequency content of the ground motion. Furthermore, Δ would tend to increase with increasing separation between the equipment frequencies as a consequence of losing coherence between the two responses, even if the spectral ordinates at the two frequencies remain the same. To investigate these effects, we repeat the preceding analysis while changing only the frequency of equipment 1 from $\omega_1 = 2\pi$ rad/s to $\omega_1 = 4\pi$ rad/s. Because of the higher frequency of this equipment, the displacement spectral ordinate is expected to be smaller. Furthermore, the separation between the two frequencies is reduced. Hence, we expect a smaller value of Δ and, therefore, reduced interaction between the two equipment items. As an example, for the Northridge record we obtain $\Delta = 0.1369$ m, which is much smaller than the value $\Delta = 0.3163$ m obtained for the previous system. Figure 4.19 shows plots of the response ratios R_1 and R_2 for the five recorded ground motions. Note that the scale used in this figure is different from the scale used in Figures 4.17 and 4.18. It is found that the interaction effect in this case is indeed greatly reduced. Furthermore, no significant interaction occurs if the normalized initial sag is greater than about 0.10.

The preceding analyses was for a cable with no vertical separation between its supports, i.e., $H = 0$. For such a cable, the initial normalized sag h_0 / L_0 represents a good measure of the flexibility and for that reason it was used to present the results in Figures 4.17-4.19. When $H > 0$, the initial cable slackness $s_0 / c_0 - 1$ is a more convenient measure of the flexibility of the cable than the initial normalized sag. Using the relation between the two measures shown in Figure 4.6, it is possible to recast the results in Figures 4.17-4.19 in terms of the slackness. However, we find it more useful to make the plots against a measure that also involves the relative displacement between the stand-alone equipment items.

Suppose one end of the cable is moved horizontally by the amount $\Delta = \max[u_{20}(t) - u_{10}(t)]$, which represents the maximum relative displacement between the stand-alone equipment items, as shown in Figure 4.20. For $\Delta << c_0$, the chord length will then increase approximately by the amount $\Delta L_0 / c_0$. One can regard this quantity as a seismic demand on the reserve cable length, $s_0 - c_0$, which can be regarded as the corresponding capacity. Obviously, if $\Delta L_0 / c_0$ is small in relation to $s_0 - c_0$, then there will be little interaction between the two equipment items. Conversely, if $\Delta L_0 / c_0$ is of the same magnitude or greater than $s_0 - c_0$, then one can expect significant interaction. It follows that the dimensionless quantity $(\Delta L_0 / c_0) / (s_0 - c_0)$, which is the ratio of the seismic demand over capacity, is a good measure to characterize the intensity of interaction. This measure can be written in the dimensionless form

$$\beta = \frac{\Delta L_0 / c_0^2}{s_0 / c_0 - 1} \tag{4.22}$$

which we define as the interaction parameter. Recall that Δ is easily computed in terms of the stand-alone equipment properties and the ground response spectrum, as described in Section 2.5 of Chapter 2. With Δ given, the interaction parameter β only depends on the initial geometry of the cable and its slackness.

Figures 4.21-4.23 show the results for the response ratios R_1 and R_2 reported in Figures 4.17-4.19, but now in terms of the interaction parameter β. Figure 4.24 shows similar results for a cable-connected system with the attachment points having the vertical separation $H = 2.5\,\text{m}$. The equipment frequencies are $\omega_1 = 2\pi\,\text{rad/s}$ and $\omega_2 = 10\pi\,\text{rad/s}$, with all other equipment and cable properties remaining the same as in the previous cases. The following noteworthy observations can be derived from the results shown in Figures 4.21-4.24:

a) There appears to be virtually no interaction between the two equipment items when β is less than about 1, regardless of the nature of the ground motion, values of the equipment frequencies, or the initial geometry of the cable.

b) For values of β greater than 1, significant interaction between the two equipment items occurs for all cable geometries. However, the degree of interaction strongly depends on the nature of the ground motion. Closer examination of the results reveals that the interaction effect is particularly sensitive to the positions of the equipment frequencies relative to the frequency content of the ground motion. As demonstrated earlier, the interaction tends to amplify the response of the higher frequency equipment item much more than that of the lower frequency item.

c) It appears from the results in Figures 4.21-24 that, for values of β greater than 1, detailed dynamic analysis of the combined system is necessary to accurately determine the peak responses of the two equipment items, particularly that of the higher frequency item. Otherwise, to be on the safe side, it is necessary to assure a capacity for the higher frequency equipment item that is anywhere from 4 to 8 times larger than the demand placed upon it by the earthquake in its stand-alone configuration.

Given the above facts, it appears to be prudent to design cable-connected equipment items in such a way that the interaction parameter β is no greater than 1.*

* See Epilogue on page 94.

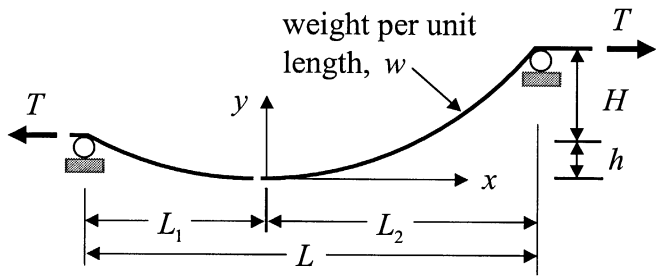

Figure 4.1 Catenary cable

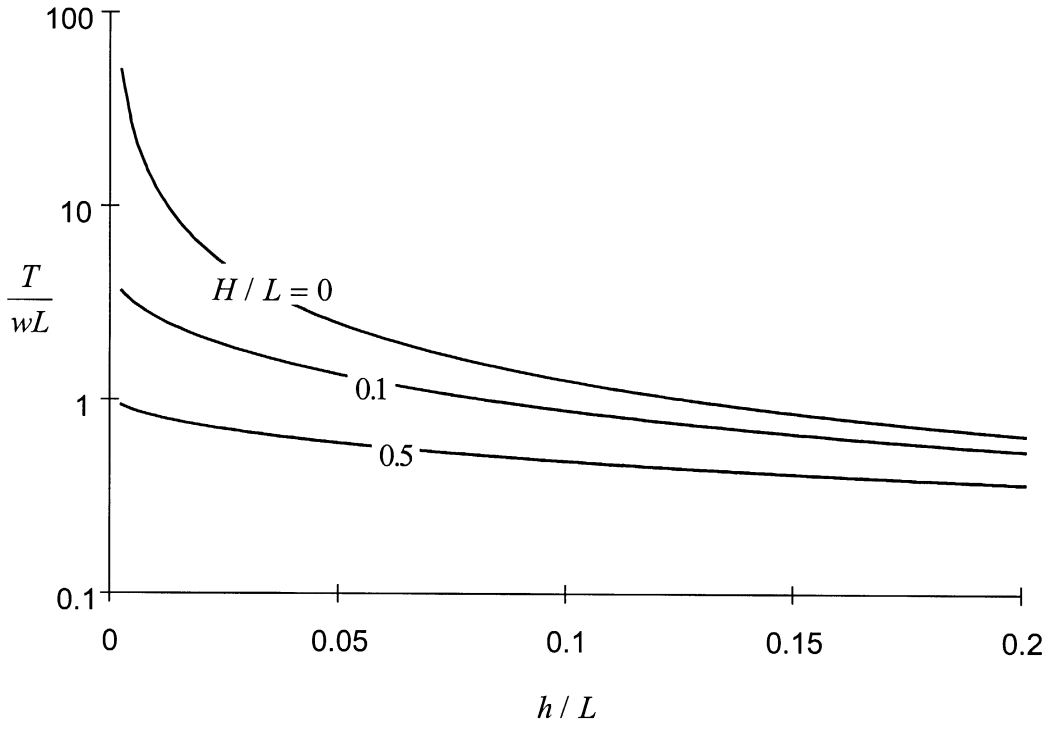

Figure 4.2 Normalized horizontal cable force versus normalized sag

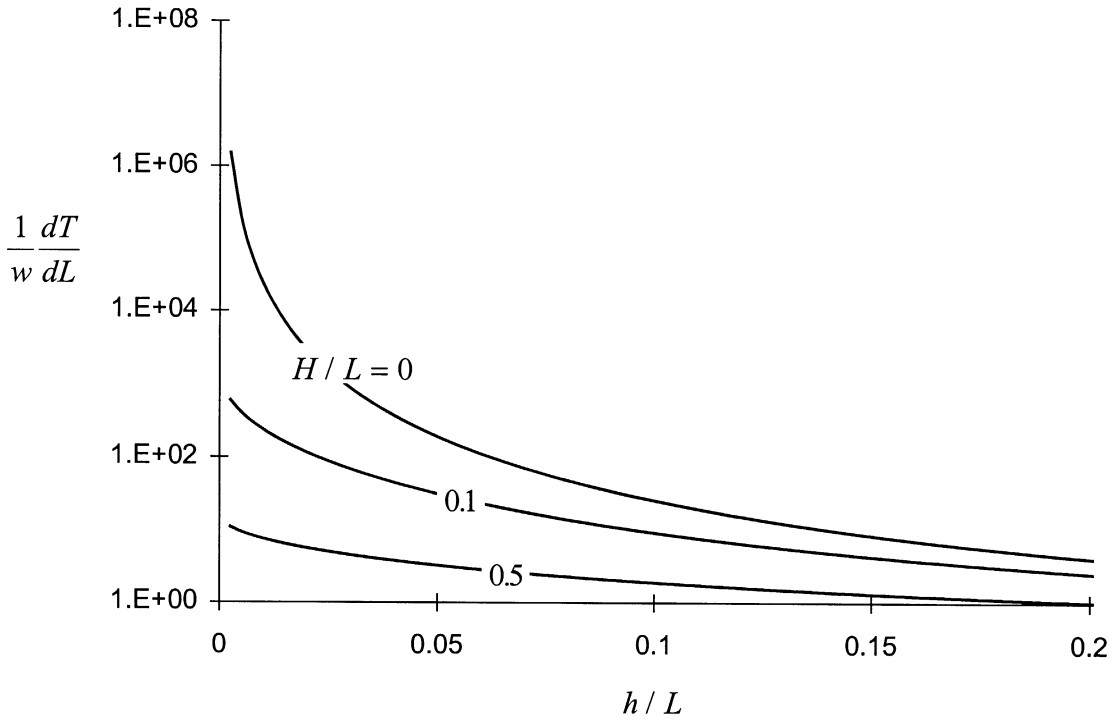

Figure 4.3 Normalized cable stiffness versus normalized sag

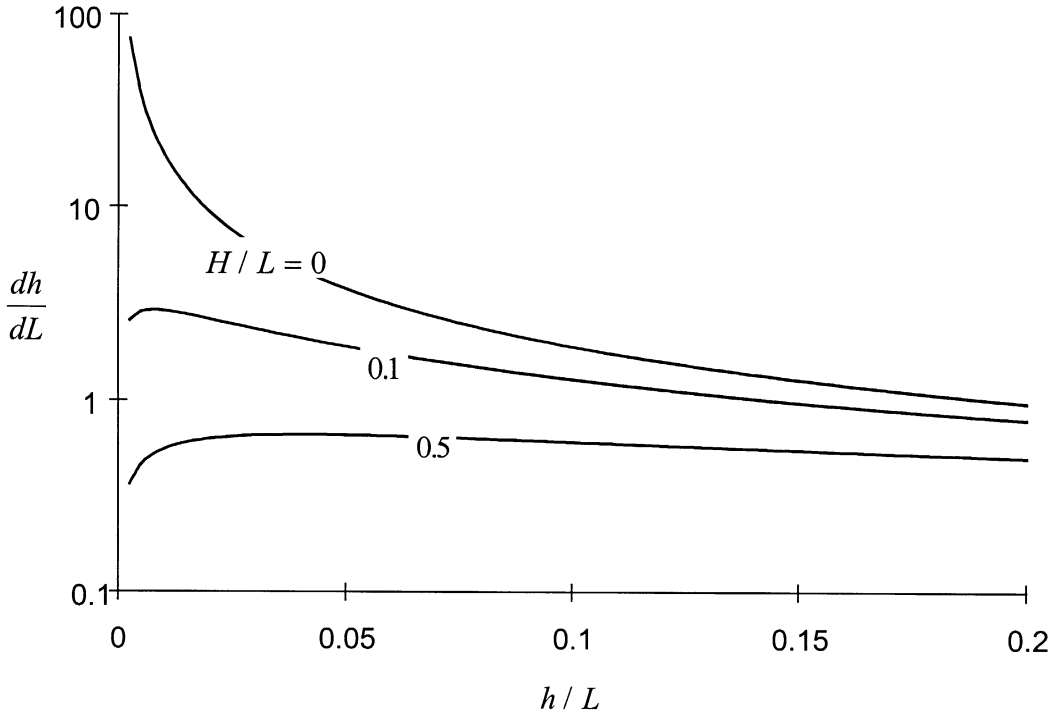

Figure 4.4 Rate of change of cable sag with respect to span length versus normalized sag

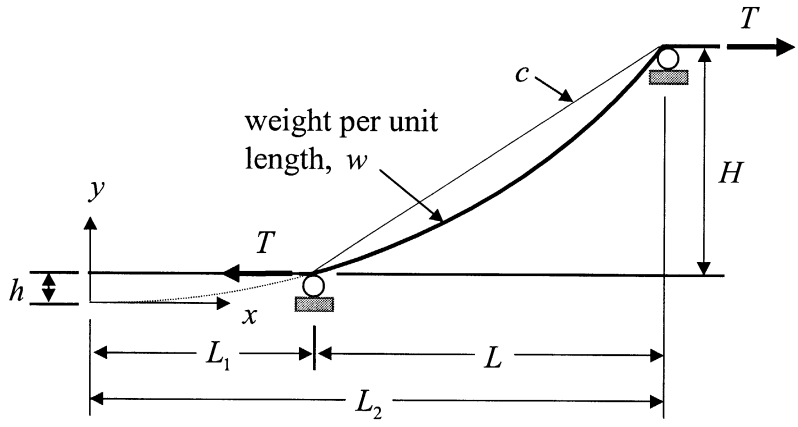

Figure 4.5 Cable configuration with virtual sag

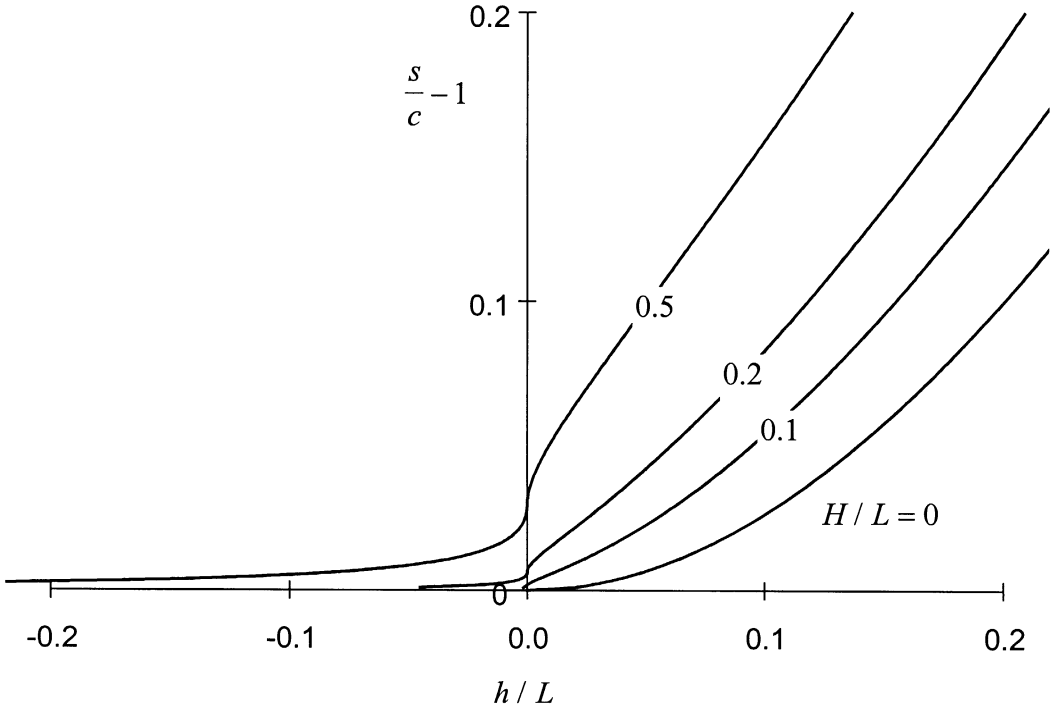

Figure 4.6 Normalized sag versus slackness

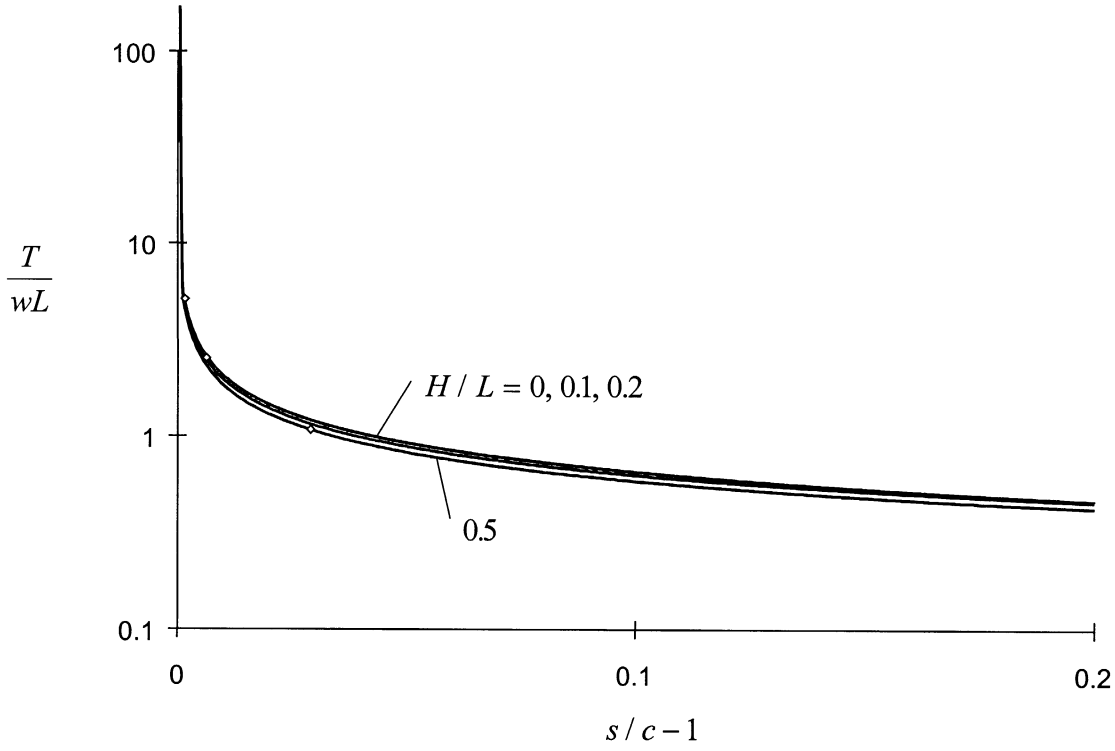

Figure 4.7 Normalized horizontal cable force versus slackness

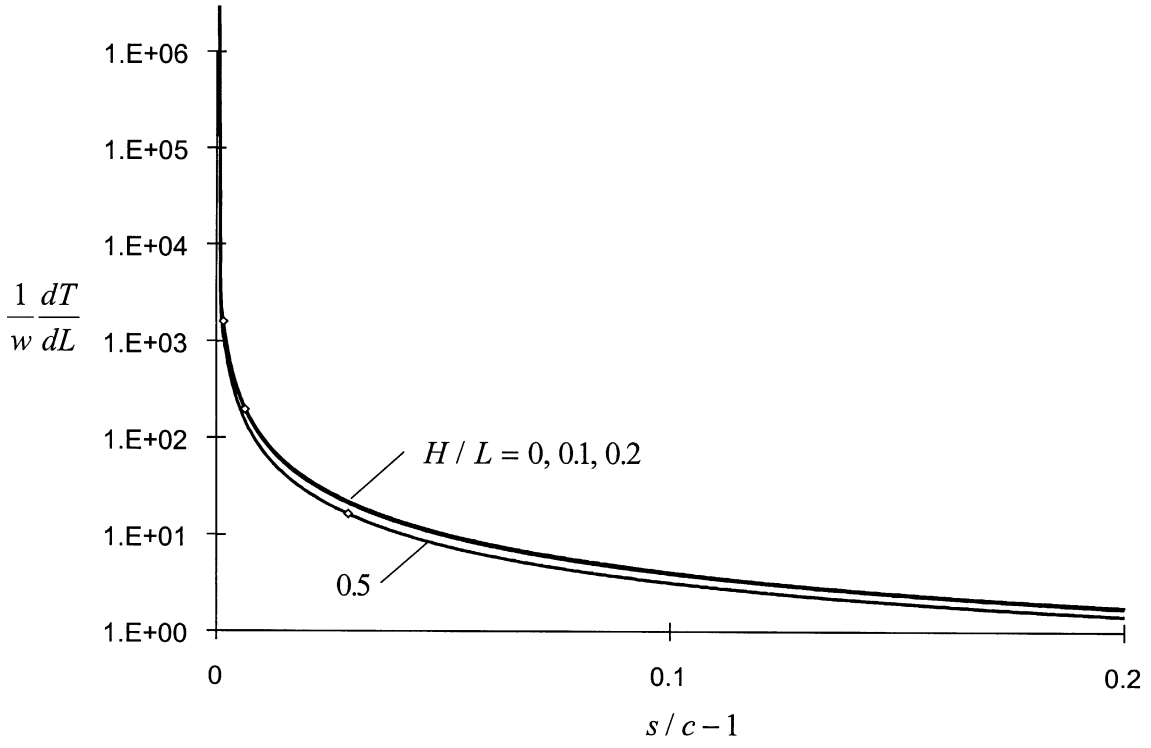

Figure 4.8 Normalized cable stiffness versus slackness

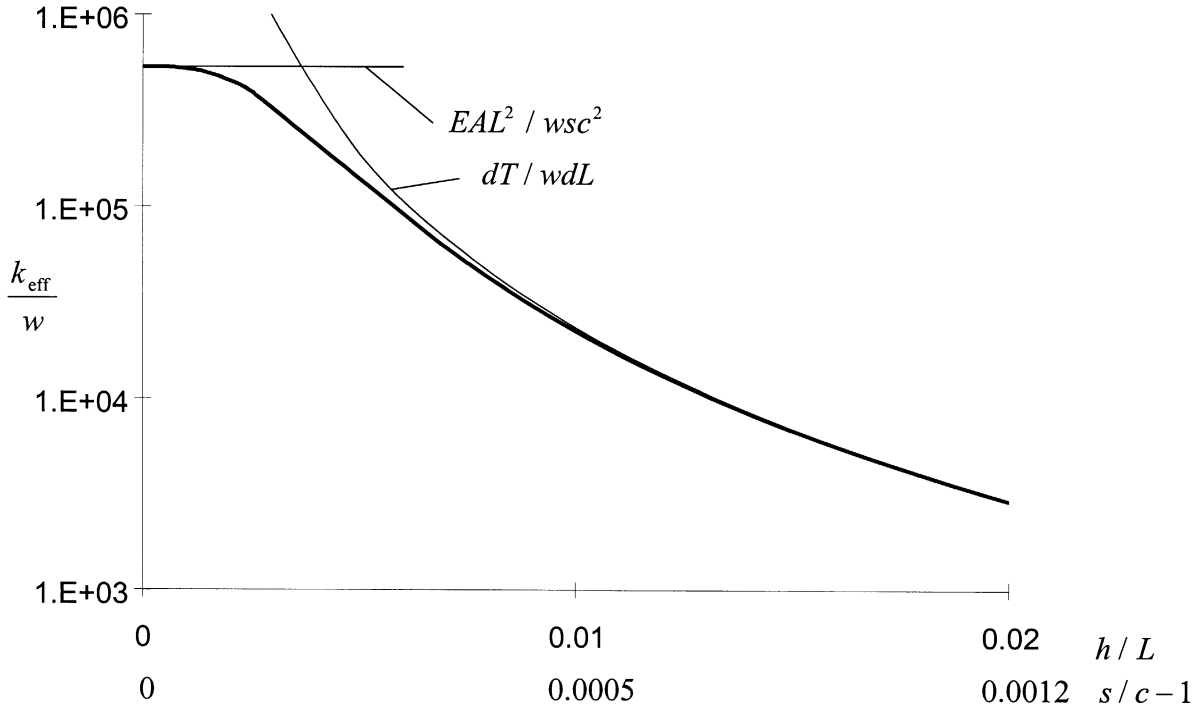

Figure 4.9 Normalized effective stiffness of example cable versus normalized sag, accounting for cable extensibility

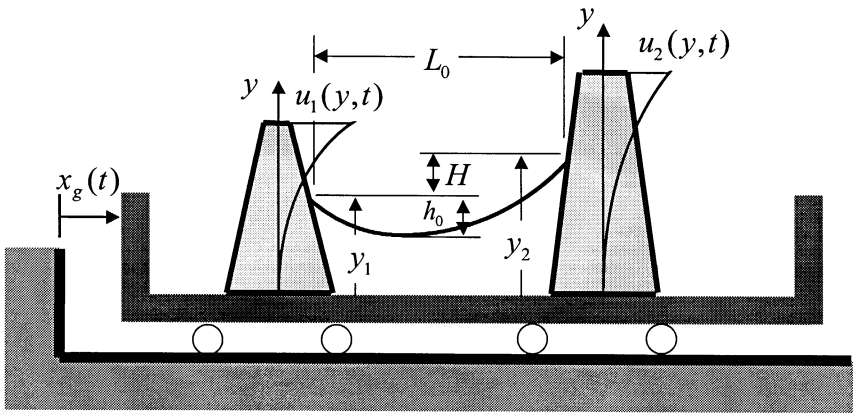

Figure 4.10 Cable-connected equipment items

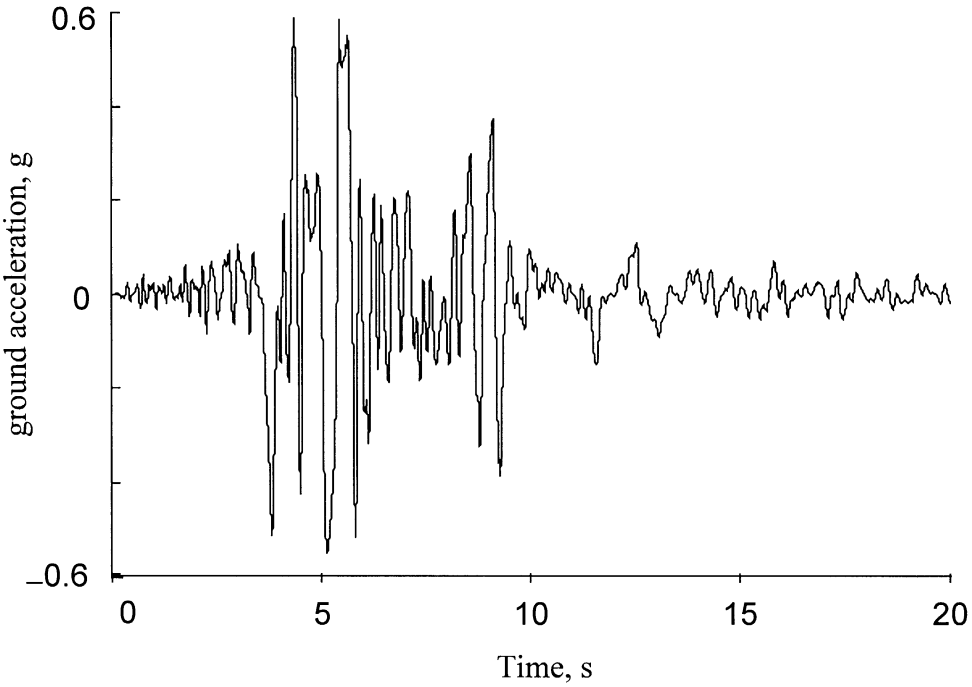

Figure 4.11 N-S component of Newhall record, 1994 Northridge Earthquake

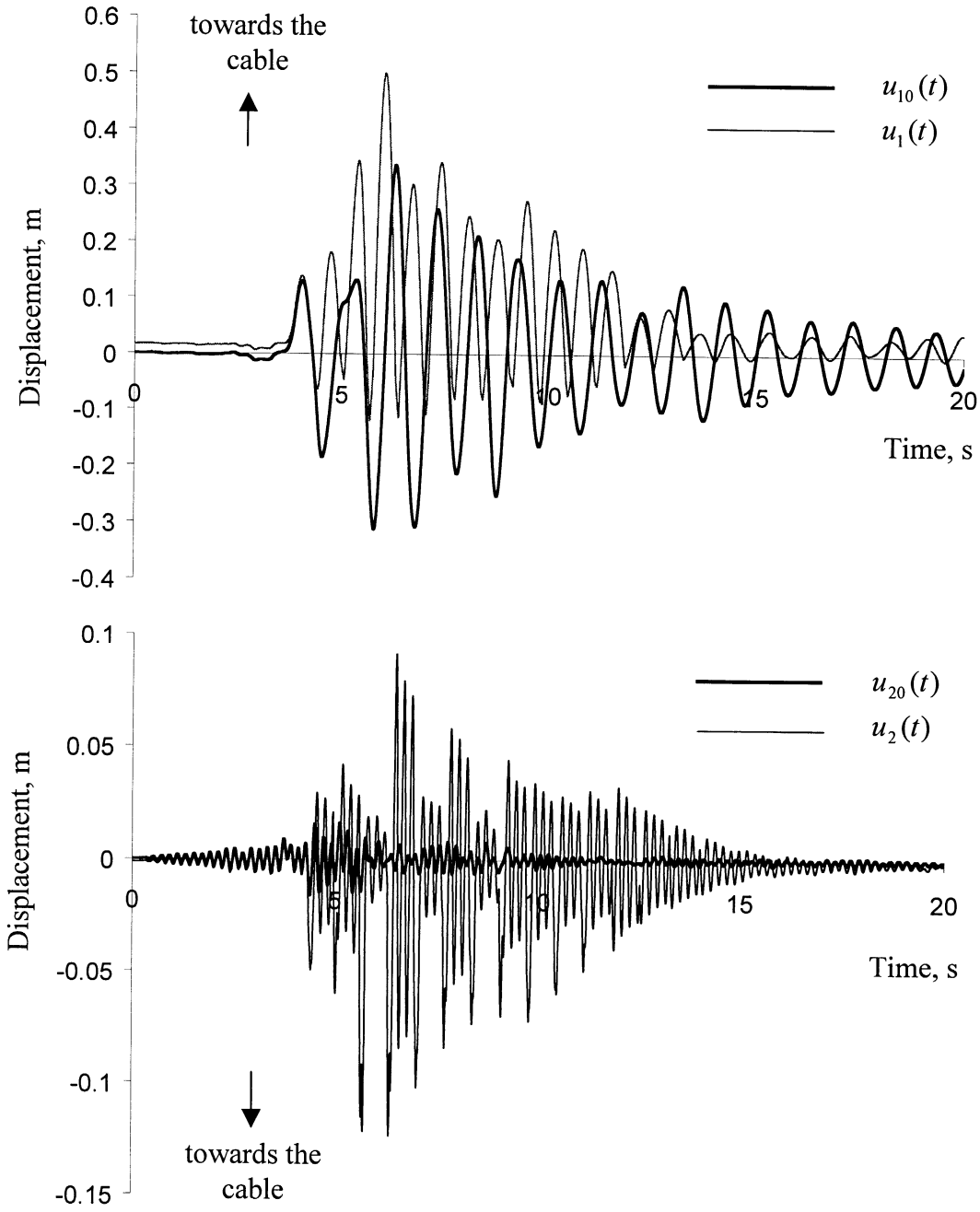

Figure 4.12 Displacement time histories for stand-alone and connected equipment items

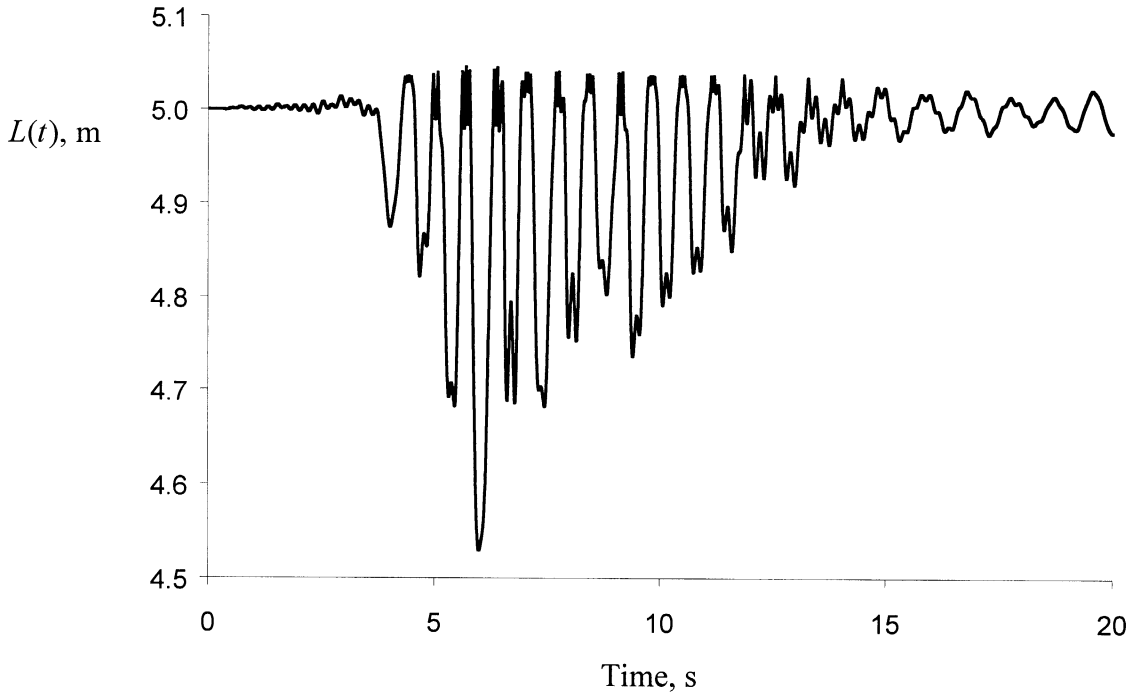

Figure 4.13 Time history of the cable span length

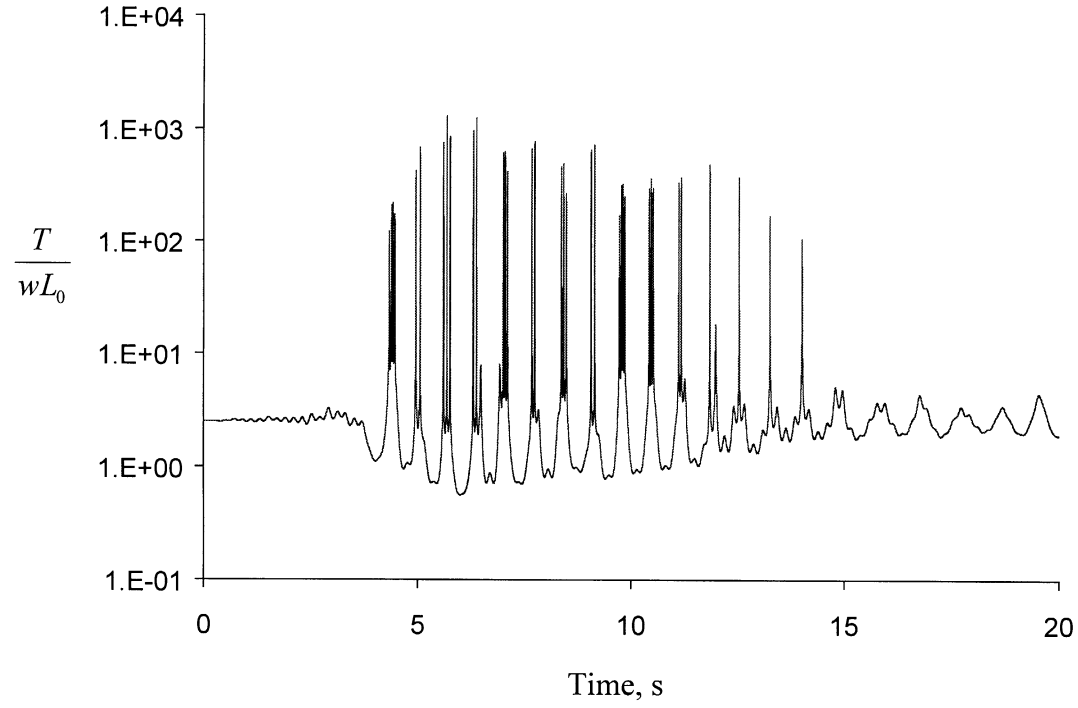

Figure 4.14 Time history of the normalized cable force

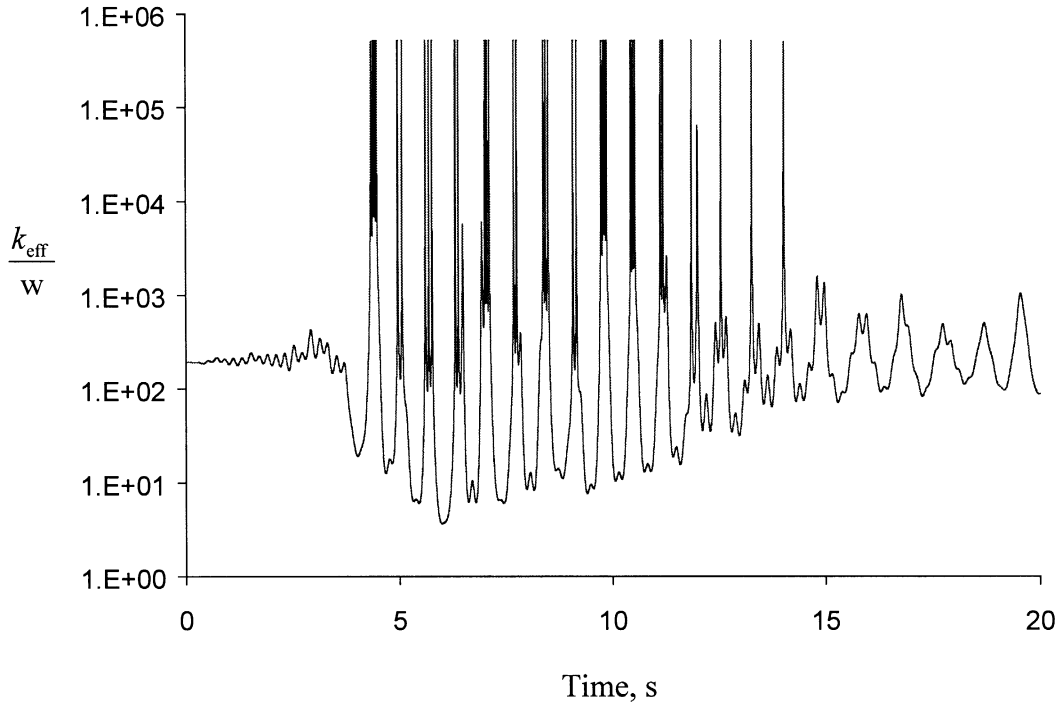

Figure 4.15 Time history of the normalized effective cable stiffness

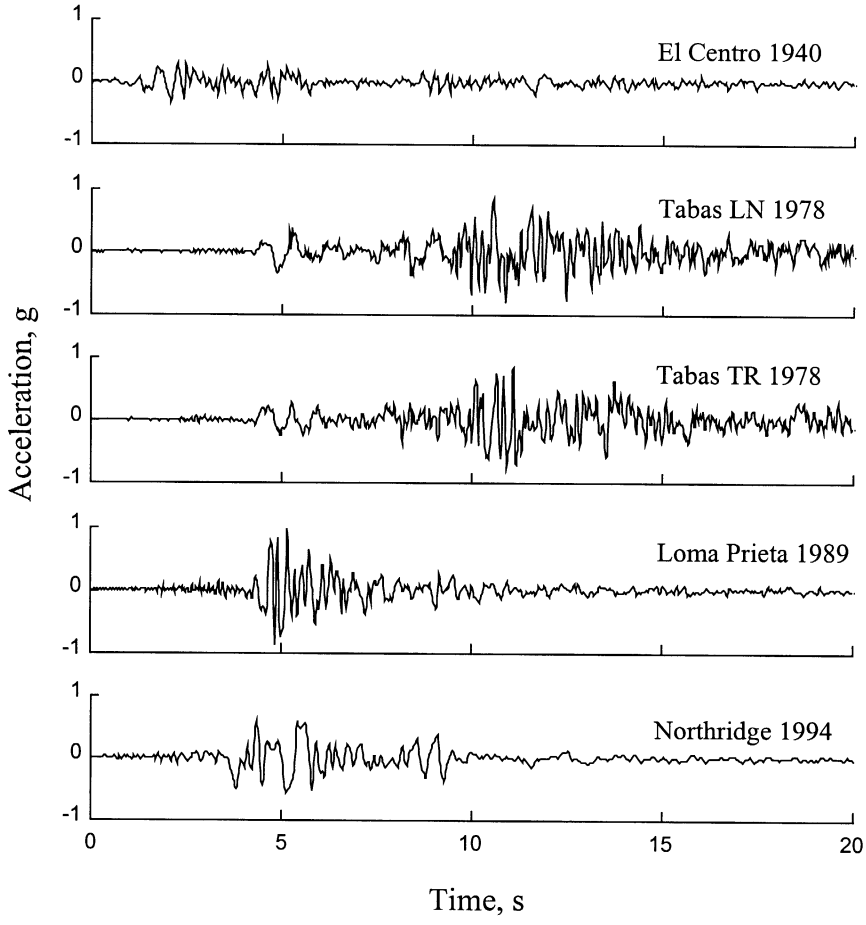

Figure 4.16 Selected accelerograms

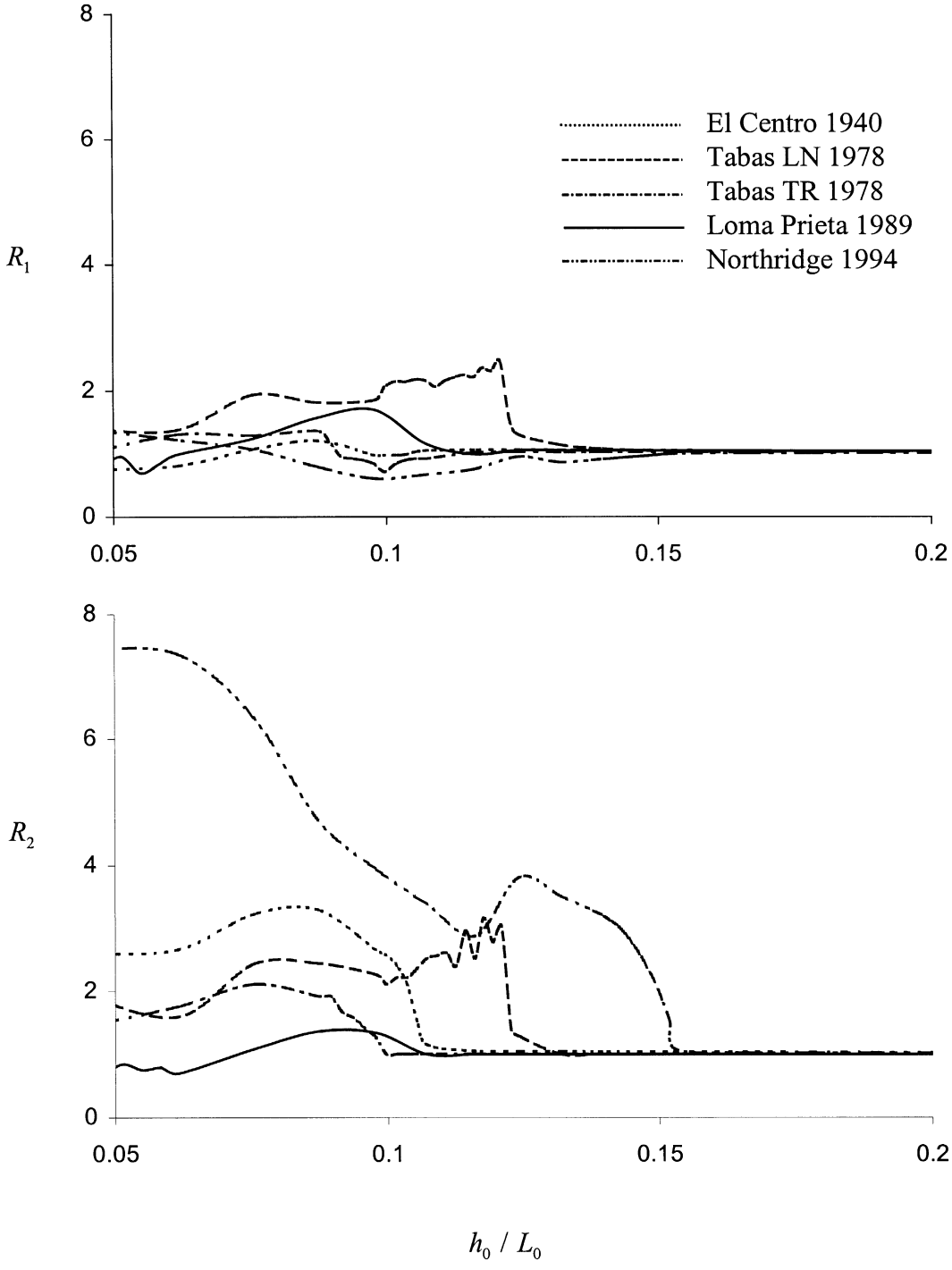

Figure 4.17 Response ratios for five earthquakes as functions of the initial sag for $\omega_1 = 2\pi$ rad/s and $\omega_2 = 10\pi$ rad/s

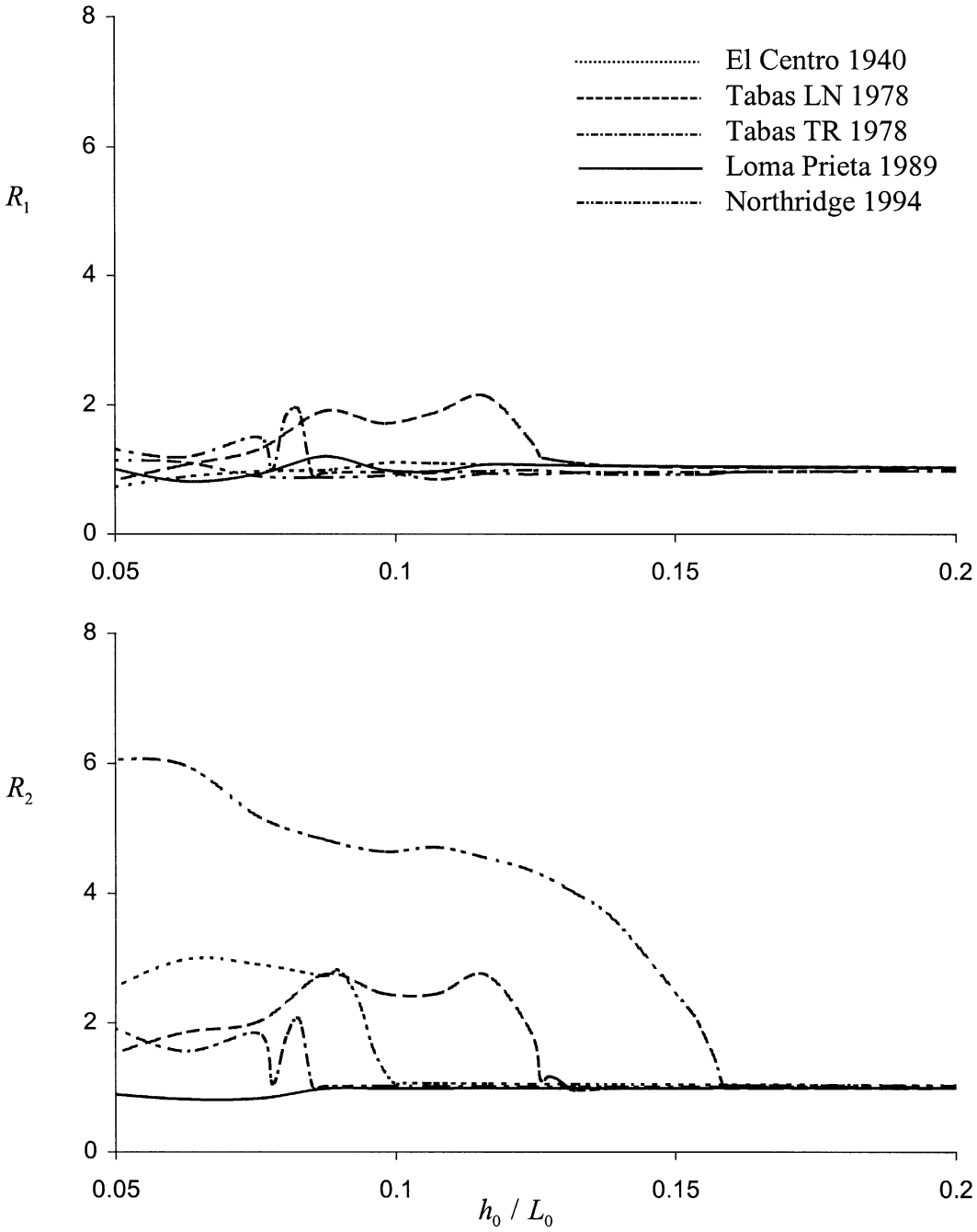

Figure 4.18 Response ratios for five earthquakes as functions of the initial sag for $\omega_1 = 2\pi$ rad/s and $\omega_2 = 10\pi$ rad/s with equipment positions switched

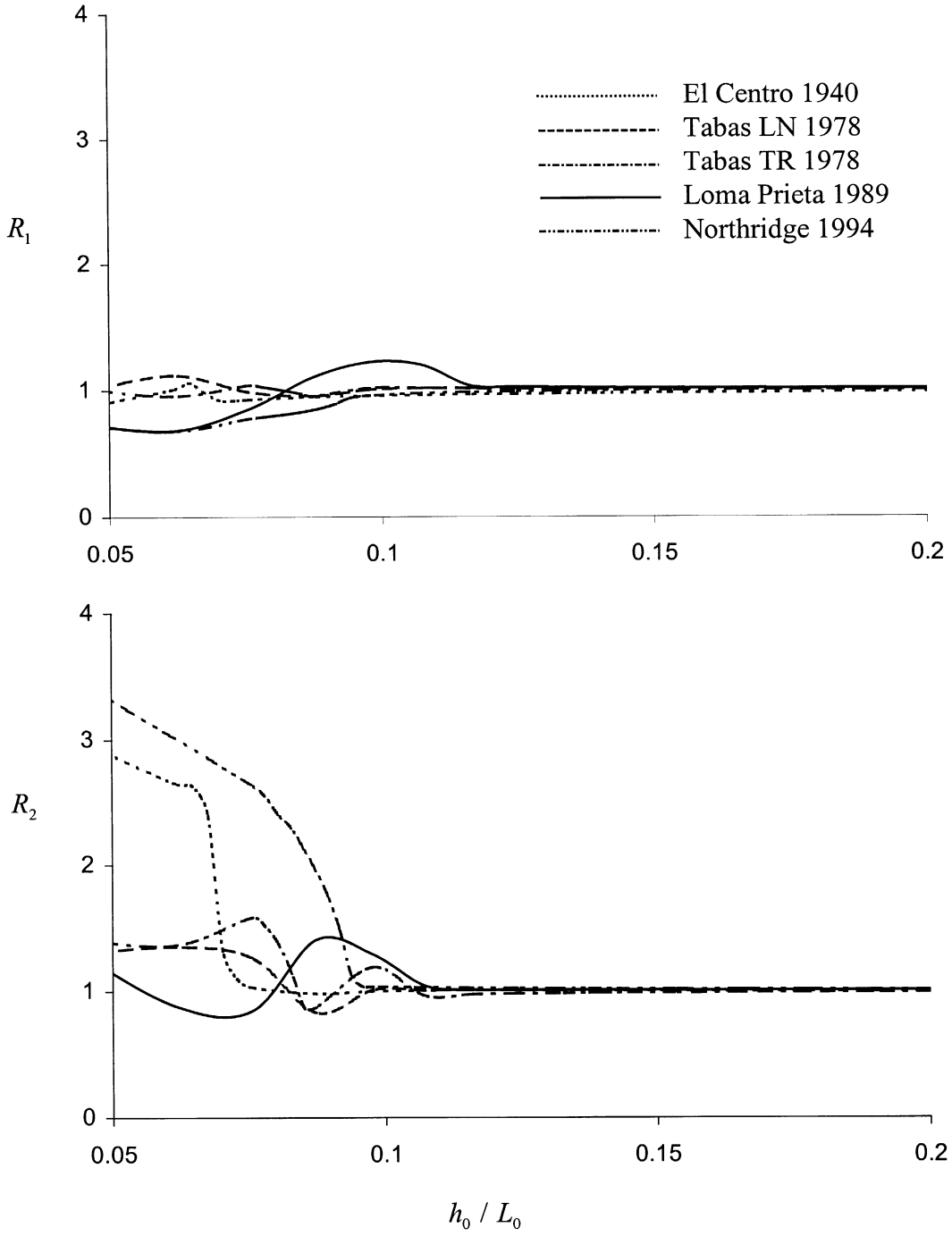

Figure 4.19 Response ratios for five earthquakes as functions of the initial sag for $\omega_1 = 4\pi$ rad/s and $\omega_2 = 10\pi$ rad/s

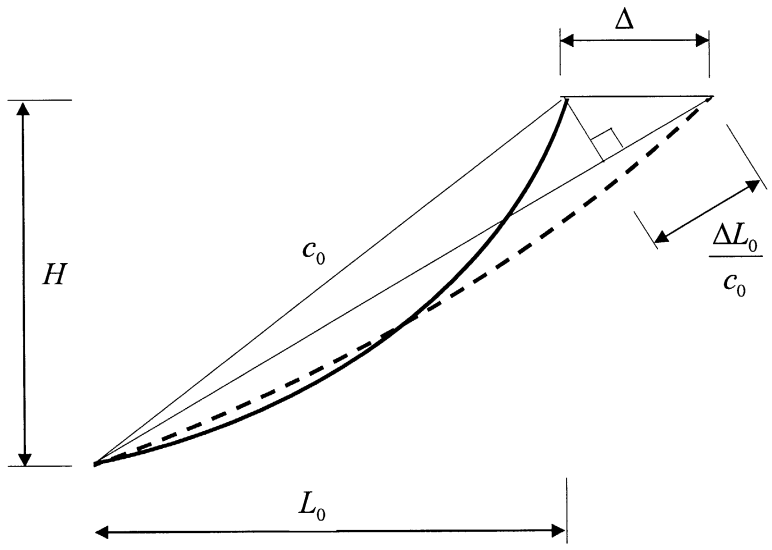

Figure 4.20 Change in slackness due to relative displacement Δ

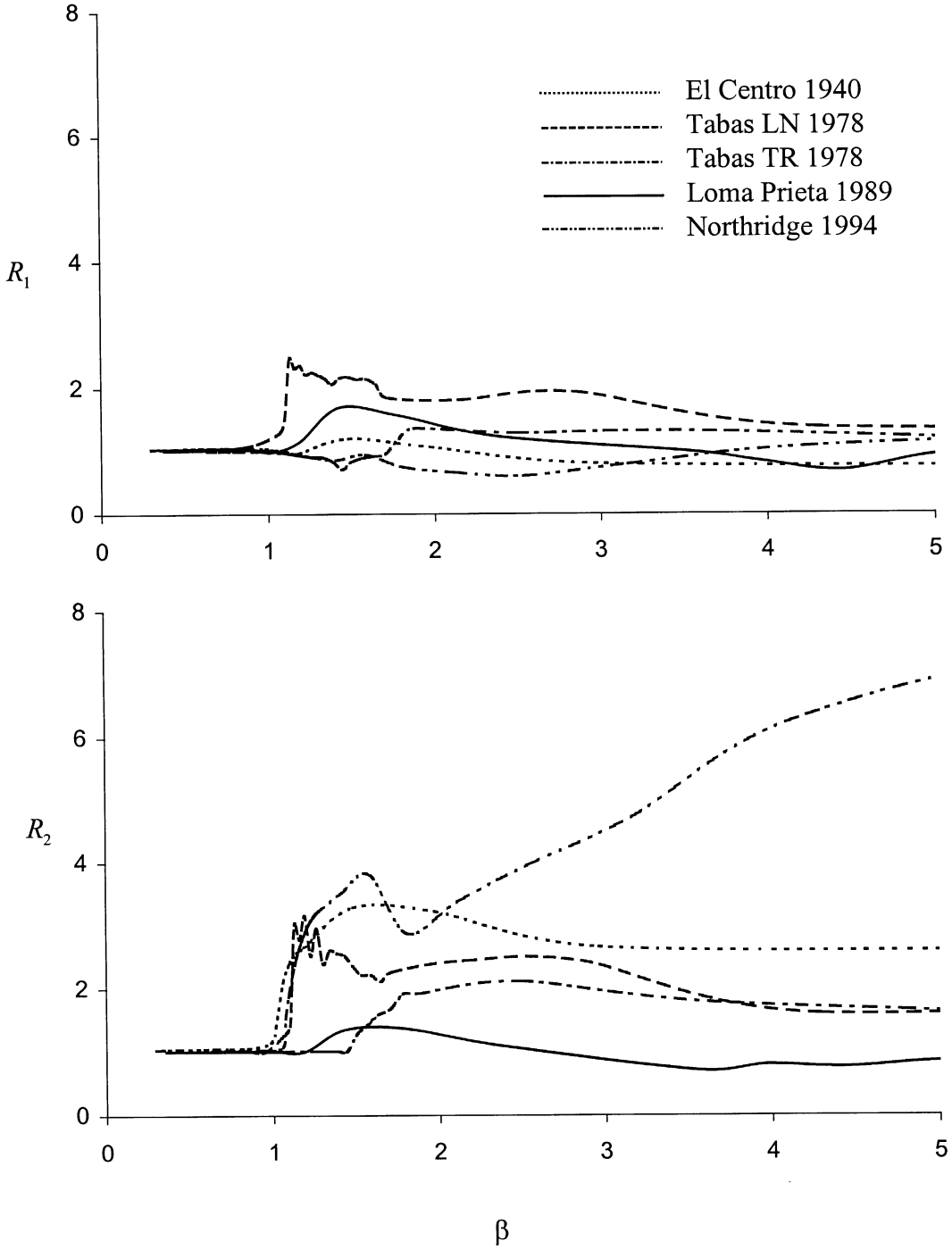

Figure 4.21 Response ratios for five earthquakes as functions of the interaction parameter for $\omega_1 = 2\pi$ rad/s and $\omega_2 = 10\pi$ rad/s ($H / L_0 = 0$)

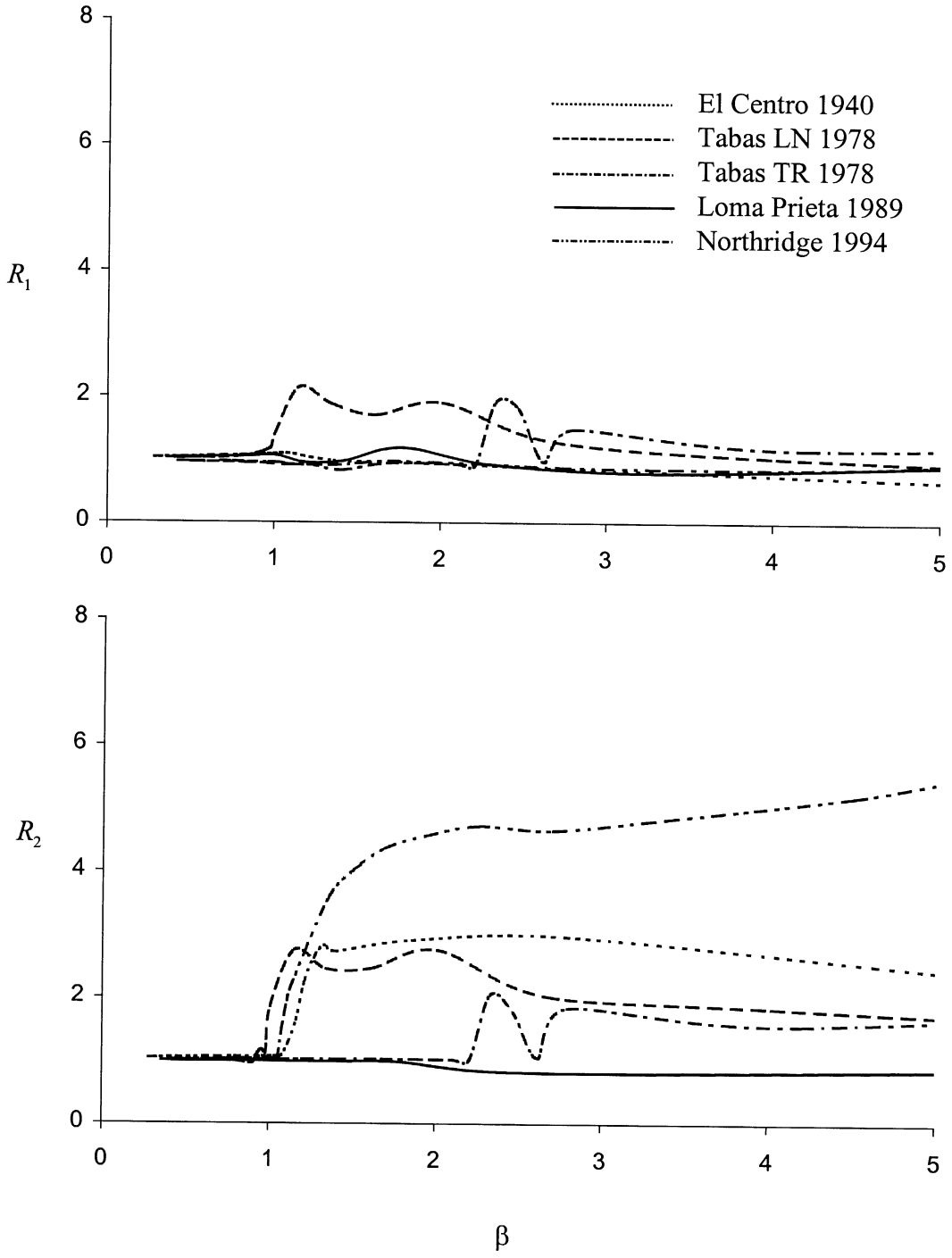

Figure 4.22 Response ratios for five earthquakes as functions of the interaction parameter for $\omega_1 = 2\pi$ rad/s and $\omega_2 = 10\pi$ rad/s with equipment positions switched ($H / L_0 = 0$)

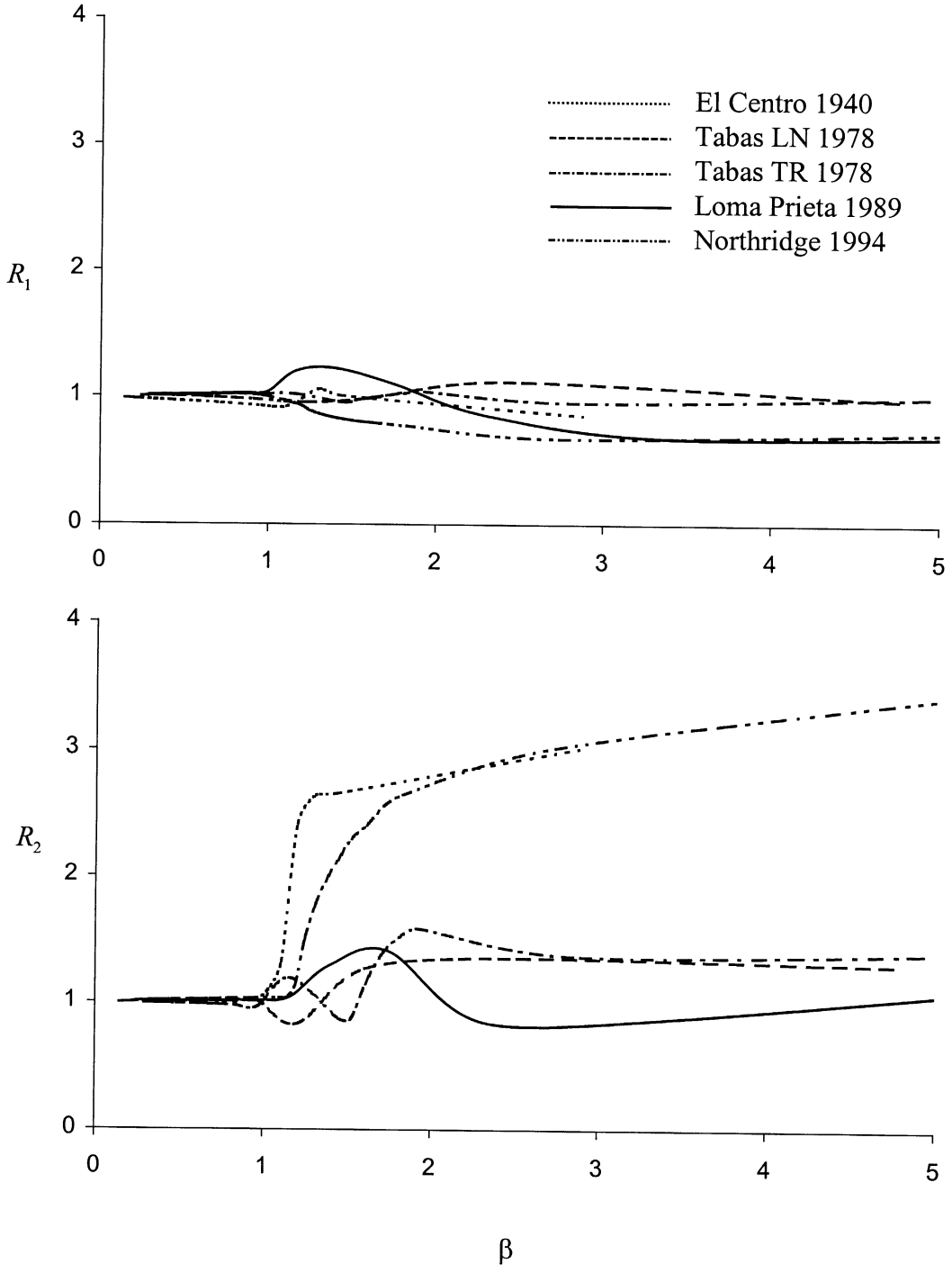

Figure 4.23 Response ratios for five earthquakes as functions of the interaction parameter for $\omega_1 = 4\pi$ rad/s and $\omega_2 = 10\pi$ rad/s ($H / L_0 = 0$)

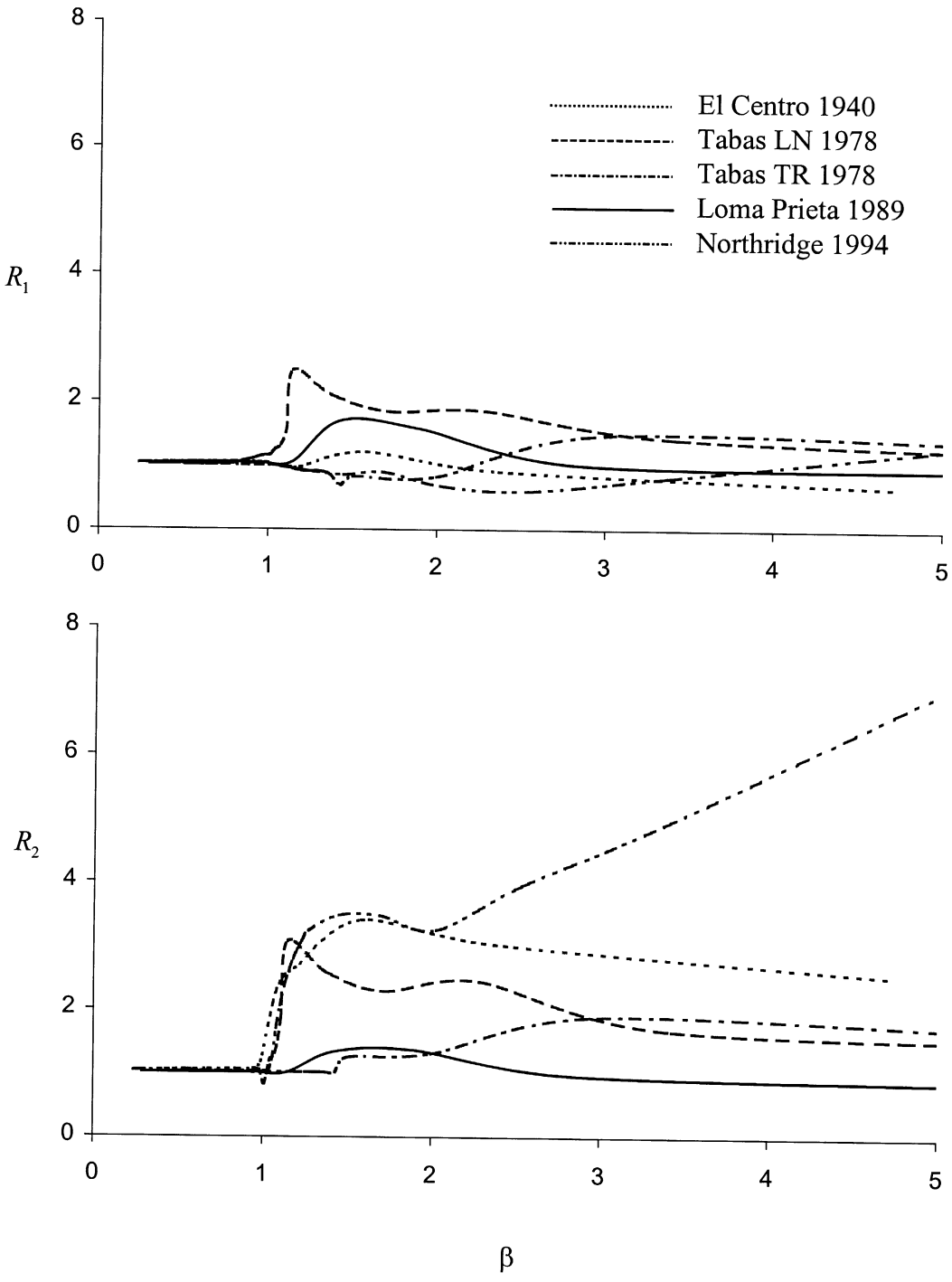

Figure 4.24 Response ratios for five earthquakes as functions of the interaction parameter for $\omega_1 = 2\pi$ rad/s and $\omega_2 = 10\pi$ rad/s ($H / L_0 = 0.5$)

CHAPTER 5

RECOMMENDATIONS AND GUIDELINES FOR DESIGN OF CONNECTED EQUIPMENT

5.1 Introduction

In this chapter, we first summarize the major findings of the study. These findings form the bases for a set of recommendations and guidelines for design of connected equipment items. Attention is given to both linear connecting elements, representative of rigid buses, and cable connections. Where appropriate, references are made to specific sections of the report, where appropriate formulas or analysis methods are given.

5.2 Major Findings

Response Ratios

Response ratios R_0, R_1 and R_2 introduced in this study provide valuable information on the effect of interaction between two connected equipment items. Ratio R_0, relating the response of the connecting element to the maximum absolute relative displacement between the stand-alone equipment items, is useful for the design of the connecting element. Response ratios R_1 and R_2 relate the responses of the two equipment items in the connected system to their corresponding responses in the stand-alone configurations. As such, they are acute measures of interaction between the two equipment items. A value for R_1 or R_2 that is greater than unity indicates an amplification of the corresponding equipment response due to the interaction effect, whereas a value smaller than unity indicates a de-amplification. A designer can use these ratios together with estimated responses of the stand-alone equipment items to determine the seismic demands on the equipment items in their connected configurations. This information could then be used to provide adequate strength to the equipment and their supports in order to withstand the seismic forces in both their stand-alone and connected configurations.

Parameters Influencing Interaction Between Equipment Items with Linear Connecting Element

Parameters having major influences on the effect of interaction between two equipment items connected by a linear element, such as a rigid bus with linear or linearized stiffness, include the following: (a) ratio of the frequencies of the stand-alone equipment items, (b) ratio of equipment masses, (c) stiffness of the connecting element, (d) location of attachment point of the connecting element to each equipment item, and (e) damping of the connecting element. Lesser influence is provided by the mass of the connecting element and the shape of the response spectrum. Damping of individual equipment items has little influence on the response ratios. No interaction occurs between equipment items with identical frequencies and damping ratios, as long as the connecting element has negligible mass and the attachment configuration is such that the same fraction of each equipment mass acts as the external inertia force.

Parameters Influencing Interaction Between Cable-Connected Equipment Items

The parameters described above have similar influences on the interaction effect in the cable-connected system. However, when the cable is taut, the response of the connected system is highly nonlinear and strongly sensitive to the details of the ground motion, including its frequency content. A measure that characterizes the influence of the cable on the system response is the normalized sag, h / L, where h is the sag and L is the span length. However, this measure is appropriate only when the cable supports are at the same level. A more general measure is the cable slackness, $s / c - 1$, where s is the cable length and c is the chord length. This measure is appropriate for cables of arbitrary vertical separation between the supports. Generally speaking, small values of cable slackness may result in strong interaction between the equipment items. Due to the strong nonlinearity of the response, a response spectrum method of analysis is inappropriate in this case. For this reason, an algorithm for nonlinear time-history analysis of such systems is developed in this study. No interaction occurs between cable-connected equipment items with identical frequencies and damping ratios, as long as the cable has

negligible mass and the attachment configuration is such that the same fraction of each equipment mass acts as the external inertia force.

Maximum Relative Displacement Between Stand-Alone Equipment Items

An important quantity for determining the effect of interaction between connected equipment items is the maximum relative displacement between them when they are in their stand-alone configurations. The larger this relative displacement, the larger will be the interaction effect. For the linear connecting element, the absolute value of the maximum relative displacement is the relevant quantity, whereas for the cable-connected system, the maximum relative displacement of the two equipment items away from one another is the quantity of interest. As described in Chapter 2, these two quantities have almost equal magnitudes. A simple formula for computing this measure that involves only the properties of the individual equipment items and the prescribed response spectrum is developed in Chapter 2. The maximum relative displacement between two equipment items is zero when they have identical frequencies and damping ratios, provided the attachment configuration is such that the same fraction of each equipment mass acts as the external inertia force

Effect of Interaction on Equipment Items

In general, when two equipment items are connected, interaction amplifies the response of the item with higher frequency. The magnitude of the amplification depends on the parameters described above and can be as large as a factor of 8 or even larger. Under certain conditions, the response of the lower-frequency equipment item may also be amplified. However, this amplification, if it occurs, is generally small and seldom reaches the factor 2. The amplification of the higher frequency equipment response tends to increase with increasing stiffness of the connecting element, increasing mass of the lower frequency equipment, increasing separation between equipment frequencies, and increasing relative displacement between the stand-alone equipment items. This amplification also increases when the connecting element is attached to a point near the base of the higher frequency equipment item and at a point at or near the top of the lower frequency equipment item. Damping in the connecting element has a significant effect in

reducing the amplification due to interaction. The mass of the connecting element tends to increase the amplification by only a small amount, as long as this mass is small in relation to the total mass of the equipment items.

The interaction effect in a cable-connected system strongly depends on the slackness of the cable. If the cable retains even a small amount of slackness during the excitation, the effect of interaction between the two equipment items would be small. However, if during the course of the excitation, the cable is stretched beyond its original length, then the effect of interaction can be very significant. In that case the response of the interacting system is strongly nonlinear. Even small variations in the time history can result in large variations in the equipment responses. Therefore, from a design stand-point, it is advisable to provide sufficient slackness in the cable so that the interaction effect is essentially avoided.

Effect of Interaction on the Connecting Element

For a linear connecting element, the response ratio R_0 provides the necessary information to determine the maximum restoring force in the element. In general this force is smaller than the force in the element were it to be elongated by the relative displacement between the stand-alone equipment items. For most cases, the connecting element can be safely designed for an elongation smaller than 60% of the stand-alone relative displacement. In a cable-connected system, when the cable is initially taut, the tension force in the cable can vary by several orders of magnitude during the course of the seismic response. Furthermore, the cable can be almost fully stretched, in which case its stiffness reaches its axial stiffness. These variations, if not avoided, can have severe effects on the cable and its connections.

Other New Results

In addition to results derived for connected equipment items, new results are developed to characterize the force, stiffness and geometric properties of the catenary cable. These include closed form expressions for the tangent stiffness of the cable, while accounting for its extensibility, and for variations in the cable sag. A numerical algorithm for computing

the strongly nonlinear and asymmetric response of the cable-connected system was developed and tested.

5.3 Guidelines for Design of Equipment Connected by Rigid Bus

Characterization of Equipment Items

In order to determine the interaction effect, characterize each stand-alone equipment item together with its support structure by a mass and a stiffness distribution, or a mass distribution and the fundamental frequency. An appropriate displacement shape should be selected to determine the effective mass and stiffness properties, as well as the fraction of the mass that acts as the external inertia force. Assign a damping ratio to characterize the energy dissipation capacity of the equipment and its support structure. Alternatively, these equipment parameters can be determined by laboratory or field tests. These parameters for equipment i, $i = 1, 2$, were denoted in this report as follows: m_i = effective mass, k_i = effective stiffness, l_i / m_i = fraction of mass acting as the external inertia force, ω_i = fundamental frequency, and ζ_i = damping ratio.

Characterization of the Connecting Element

Characterize the connecting element by its axial stiffness k_0, its damping coefficient c_0, and its mass m_0. These parameters could be effective values obtained by assuming an appropriate deformation shape function for the element. Appropriate linearization methods may be employed to approximately characterize elements that have nonlinear behavior. Alternatively, these connecting element properties can be obtained by laboratory or field tests.

Characterization of Input Ground Motion

For analysis of the interaction effect between connected equipment items, it is most convenient to characterize the input ground motion in terms of a design response spectrum, such as that described in IEEE (1997), and a peak ground acceleration that scales the spectrum. The spectrum shape should be selected in accordance with the soil conditions

at the site of the equipment. The peak ground acceleration should be selected on the basis of the seismic zone associated with the site.

Evaluate the Effect of Interaction on Equipment Items

For a linear connecting element, the interaction effect tends to de-amplify the response of the lower frequency equipment item and amplify the response of the higher frequency equipment item. For design purposes, it is advisable not to take advantage of the de-amplification in the response of the lower frequency equipment item in the connected system, so as to ensure its safety were it to be subjected to an earthquake in its stand-alone configuration. The amplification in the response of the higher frequency equipment item, however, should be properly determined so that adequate strength to resist the earthquake forces in the connected configuration can be provided. As we have seen above, system parameters having important influences on the amplification factor (response ratio R_2) are the ratio of the frequencies of the stand-alone equipment items, the ratio of equipment masses, the stiffness of the connecting element, the location of attachment points, and damping of the connecting element. For a wide range of these system parameter values, the response ratio R_2 can be readily read from the graphs in Figures 3.1-3.4, 3.6 and 3.9. For system parameter values not in this range, the response ratio should be determined by use of the response spectrum method described in Chapter 2. The seismic demand in the equipment in the connected system is determined by multiplying the demand for the stand-alone configuration by the response ratio R_2.

Reducing the Effect of Interaction on the Higher-Frequency Equipment Item

When the seismic demand on the higher frequency equipment item exceeds its capacity, the design engineer has two alternative recourses: increase the capacity of the equipment; reduce the amplification due to the interaction. The following measures can be employed to reduce the interaction effect on the higher frequency equipment item:

- Reduce the separation between the stand-alone equipment frequencies. This can be done by increasing the stiffness or reducing the mass of the lower frequency equipment item. Another alternative is to place the higher frequency equipment item on an

isolation system such that its base-isolated frequency is close to that of the lower frequency equipment item.

- Reduce the stiffness of the connecting element by, e.g., providing special expansion connectors.
- Increase the energy dissipation capacity of the connecting element. This can be done by installing a special device, such as a viscous damper, on the connecting element, or, more practically, by providing an expansion connector that dissipates energy through plastic deformation.
- Attach the connecting element to a point at or near the top of the higher frequency equipment item and to a point near the base of the lower frequency equipment item, subject to electrical clearance requirements.

5.4 Guidelines for Design of Equipment Connected by Flexible Cables

Characterization of Equipment Items

Characterize equipment items in the manner described in Section 5.3.

Characterization of the Connecting Cable

Provided the flexural rigidity of the cable is negligible (see Appendix A), we can model the connecting cable as a catenary cable with axial extensibility. Characterize the cable by its span length L_0, vertical separation H of the attachment points, chord length $c_0 = \sqrt{L_0^2 + H^2}$, length s_0, sag h_0, weight per unit length w, and axial stiffness AE/s_0. The quantities L_0, c_0, s_0 and h_0 should correspond to the initial values of the cable in the equilibrium position of the combined system. The cable length can be determined from the relevant equations of the catenary cable in Chapter 4, or by reading from the plots of slackness versus normalized sag in Figure 4.6.

Characterization of Input Ground Motion

A characterization of the input ground motion in terms of a design response spectrum as described in the previous section is also useful for cable-connected equipment items, as

we will see below. However, such a characterization does not allow an accurate analysis of the interaction effect caused by a taut cable that has a strongly nonlinear response. If such analysis is necessary, one alternative is to describe the ground motion by a suite of time histories that are typical for the site. Another alternative, not developed in this study, is to employ a stochastic model of the ground motion and evaluate the interaction effect through nonlinear stochastic dynamic analysis. These alternatives, however, are time consuming, cumbersome and not well suited for design and analysis of electrical substation equipment items that come in many different configurations and characteristics. A simple design rule that eliminates the need for such complex analyses is described below.

Evaluate the Maximum Relative Displacement Between Stand-Alone Equipment Items

For a cable connection, an important parameter is the maximum amount that the two equipment items displace away from each other, defined as $\Delta = \max[u_{20}(t) - u_{10}(t)]$. With the equipment items characterized as described above, this quantity can be computed by use of the response spectrum method in the manner described in Section 2.5.

Determine Minimum Cable Slackness to Avoid Adverse Interaction[*]

As mentioned earlier, the response of the cable-connected system can be strongly nonlinear when the cable slackness $(s_0 / c_0 - 1)$ is small and the cable is stretched beyond its original length during the course of the excitation. In that case, significant interaction between equipment items occurs, which can result in large amplification of the higher frequency equipment item and moderate amplification of the lower frequency equipment item. Unfortunately, these effects cannot be predicted by simple response spectrum analysis. We recommend providing sufficient slackness in the cable to entirely avoid this problem. Based on results in Section 4.4, the minimum slackness that accomplishes this objective is determined by using the rule $\beta < 1$, where β is the interaction parameter defined in Section 4.4. Based on this rule, the minimum cable slackness to avoid adverse interaction effect in the equipment items is computed from

[*] See Epilogue on page 94.

$$\frac{s_0}{c_0} - 1 > \frac{\Delta L_0}{c_0^2} \tag{5.1}$$

For a given L_0 and c_0 dictated by the locations of the equipment items in the substation, the above requirement can be satisfied in two ways. One is to increase the cable length s_0, subject to electrical clearance requirements. The other is to reduce Δ. The latter can be accomplished by several means, including:

- Reduction of the separation between the stand-alone equipment frequencies. This can be done by increasing the stiffness or reducing the mass of the lower frequency equipment item. Another alternative is to place the higher frequency equipment item on an isolation system such that its base-isolated frequency is close to that of the lower frequency equipment item.
- Attach the connecting element to a point at or near the top of the higher frequency equipment item and to a point near the base of the lower frequency equipment item, subject to electrical clearance requirements.

CHAPTER 6

SUMMARY AND RECOMMENDATIONS FOR FURTHER STUDY

6.1 Summary

This study investigates the effect of interaction between connected electrical substation equipment items that are subjected to earthquake motions. To the best of our knowledge, this is the first analytical study of this subject. Equipment items are modeled as lumped- or continuous-mass linear systems idealized by a single degree of freedom. The connecting element is modeled either as a linear spring-dashpot-mass element, or an extensible cable with negligible inertia. The effect of interaction is represented in terms of the ratio of peak equipment responses in the combined system to their corresponding responses in the stand-alone equipment configurations.

Study of the combined system with the linear connecting element reveals that the interaction effect tends to amplify the response of the higher frequency item, and de-amplify the response of the lower frequency item. Parameters having major influences on the effect of interaction include the frequencies of the stand-alone equipment items, the ratio of equipment masses, the stiffness of the connecting element, the location of attachment of the connecting element to each equipment item, and the damping of the connecting element. Lesser influence is provided by the mass of the connecting element and the shape of the response spectrum of the ground motion. Damping of individual equipment items has little influence on the response ratios. No interaction occurs between equipment items with identical frequencies and damping ratios, as long as the connecting element has negligible mass and the attachment configuration is such that the same fraction of each equipment mass acts as the external inertia force.

Study with the cable-connected system reveals that the response of this system when the cable is taut is highly nonlinear, asymmetric and strongly sensitive to the details of

the ground motion, including its frequency content. The amplification of the higher frequency equipment relative to its stand-alone response in this case can be large; furthermore, the lower frequency equipment item may also experience a moderate amplification in its response, depending on the frequency content of the ground motion. A convenient measure that characterizes the severity of the interaction effect for this system is identified as the slackness $s/c-1$, where s is the length of the cable and c is its chord length. This measure is appropriate for cables of arbitrary geometry. Through a comprehensive set of time history analysis, a simple rule for determining the minimum required slackness to avoid the adverse interaction effect is developed in this study.

A more detailed description of the major findings of this study are presented in Chapter 5. Included in there are also a set of recommendations and guidelines for design of connected equipment items, and for reducing the adverse effect of interaction.

In addition to results derived for connected equipment items, new results are developed in this study that characterize the force, stiffness and geometric properties of the catenary cable. These include closed form expressions for the tangent stiffness of the cable, while accounting for its extensibility, and for variations in the cable sag.

While this has been a comprehensive study of the effect of interaction between connected equipment items, the investigation has been conducted based on a set of idealizations and within a prescribed scope. The following section lists recommendations for further study that in our opinion will broaden the scope of application of the results derived in this study, while relaxing some of the idealizations that were made.

6.2 Recommendations for Further Study

Based on the experience gained from the present study, we believe pursuing further research on the following topics would lead to a better understanding of the behavior of interacting equipment items and would result in more reliable and safe design methods.

a) *Study of interaction among multiple equipment items with multiple connections:* The present study is limited to two equipment items with only one connecting element. The interaction phenomenon in several equipment items that are multiply connected

to each other is expected to be far more complex. It would be useful to investigate and determine whether the results derived from the present study can be carried over to such systems. If not, then new results for such systems need to be developed.

b) *Refined modeling of rigid bus connectors*: In this study, the rigid bus connector was modeled as a linear spring-dashpot-mass element. In reality, these elements may act nonlinearly, either because of closing of their expansion gap or because of inelastic deformation of their expansion loop. It is worthwhile to investigate nonlinear models of the connecting element with the objective of understanding their behavior and possibly deriving rules for their equivalent linearization. Such rules would then allow utilization of the results reported in the present study for rigid buses having nonlinear behavior.

c) *Flexible bus connector with flexural rigidity*: In the present study, the flexible bus connector was modeled as an extensible cable with negligible flexural stiffness. A criterion for the conditions under which the flexural rigidity can be neglected was derived. In the field there are many flexible connectors (made of braided aluminum wires) that have significant flexural stiffness and are in fact pre-formed into standard shapes before attaching to equipment items. It is important to investigate the influence of the flexural rigidity of such elements to fully understand the effect of interaction between the connected equipment items. It may also be worthwhile to investigate the influence of damping in the flexible connector that arises from friction between braided wires. We believe the results developed in the present study provide the proper foundation for such an investigation.

d) *Correlation with laboratory and field studies:* The present study is based on idealized mathematical models. It is highly desirable to correlate the results derived from this study with results obtained from laboratory or field experiments. It is particularly important to obtain experimental data on the stiffness, damping and elastic/inelastic properties of rigid and flexible connectors, as well as on the dynamic characteristics of typical equipment items. Experimental or field observations can also be used to validate the analytical predictions of the interaction effect made in this study.

APPENDIX A

CRITERION FOR NEGLECTING FLEXURAL STIFFNESS OF CABLE

In Chapter 4, we have developed formulas for the connecting cable assuming that the flexural stiffness of the cable is negligible. Here, we develop a criterion to examine the circumstances under which this assumption is valid.

Consider the symmetric cable in Figure A1 having span L, sag h, weight per unit length w, section moment of inertia I, and elastic modulus E. Let s denote the length of the cable and T denote the horizontal component of the cable force. The stiffness due to cable action is given in (4.8) of Chapter 4, which for $H = 0$ is

$$k_{\text{cable}} = \frac{T + wh}{\frac{wL}{T}h - (s - L)} \tag{A1}$$

Our interest here is in shallow cables. For such cables, $s \cong L$ and $T \cong wL^2/8h$ (Meriam and Kraige 1997) and (A1) reduces to

$$k_{\text{cable}} = \frac{wL^3}{64h^3} \tag{A2}$$

To determine the flexural stiffness, consider a simply-supported curved beam having the shape of the cable, which we approximate as a parabola $y = 4hx^2/L^2$, as shown in Figure A2. Let dL denote the differential displacement of the beam at the right support caused by the application of a horizontal differential force dT. The bending moment along the beam is given by $dM = dT(h - y)$, and the change in curvature is $d\psi = dM/(EI)$. The horizontal displacement at the right support from the bending of a differential segment dx of the beam is given by $y\,d\psi\,dx$. The total displacement is obtained by integration along the beam, i.e.,

$$
\begin{aligned}
dL &= \int_{-L/2}^{L/2} y \, d\psi \, dx \\
&= \int_{-L/2}^{L/2} \frac{4hx^2}{L^2} \frac{dT}{EI} \left(h - \frac{4hx^2}{L^2} \right) dx \\
&= \frac{2Lh^2}{15EI} dT
\end{aligned} \tag{A3}
$$

It follows that the stiffness due to bending is

$$
k_{\text{flexure}} = \frac{15EI}{2Lh^2} \tag{A4}
$$

A measure of the significance of the flexural stiffness is given by the ratio $k_{\text{flexure}} / k_{\text{cable}}$. For a given cable, one is justified in neglecting the flexural rigidity if this ratio is small in comparison to unity. Using (A2) and (A4), we obtain the following criterion:

$$
\frac{k_{\text{flexure}}}{k_{\text{cable}}} = 480 \frac{EI}{wL^3} \frac{h}{L} << 1 \tag{A5}
$$

It is clear that the flexural stiffness can only be significant for large values of the sag. It is noted that as $h \to 0$, both k_{flexure} and k_{cable} become very large. In that case, the flexibility of the system is governed by the axial deformation of the cable, which is accounted for in our analysis in Chapter 4.

As an example, we consider a Class A Trillium cable made by ALCAN according to ASTM Standard B230 (PG&E 1998). This cable consists of 127 strands each having a diameter of 0.154in, which is equivalent to 3.90×10^{-3} m. The weight per unit length of the cable is $w = 41.5$ N/m. Assuming negligible friction between the strands, the effective moment of inertia of the cable cross section is equal to the sum of the moments of inertia of the strands, thus yielding $I = 127 \times \pi \times (3.90 \times 10^{-3})^4 / 64 = 1.44 \times 10^{-9}$ m^4. (If friction were to be accounted for, this value would be larger by an amount depending on the coefficient of friction.) For aluminum, the elastic modulus is approximately

$E = 7.27 \times 10^{10}\,\mathrm{N/m^2}$. Substituting these values in (A5) for a cable of length $L = 5\,\mathrm{m}$, the ratio of stiffnesses is

$$\frac{k_{\text{flexure}}}{k_{\text{cable}}} = 9.7\frac{h}{L} \tag{A6}$$

For a normalized sag $h/L = 0.05$, the above gives $k_{\text{flexure}}/k_{\text{cable}} = 0.485$. At first sight, this value may not appear sufficiently small in relation to unity. However, as pointed out in Chapter 4, the stiffness of the cable for this value of the sag is negligible in relation to the stiffnesses of the two equipment items and consequently induces little interaction between the two equipment items. (See discussion of values of parameter κ in the second paragraph of Section 4.4.) It follows that the flexural stiffness, which is even smaller, will also induce insignificant interaction. For smaller values of the sag, the cable stiffness rapidly increases (in proportion to h^{-3}), whereas the flexural stiffness increases more slowly (in proportion to h^{-2}). Hence, the cable stiffness dominates the behavior of the connecting element when the total stiffness becomes significant in relation to the stiffnesses of the equipment items. This shows that, for the cable under consideration, it is reasonable to neglect the flexural stiffness in determining the interaction effect between the two equipment items.

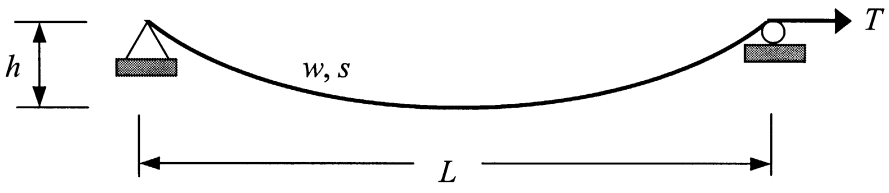

Figure A1. Cable with no flexural stiffness

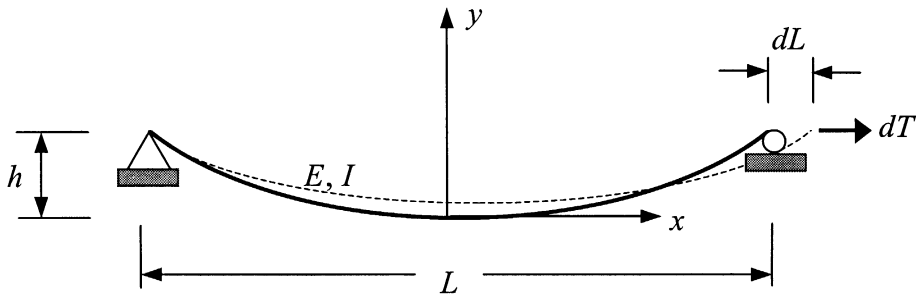

Figure A2. Horizontal support displacement of curved beam

REFERENCES

Benuska, L. (Editor) 1990. Chapter 8 — Lifelines. *Earthquake Spectra* (Supplement) 6: 315-338.

Chopra, A. K. 1995. *Dynamics of structures.* Prentice Hall, Englewood Cliffs, NJ.

Clough, R., and J. Penzien. 1993. *Dynamics of structures.* McGraw-Hill, New York.

Der Kiureghian, A. 1980. Structural response to stationary excitation. *Journal of Engineering Mechanics Division,* ASCE, 106(6): 1195-1213.

Der Kiureghian, A. 1981. A response spectrum method for random vibration analysis of MDF systems. *Earthquake Engineering & Structural Dynamics,* 9(5): 419-435.

Der Kiureghian, A., and Y. Nakamura. 1993. CQC modal combination rule for high-frequency modes. *Earthquake Engineering &. Structural Dynamics,* 22(11), 943-956.

Hall, J. (Editor) 1995. Chapter 4 — Lifelines. *Earthquake Spectra* (Supplement C) 11: 188-217.

IEEE 1997. *IEEE 693 — Recommended practices for seismic design of substations.* IEEE Standard Draft No. 6. 1, IEEE Standards Department, Piscataway, NJ.

Igusa, T., and A. Der Kiureghian. 1985. Generation of floor response spectra including oscillator-structure interaction. *Earthquake Engineering & Structural Dynamics,* 13(5): 661-676.

Matsuda, E., N. Abrahamson, and Y-B. Tsai. 1996. *Effects of strong ground motion on substations in the January 17, 1994 Northridge earthquake.* Report 005-96.23, Pacific Gas and Electric Company, San Ramon, CA.

Meriam, J. L. and L. G. Kraige. 1997. *Engineering mechanics: Volume I — Statics.* 4th ed., John Wiley & Sons, New York.

PG&E. 1998. Tables of Physical Properties of Aluminum Cables. (Provided to the authors by E. Fujisaki.)

Tsai, Y-B. 1993. Impact of earthquake strong ground motion on substations. *Report 009.3-93.1*, Pacific Gas and Electric Company, San Ramon, CA.

EPILOGUE

The formulation and results for the cable-connected equipment system in Chapter 4 and the corresponding recommendations in Chapter 5 were derived based on the assumption that the influence of the inertia associated with the cable mass was negligible. After completing this study, while this report was being printed, we came across an important paper by J.-B. Dastous and J.-R. Pierre (1996)*. They performed experiments on flexible conductors under imposed dynamic displacement at one or both ends. Their results indicate a strong influence of the cable inertia on the horizontal cable force. Our preliminary analytical investigation reveals that indeed, under certain conditions, the cable inertia can have an important influence on the interaction between the two equipment items and on the force transmitted by the cable to each equipment item. It appears that this influence could further amplify the response of the equipment items beyond that estimated in Chapter 4 of this report. Furthermore, when this effect is significant, the rule described in (5.1) can be unconservative.

This issue is a subject of our current study that deals with flexible conductors having flexural stiffness. The results reported in Chapter 4 and the recommended rule (5.1) should be regarded as preliminary until their re-evaluation at the completion of the present investigation.

* Dastous, J.-B., and J.-R. Pierre (1996). Experimental investigation on the dynamic behavior of flexible conductors between substation equipment during an earthquake. IEEE Transactions on Power Delivery, 11(2), 801-807.